Best Available Copy

OIPE SEP 05 2000 JC116 PATENT & TRADEMARK OFFICE

IN THE UNITED STATES PATENT AND TRADEMARK OFFICE
BEFORE THE BOARD OF PATENT APPEALS AND INTERFERENCES

First Named Inventor : Kumar	Appeal No.
Appln. No.: 09/136,483	
Filed : August 19, 1998	Group Art Unit: 1755
For : ALUMINUM OXIDE PARTICLES	Examiner: M. Marcheschi
Docket No.: N19.12-0016	

TRANSMITTAL OF APPEAL BRIEF
(PATENT APPLICATION - 37 C.F.R. § 192)

BOX AF
Assistant Commissioner for Patents
Washington, D.C. 20231

I HEREBY CERTIFY THAT THIS PAPER IS BEING SENT BY U.S. MAIL, FIRST CLASS, TO THE ASSISTANT COMMISSIONER FOR PATENTS, WASHINGTON, D.C. 20231, THIS

30 DAY OF August, 2000.

Peter S. Dardi
PATENT ATTORNEY

Sir:

Transmitted herewith in triplicate is the Appeal Brief in this application with respect to the Notice of Appeal filed on May 30, 2000.

FEE STATUS

[X] Small entity status under 37 C.F.R. §§ 1.9 and 1.27 is established by a verified statement previously submitted.

FEE FOR FILING APPEAL BRIEF

Pursuant to 37 C.F.R. 1.17(c) the fee for filing the Appeal Brief is $150.00.

The Commissioner is authorized to charge any additional fees associated with this paper or credit any overpayment to Deposit Account No. 23-1123. A duplicate copy of this communication is enclosed.

Respectfully submitted,

WESTMAN, CHAMPLIN & KELLY, P.A.

By: Peter S. Dardi

Peter S. Dardi, Reg. No. 39,650
Suite 1600 - International Centre
900 Second Avenue South
Minneapolis, Minnesota 55402-3319
Phone: (612) 334-3222 Fax: (612) 334-3312

PSD:slg

RECEIVED SEP - 7 2000 TECH. CENTER 1700

OIPE
SEP 0 5 2000
PATENT & TRADEMARK OFFICE
TC1700

IN THE UNITED STATES PATENT AND TRADEMARK OFFICE
BEFORE THE BOARD OF PATENT APPEALS AND INTERFERENCES

Applicant : Kumar et al.	Appeal No.
Applic No.: 09/136,483	
Filed : August 19, 1998	Group Art Unit: 1755
For : ALUMINUM OXIDE PARTICLES	Examiner: M. Marcheschi
Docket No.: N19.12-0016	

BRIEF FOR APPELLANT

09/06/2000 YPOLITE1 00000048 09136483
01 FC:220 150.00 OP

RECEIVED
SEP -7 2000
BOARD MAIL ROOM

PATENT & TRADEMARK OFFICE
SEP 05 2000
TECHNOLOGY CENTER 1700

IN THE UNITED STATES PATENT AND TRADEMARK OFFICE
BEFORE THE BOARD OF PATENT APPEALS AND INTERFERENCES

Applicant : Kumar et al.	Appeal No.
Applic No.: 09/136,483	
Filed : August 19, 1998	Group Art Unit: 1755
For : ALUMINUM OXIDE PARTICLES	Examiner: M. Marcheschi
Docket No.: N19.12-0016	

BRIEF FOR APPELLANT

BOX AF
Assistant Commissioner for Patents
Washington, D.C. 20231

I HEREBY CERTIFY THAT THIS PAPER IS BEING SENT BY U.S. MAIL, FIRST CLASS, TO THE DIRECTOR OF PATENTS, WASHINGTON, D.C. 20231, THIS
30 DAY OF August, 2000.
Peter S. Dardi
PATENT ATTORNEY

Sir:

This is an appeal from the Final Office Action dated February 29, 2000 in which claims 1-3 and 5-22 were finally rejected.

REAL PARTY INTEREST

NanoGram Corp., a corporation organized under the laws of the state of Delaware, and having offices at 46774 Lakeview Bld., Fremont, CA, has acquired the entire right, title and interest in and to the invention, the application, and any and all patents to be obtained therefor, as set forth in the Assignment filed with the patent application and recorded on Reel 9402, frame 0196.

RECEIVED
SEP 7 2000
TECHNOLOGY CENTER 1700

RELATED APPEALS AND INTERFERENCES

There are no related appeals or interferences regarding the present appeal.

STATUS OF THE CLAIMS

Claims 1-3 and 5-22 are pending and stand rejected. Applicants appeal the final rejection of claims 1-3 and 5-22. The pending claims are presented in Appendix A below.

STATUS OF AMENDMENTS

An Amendment After Final was filed on May 1, 2000. In an Advisory Action dated May 19, 2000, the Examiner indicated that the Amendment would be entered following the filing of a Notice of Appeal and An Appeal Brief. Thus, all Amendments have been entered.

SUMMARY OF INVENTION

Applicants' invention involves novel forms of aluminum oxide particles and methods for producing aluminum oxide particles. Specifically, with respect to the aluminum oxide particles, the invention is directed to collections of submicron aluminum oxide particles. Submicron particles have an average diameter less than about 1000 nm (one micron), although the claims are limited to particles with an **average** diameter less than about 500 nm. The collections of particles have an extremely uniform particle size. This uniformity can be expressed in two ways. First, the distribution of particle sizes around the average drops off very quickly. In addition, the particle size distribution does not have a tail, such that there are no particles above a certain cut off value.

The production of highly uniform particles is enabled by the use of laser pyrolysis. These processes are the subject of claims 17 and 18. Unlike standard chemical reactions under equilibrium conditions, the light bean defines a reaction zone in which the reaction is driven to completion. See the specification, for example, at page 4, line 34 to page 5, line 2, page 6, lines 16-27 and page 12, lines 12-23. The extreme amounts of heat in the reaction zone tends to dissociate reactants within the reaction zone. The species then recombine to form the product compositions. The reaction is rapidly quenched as the particles leave the reaction zone. See page 12, lines 12-23. This quenching terminates further reaction and corresponding particle growth.

Since the reaction zone is small and well defined, the product particles are correspondingly uniform.

Pending claim 1 is directed to the uniformity of the particle collection through the cut off in the particle size distribution. In other words, the plot of particle diameters does not have a tail at large diameters. For further description of these uniform particle collections, see the specification, for example, at page 20, line 16 to page 21, line 10. Specifically, less than one particle in one million particles have a diameter more than three times the average diameter. Similarly, pending claim 19 is specifically directed to the sharp drop in the distribution of particle sizes away from the average particle size. This narrow distribution about the average is independent from the lack of a tail in the distribution, although they both relate to the overall particle size distribution. Foe example, a distribution could be narrow near its peak but have a tail at larger diameters. Applicants have produced powders with a distribution of particle sizes that is both narrow near its peak and without a tail at larger distributions. This distribution is shown in Fig. 11 of Applicants' specification.

ISSUES

Whether claims 1-3 and 5-16 are indefinite under 35 U.S.C. §112, second paragraph?

Whether claims 1-3, 5-8, and 19-22 are obvious under 35 U.S.C. §103(a) over any one of U.S. Patent 4,861,572 to Sugoh et al., U.S. Patent 4,705,762 to Ota et al., U.S. Patent 5,635,154 to Arai et al., U.S. Patent 5,417,956 to Moser and U.S. Patent 5,447,708 to Helble et al.?

Whether claims 1-3, 5-16 and 19-22 are unpatentable under 35 U.S.C. §103(a) over either U.S. Patent 5,804,513 to Sakatani et al. alone or in view of U.S. Patent 5,697,992 to Ueda et al., the Ueda patent alone, U.S. Patent 5,868,604 to Atsugi et al. alone or

in view of the Ueda patent, U.S. Patent 4,021,263 to Rosenblum alone or in view of the Ueda patent, U.S. Patent 5,228,886 to Zipperian alone or in view of the Ueda patent, U.S. Patent 5,300,130 to Rostoker alone or in view of the Ueda patent, U.S. Patent 5,389,194 to Rostoker et al. alone or in view of the Ueda patent, or U.S. Patent 5,527,423 to Neville et al. alone or in view of the Ueda patent?

Whether claims 17 and 18 are obvious under 35 U.S.C. §103(a) over U.S. Patent 5,064,517 to Shimo?

Whether claims 17 and 18 are unpatentable under 35 U.S.C. §103(a) over 1) Sugoh et al., 2) Ota et al., 3) Arai et al., 4) Moser, 5) Helble et al., 6) Sakatani et al., 7) Ueda et al., 8) Atsugi et al., 9) Rosenblum, 10) Zipperian, 11) Rostoker '130, 12) Rostoker et al. '194, or 13) Neville et al., as applied to claim 1, further in view of Shimo?

Whether the claims are obvious over the claims of copending application 08/961,735?

Whether the claims are obvious over the claims of copending application 09/433,202?

GROUPING OF CLAIMS

Claims 1-3, 5-16 form a first group of claims directed to aluminum oxide particles having essentially a cut off in the particle size distribution.

Claims 17 and 18 form a second group of claims directed to a method of producing aluminum oxide particles using light radiation.

Claims 19-22 form a third group of claims directed to aluminum oxide particles with a narrow particle size distribution.

ARGUMENT

I. Indefiniteness Under 35 U.S.C. §112, Second Paragraph

The Examiner rejected claims 1-3 and 5-16 under 35 U.S.C. §112, second paragraph as being indefinite. In particular, the Examiner objected to the reference to "the primary particles" because there was no explicit earlier reference to primary particles. Applicants have deleted "the" from the phrase. However, Applicants note that presence of primary particles is clearly inherent such that the use of the article "the" would not lead to indefiniteness. Also, the dependency of claim 18 has been corrected. Applicants respectfully request the withdrawal of the rejection of claims 1-3 and 5-16 under 35 U.S.C. §112, second paragraph.

II. Rejections Of Claims 1-3, 5-8 and 19-22 Under 35 U.S.C. §103(a) Over Single References

The Examiner rejected claims 1-3, 5-8 and 19-22 as being unpatentable over any one of U.S. Patent 4,861,572 to Sugoh et al. (the Sugoh patent), U.S. Patent 4,705,762 to Ota et al. (the Ota patent), U.S. Patent 5,635,154 to Arai et al. (the Arai patent), U.S. Patent 5,417,956 to Moser (the Moser patent) and U.S. Patent 5,447,708 to Helble et al. (the Helble '708 patent). The Examiner cited these five references for teaching particle sizes within the claimed range. Applicants respectfully request reconsideration of the rejections based on the following comments.

A) Legal Background

In phone conferences with the Examiner, Applicants inquired how the claimed feature regarding narrow particle sizes were disclosed in the cited prior art. The Examiner apparently was asserting, alternatively, that the cited prior art had distributions that overlapped with the claimed distributions or that the cited prior art inherently disclosed the claimed narrow particle size distribution. These and other relevant legal issues are presented in this section.

All claim limitations must be taught or suggested by the prior art. See MPEP 2143.03. "Obviousness cannot be predicated on

what is unknown." In re Rijckaert, 28 USPQ2d at 1957, citing In re Spormann, 150 USPQ 449, 452 (CCPA 1966).

The proposition is well established that the prior art only renders a composition of matter unpatentable to the extent that the prior art provides a means of obtaining the composition.

> To the extent that anyone may draw an inference from the Von Bramer case that the mere printed conception or the mere printed contemplation which constitutes the designation of a 'compound' is sufficient to show that such a compound is old, regardless of whether the compound is involved in a 35 U.S.C. 102 or 35 U.S.C. 103 rejection, we totally disagree. ... We think, rather, that the true test of any prior art relied upon to show or suggest that a chemical compound is old, is whether the prior art is such as to place the disclosed 'compound' in the possession of the public.

In re Brown, 141 USPQ 245, 248-49 (CCPA 1964)(emphasis in original)(citations omitted). Similarly, see In re Hoeksema, 158 USPQ 596, 600 (CCPA 1968)(emphasis in original):

> We are certain, however, that the invention as a whole is the claimed compound and a way to produce it, wherefore appellant's argument has substance. There has been no showing by the Patent Office in this record that the claimed compound can exist because there is no showing of a known or obvious way to manufacture it; hence, it seems to us that the 'invention as a whole,' which section 103 demands that we consider, is not obvious from the prior art of record.
>
> While there are valid reasons based on public policy as to why this defect in the prior art precludes a finding of obviousness under section 103, In re Brown, supra, its immediate significance in the present inquiry is that it poses yet another difference between the claimed invention and the prior art which must be considered in the context of section 103. So considered, we think the differences between appellant's invention as a whole and the prior art are such that the claimed invention would not be obvious within the contemplation of 35 U.S.C. 103.

The Federal Circuit has further emphasized these issues. "But to be prior art under section 102(b), a reference must be enabling. That is, it must put the claimed invention in the hands of one skilled in the art." In re Sun, 31 USPQ2d 1451, 1453 (Fed. Cir. 1993)(unpublished). Assertions in a prior art reference do not support an anticipation or obviousness rejection unless the references place the claimed invention in the hands of the public. Beckman Instruments Inc. v. LKB Produkter AB, 13 USPQ2d 1301, 1304 (Fed. Cir. 1989). "In order to render a claimed apparatus or method obvious, the prior art must enable one skilled in the art to make and use the apparatus or method." Id. While a reference is prior art for all that it teaches, references along with the knowledge of a person of ordinary skill in the art must be enabling to place the invention in the hands of the public. In re Paulsen, 31 USPQ2d 1671, 1675 (Fed. Cir. 1994). See also In re Donohue, 226 USPQ 619, 621 (Fed. Cir. 1985).

"To serve as an anticipation when the reference is silent about the asserted inherent characteristic, such gap in the reference may be filled with recourse to extrinsic evidence. Such evidence must make clear that the missing descriptive matter is **necessarily present** in the thing described in the reference, and that it would be so recognized by persons of ordinary skill." Continental Can Co. USA Inc. v. Monsanto Co., 20 USPQ2d 1746, 1749 (Fed. Cir. 1991). "Inherency, however may not be established by probabilities or possibilities. The mere fact that a certain thing **may** result from a given set of circumstances is not sufficient." Id., quoting Hansgirg v. Kemmer, 40 USPQ 665, 667 (CCPA 1939)(emphasis in original).

"In rejecting claims under 35 U.S.C. §103, the examiner bears the initial burden of presenting a prima facie case of obviousness. In re Rijckaert, 28 USPQ2d 1955, 1956 (Fed. Cir. 1993). "Only if that burden is met, does the burden of coming forward with evidence or argument shift to the applicant." Id.

The Examiner has noted that "a reference is good not only for what it teaches but also for what one of ordinary skill might reasonably infer from the teachings." However, "[t]o imbue one of ordinary skill in the art with knowledge of the invention in suit, when no prior art reference or references of record convey or suggest that knowledge, is to fall victim to **the insidious effect of a hindsight syndrome** wherein that which only the inventor taught is used against its teacher." W. L. Gore & Assocs., Inc. v. Garlock, Inc., 220 USPQ 303, 312-13 (Fed. Cir. 1983). **"Skill in the art does not act as a bridge over gaps in the substantive presentation of an obviousness case, but instead supplies the primary guarantee of objectivity in the process."** All-Site Corp. v. VSI International Inc., 50 USPQ2d 1161, 1171 (Fed. Cir. 1999)(emphasis added).

Claims covering a range of composition narrower than a broader range covered in the prior art are prima facie obvious over the prior art. In re Malagari, 182 USPQ 549, 553 (CCPA 1974). Similarly, claims covering ranges overlapping or touching upon ranges disclosed in the prior art are also prima facie obvious. Id. There is some support for the proposition that prior art disclosing ranges that overlap with claimed ranges anticipate the claims. Ex parte Lee, 31 USPQ2d 1105, 1107 (USPTO Bd. Pat. App. & Int. 1993)(an expanded seven member board). Applicants do not believe that these cases are relevant to claim 1 and claims depending from claim 1, as described in the following section. With respect to claims 19-22, none of the prior art described overlapping ranges, as described further below.

B) Overlapping Ranges

1) Claims 1-3 and 5-8

The Examiner has relied on case law relating to ranges specified in the claims to argue that they are prima facie obvious. See pages 4 and 7 of the Final Office Action of February 29, 2000. Applicants believe that there has been a misunderstanding regarding

the case law and the claims. Applicants will attempt to address these issues. The case law on ranges cited above, relate to claims that have a continuously adjustable parameter. For example, a composition of matter may have a range in the relative amount of a particular atom within the claimed composition. Since the parameter is continuously adjustable, generally a range must be specified to define the parameter unless it is limited to a specific value. **Each value of the parameter within the range describes a different physical embodiment of the article or method capable of being practiced.**

The present claims 1-3, 5-8 and 19-22 specify a range of **average particle size**. Specifically, independent claims 1 and 19 indicate an average particle size of about 5 nm to about 500 nm. This type of parameter is of the type described in the case law on parameter ranges. A particular embodiment of a claimed composition will have an average particles size within the claimed range. However, the claims further include a limitation on the particle size distribution. This characteristic is independent of the average particle size. Since the prior art **must** teach or suggest all of the claim limitations, the narrow particle size must be taught by the prior art for the claims to be obvious over the prior art. The fact that the average particle size is taught is irrelevant with respect to the uniformity. With respect to claim 1, **the narrow distribution specifies a characteristic of a collection of particles that is either satisfied or not satisfied by a real collection of particles. The characteristic does not include a range of characteristics or parameters.** This is in contrast with limitations including parameters that described a range of parameters. In any case, the relevant inquiry is whether or not the prior art describes embodiments or the obviousness of embodiments that fall within the claim limitations.

In particular, claim 1 specifies that "less than about one in 10^6 particles have a diameter greater than about three times

the average diameter of the collection of particles." This characteristic signifies that extreme uniformity of the powders disclosed and claimed by Applicants. Furthermore, this characteristic is a characteristic of every claimed embodiment and **does not specify a range** of cut off values of the distribution. It describes a **single** limitation on the covered powders. The cut off value for the distribution is three times the average diameter. If there are particles in a collection of power greater than this distance, the powder is not within the claimed compositions of matter. If there are no particles in the powder with a diameter of three times the average diameter then the powder is within the claimed compositions of matter. **There is no range with respect to the cut off in the diameters of the collection of particles in the powder.**

At the risk of causing confusion but for completeness, there is a range in the claim limitation quoted in the previous paragraph. The range is that there are no more than about 10^6 particles at the specified distance of three average diameters. The range is 1 in one million to zero. However, Applicants are confident that the 1 in a million range is not the range considered by the Examiner since this range was added for clarity in prosecution to replace "effectively no particles" (which has no range), and the Examiner introduced the range issue prior to the introduction of the 0 to one in one million range into the claim. See the Office Action of March 19, 1999. In addition, the Examiner has not indicated in two phone interviews that this one in one million range was a consideration.

Thus, in summary Applicants claims 1-3 and 5-8 and do not include a range in values that would implicate the issue of In re Malagari, supra, or Ex parte Lee, supra. Thus, Applicants firmly believe that the Examiner has failed to establish prima facie obviousness of claims 1-3 and 5-8.

2) Claims 19-22

Claims 19-22 include a limitation that the collection of particles has "a distribution of particle sizes such that at least about 95 percent of the particles have a diameter greater than about 40 percent of the average diameter and less than about 160 percent of the average diameter." This limitation is related to the distribution of particle sizes around the average. At the lower end of the distribution, no more than 5 percent of the particles have a diameter less than 40 percent of the average diameter. At the high end of the distribution, no more than 5 percent of the particles have a diameter greater than 160 percent of the average diameters. The range in this limitation is about 95 percent to 100 percent of the particles fall within the specified cut offs at large and small diameter values relative to the average value.

The Examiner has **NOT** asserted that the cited prior art discloses overlapping ranges in the sense of values of the distribution such that between 0 and 5 percent of the particles in the prior art have diameters less than 40 percent of the average or greater than 160 percent of the average. **The Examiner has made an unsubstantiated assertion that the particles size distribution limitation can be selected by a person of skill in the art as a selectable parameter.** The Examiner is simply using hindsight based on Applicants' claims to make bald assertions of obviousness while completely ignoring actual disclosure in the references themselves. The only support provided by the Examiner is the fact that the prior art discloses overlapping average particle sizes. But **average particle sizes is an independent parameter** relative to the distribution of particle sizes.

At page 9, of the Final Office Action of February 29, 2000, it is stated that "these references teach broad particle size ranges which overlap the instantly claimed ranges and it is well know that overlapping ranges are obvious." This statement misses the point for two reasons. First, the **ranges** relating to

obviousness must relate to a claim parameter not some characteristic of the claimed article that the Examiner arbitrarily points out. Second, a size distribution is a characteristic of a single embodiment. Parameter ranges in the case law relate to a plurality of embodiments that fall within a claim. To apply the case law, one must examine how different embodiments relate to the claim, and specific ranges within the claim scope.

In addition, to argue that a more uniform composition of matter overlaps a less uniform composition of matter is unreasonable and illogical. The fact that one composition is embedded within another does not make the more uniform composition of matter inherently old or obvious unless there is an old or obvious way of making the new composition and a motivation to form the composition. As an analogous example, a purified protein is not obvious over a native organism with the protein unless the existence of the protein was know, and there was an obvious way of purifying the protein and a motivation to purify it. Based on the Examiner's reasoning, the purified protein overlaps with the unpurified form. Furthermore with respect to uniform aluminum oxide powders, the Examiner has ignored the contrary evidence on the availability of uniform aluminum oxide particles presented in Dr. Kambe's Declaration and the Applicants' arguments presented regarding the specific cited references. Dr. Kambe's Declaration and resume, as originally filed on May 1, 2000, are attached as Appendix C. Applicants do not believe that the Examiner has established prima facie obviousness, and assuming arguendo prima facie obviousness, Applicants have rebutted these assertions.

3) Summary of Range Issues

Applicants believe that the aluminum oxide powders described and claimed in their application are unique compositions of matter that have not been disclosed publicly prior to their filing date. If these compositions of matter were not in the hands of the public prior to the filing date, Applicants believe that

they should be patentable subject matter. In view of the specific references cited by the Examiner, Applicants review below why they believe that these references do not render the present invention unpatentable. Applicants have no responsibility to establish patentability if the Examiner has not established prima facie obviousness. In spite of the fact that the Examiner has not established prima facie obviousness, Applicants have presented arguments why the cited references do not render the claimed invention obvious.

Applicants acknowledge that the cited references disclose aluminum oxide particles with overlapping **average particle sizes**. However, Applicants do not believe that the Examiner has established prima facie obviousness because the claims include additional characterization other than average particle diameter. Specifically, Applicants' claims include values corresponding to the **distribution of particle sizes around the average**. The particle size distribution is an **independent property** of the powders. Thus, two collections of powders can have the same average particle size, but a very different particle size distribution.

In response to Applicants' arguments regarding differences in particle size distributions, the Examiner responded that "the ranges defined by the references imply a variety of distributions, including the claimed one." Applicants believe that this unsubstantiated assertion is untrue. The particle size distribution is a direct consequence of the method used to produce the particles. The particle size distribution is not an arbitrary parameter that can be selected arbitrarily to meet Applicants' claim parameters. Until Applicants developed their approach for the synthesis of aluminum oxide, no approach was available for the production of aluminum oxide nanoparticles having an average particle diameter less than about 500 nm **with the narrow particle size distributions disclosed and claimed by Applicants. This**

proposition is supported by the enclosed Declaration by Dr. Nobuyuki Kambe, one of the present inventors. Dr. Kambe's Declaration and resume are attached as Appendix C.

Applicants believe that the Examiner has failed to establish prima facie obviousness based on the cited references. To the extent that the Examiner has established prima facie obvious, Applicants have rebutted the asserted obviousness by submitting Dr. Kambe's Declaration substantiating that approaches for the production of aluminum oxide particles with the claimed narrow particles size distributions were not available to a person of ordinary skill in the art prior to Applicants' invention.

C) Sugoh Patent

With respect to the Sugoh patent, the Sugoh patent describes a solution based method for the production of metal oxides. Examples 1 and 2 of the Sugoh patent relate to silica (SiO_2). The particle size growth for the silica particles is shown in Fig. 5. Table 1 includes a summary of the final particle sizes for aluminum oxide. The final particle size in the Sugoh patent for alumina is 1.2 microns, which is more than a factor of two larger than Applicants' claimed particle size. Furthermore, the Sugoh patent does not teach or suggest the claimed narrow particle size distributions claimed by Applicants.

D) Ota Patent

With respect to the Ota patent, the Ota patent discloses a flame synthesis method for producing ultra-fine powders. Flame methods are a well known approach for the production of inorganic powders. As demonstrated by the Ota patent, nanoscale powders can be produced using flame methods. However, the explosive nature of the flame process results in particles with a significant range in particle sizes. As reported in Table 1 of the Ota patent, the Al_2O_3 particles are reported to have particle sizes ranging from 10-100 nm. They do not report an average particle size, although it is presumably about 50 nm. Generally, when reporting values in this

way, the range covers a reasonable majority (perhaps covering 90-95 percent) of the particles excluding the tails of the particle distribution. These broad distributions are very different from those disclosed and claimed by Applicants. The Helble patent describes a similar flame process and provides a plot of the particle size distribution.

E) Arai Patent

With respect to the **Arai** patent, Applicants do not disagree that the Arai patent discloses the production of metal oxides. But Applicants assert that **these metal oxides do not include alumina**. The Arai patent discloses the production of iron oxide, nickel oxide and **aluminum oxyhydroxide**. See column 4, lines 31-34 and Table 1. It is ambiguous from the disclosure of the Arai patent whether **they** consider aluminum oxyhydroxide to be a metal oxide. On the other hand, it is clear from **Applicants' specification** and from conventional usage that **aluminum oxyhydroxide** is not a metal oxide, as used in the claims. Applicants have previously enclosed relevant pages from the CRC Handbook of Chemistry and Physics to indicate the distinction between aluminum oxide with a hexagonal crystal structure (Al_2O_3) and aluminum oxyhydroxide with an orthorhombic crystal structure (AlOOH). These pages are reproduced in Appendix D. The Arai patent does not claim to be able to produce aluminum oxide as claimed by Applicants since the method in the Arai patent produces aluminum oxyhydroxide rather than aluminum oxide. Thus, the Arai patent does not teach or suggest Applicants claimed invention.

With respect to the Arai patent, the portion of the patent cited by the Examiner (column 2, lines 1-15 and column 3 [column 4?], line 47) do not contradict in any way, Applicants' assertion that the Arai patent does not disclose the production of aluminum oxide. The Arai patent discloses the production of aluminum oxyhydroxide not aluminum oxide. Thus, the Arai patent cannot render Applicants' claimed invention obvious. The following

comments are also applicable to the Arai patent as well as the other cited references.

F) Moser Patent

With respect to the **Moser** patent, the Moser patent describes a solution based approach for the production of metal oxide powders. Applicants note that in Table II of the Moser patent, the chemical formula is presented for each of the species except for the aluminum species. This strongly suggests that Moser et al. were not confident that they had produced alumina (Al_2O_3). At column 6, lines 1-6, the Moser patent indicates that Transmission Electron Microscopy was used to evaluate **each** of the materials. However, no particle morphology or particle size is given for alumina. Thus, the results in the Table suggest that no nanoscale particles were formed of alumina. Even for the TiO_2 particles, Fig. 6 of the Moser patent shows large agglomerates with no distinguishable particles indicative of a particle size distribution extremely different from the distributions disclosed and claimed by Applicants. Thus, in the Moser process, the particle size distribution would clearly be much larger than the particle sizes presented in Applicants' claims. In summary, the Moser process does not inherently disclose the claimed aluminum oxide nanoparticles and does not disclose methods suitable for the production of the claimed highly uniform nanoparticles with an extremely narrow particle size distribution.

G) Helble '708 Patent

In the Helble '708 patent, the flame apparatus is designed to produce a short residence time. See, for example, the abstract. A short residence time should lead to a narrower particle size distribution. In Applicants' approach, the light beam creates a small, well defined reaction zone for particle formation. The well defined reaction zone leads to the extremely small particle size distributions. In contrast, in the Helble method, the particles have a wide range in particle sizes, as

visibly seen in their Figs. 3A and 3B. The resulting particle size distribution is plotted in Fig. 4 of the Helble patent. First, it is clearly seen that there are many particles with larger diameters greater than 100 nm. This corresponds to a large tail in the distribution. The distribution is plotted in a log scale, which dramatically constricts the spread of the distribution. If the average particle size is about 15 nm, there are many particles with a diameter greater than 4 times the average, i.e., 60 nm. Similarly, many more than 5 percent have diameter greater than 60 percent more than the average. Thus, the Helble process does not lead to the claimed materials. Similarly, the Ota process, which is similar to the Helble process, cannot lead to the claimed materials.

H. Summary

Applicants believe that they have established that none of the five cited patents above inherently disclose Applicants' claimed invention. Furthermore, none of the methods disclosed in these patents are suitable for the production of Applicants' claimed materials. Applicants respectfully request withdrawal of the rejection of claims 1-3, 5-8 and 19-22 as being unpatentable over any one of the Sugoh patent, the Ota patent, the Arai patent, the Moser patent and the Helble '708 patent.

III. Rejection Of Claims 1-3, 5-16 and 19-22 Over Single References or Alternatively Over a Combination of References

The Examiner rejected claims 1-3, 5-16 and 19-20 under 35 U.S.C. §103(a) as being unpatentable over either U.S. Patent 5,804,513 to Sakatani et al. (the Sakatani patent) alone or in view of U.S. Patent 5,697,992 to Ueda et al. (the Ueda patent), the Ueda patent alone, U.S. Patent 5,868,604 to Atsugi et al. (the Atsugi patent) alone or in view of the Ueda patent, U.S. Patent 4,021,263 to Rosenblum (the Rosenblum patent) alone or in view of the Ueda patent, U.S. Patent 5,228,886 to Zipperian (the Zipperian patent)

alone or in view of the Ueda patent, U.S. Patent 5,300,130 to Rostoker (the Rostoker '130 patent) alone or in view of the Ueda patent, U.S. Patent 5,389,194 to Rostoker et al. (the Rostoker '194 patent) alone or in view of the Ueda patent, or U.S. Patent 5,527,423 to Neville et al. (the Neville patent) alone or in view of the Ueda patent. These rejections, like the rejections above in section II, are based on the disclosure in the prior art of overlapping average particle sizes and the unsubstantiated bald assertion that the particle size distribution involves overlapping distributions. For the reasons discussed in the previous section, Applicants do not believe that the Examiner has established prima facie obviousness of claims 1-3, 5-16 and 19-20 based on the references listed at the beginning of the paragraph. The discussion in Section II above is also completely applicable here as well. However, Applicants again present arguments based on the specific references that these references do not render the claims obvious because they do not teach or suggest the narrow particle size distributions or method of generating particles with the narrow particle size distributions.

Applicants first note that the Sakatani patent, the Ueda patent, the Atsugi patent, the Rosenblum patent and the Zipperian patent do not assert that they are producing aluminum oxide by any new methods. Only the Neville patent and the Rostoker patent assert the availability of new forms of aluminum oxide. Applicants discuss the Neville patent and Rostoker patent in more detail below after briefly discussing the other patents.

The Sakatani patent discloses the use of known approaches for the production of aluminum oxides. See column 4, lines 64-67. A solution based method and a flame method are specifically mentioned. See column 5, lines 1-14. Flame methods were discussed above in Section II with respect to the Helble patent. Flame methods do not lead to the narrow particle size distributions claimed by Applicants. Equilibrium solution based methods also

lead to large particle size distributions. Specifically, the Sakatani patent discusses the hydrolysis of an aluminum alkoxide. Hydrolysis of an alkoxide is the subject of the Sugoh patent discussed above. Such a hydrolysis approach similarly does not lead to the claimed narrow particle size distributions.

The Ueda patent has the same assignee as the Sakatani patent and has overlapping disclosure. The Ueda patent does not disclose any information beyond what was disclosed in the Sakatani patent. See, for example, column 3, line 12 to column 4, line 15 and Example 1 in comparison with Example 1 of the Sakatani patent.

The Atsugi patent describes the use of commercially available aluminum oxide. See column 3, lines 4-9 and 56-65. Commercially available aluminum oxide particles certainly do not have the narrow distributions of particle sizes disclosed and claimed by Applicants. The Declaration of Dr. Kambe attests to this issue.

The Rosenblum patent and the Zipperian patent do not disclose methods or sources for their aluminum oxide. Presumably, they refer to the use of commercially available aluminum oxides. Thus, these patents are not particularly relevant to the rejections since they cannot inherently disclose the present invention since commercial materials are not available that meet the claimed particle size distributions. The extensive discussion herein and Dr. Kambe's earlier Declaration provide further support of the irrelevance of these references.

The Neville patent discloses a flame synthesis method for production of aluminum oxide particles. The Neville patent not only describes polishing with alumina particles with an average diameter less than 500 nm, but the patent also describes the production approach and particle size distribution of the secondary particles in a dispersion. The Neville patent discloses a flame synthesis approach without disclosing significant details of the process, column 6, lines 6-34. The secondary particle size

distribution for flame synthesized particles is presented in Fig. 2 of Neville. No information is presented for the primary particle sizes, although the primary particles sizes for flame synthesized particles is presented by the Helble '708 patent, as described above. However, their secondary particle size distribution is significantly narrower than the primary particle size distribution of particles produced by a flame synthesis approach described in the Helble '708 patent, for example, see figure 4 of the Helble '708 patent discussed above. Nevertheless, even the narrower secondary particle size distribution shown in Fig. 2 of the Neville patent is considerably broader than the distribution disclosed and claimed by Applicants.

Assuming for argument that the secondary particle size distribution presented in the Neville patent corresponds to the primary particle size distribution, with respect to Applicants' claim 1, the distribution in Fig. 2 of the Neville patent has a significant tail. At the tail, the distribution is dropping off about a factor of five for every 50 nm along the Y axis. Thus, the distribution would not fall off to having less than 1 per million particles until about 500 nm, more than a factor of five greater than the average diameter. Nevertheless, Applicants have previously amended claim 1 to indicate that the particle size distribution has a value of less than 1 per million particles by a diameter that is a factor of three relative to average diameter. As presently amended, Applicants' claim 1 accounts for any possible moderation of the tail in the Neville distribution at larger particle diameters. However, any error in the tail of the distribution shown in the Neville patent almost certainly would correspond to a corrected distribution with an extended tail more similar to the tail shown in the Helble '708 patent.

Thus, the Neville patent falls far short of Applicants' claimed distribution. With respect to claim 19, the Neville patent is significantly broadened at both small particle sizes and at

larger particles sizes relative to Applicants' claimed distribution. In conclusion, the Neville patent does not teach or suggest Applicants' claimed invention.

The Rostoker patent described the use of nanoparticles of Al_2O_3. The Rostoker patent discloses only one approach for obtaining nanoparticles of Al_2O_3, a process described in U.S. Patent 5,128,081 to Siegel et al. (the Siegel patent). The Siegel patent is attached in Appendix D. The Siegel patent describes the use of a gas phase condensation approach to producing the particles. This approach leads to a tail at larger particle sizes that brings the distribution outside of Applicants' claimed ranges. As evidence of this, Applicants previously filed a copy of a reference by Siegel et al., J. de Physique C5: Supplement 10 681-686 (October 1988). A copy of this article is presented in Appendix D. The inset in figure 1 shows a particle size distribution for titanium dioxide produced by the gas phase condensation approach. The discussion below figure 1 refers to the distribution as "typical of the particle-size distribution produced in the gas-condensation method."

The long tail at larger particle sizes in the distribution clearly distinguishes the materials from those claimed by Applicants. The average "grain size" is about 13 nm, and a significant fraction of the particles have a size larger than 160 percent of the average, i.e., about 21 nm. The elimination of larger particle sizes is critical for polishing applications since larger particles can scratch the surface of the material being polished.

With respect to other availability of the aluminum oxide nanoparticles with a narrower size distribution, we note that Dr. Siegel was instrumental in the formation of Nanophase Technologies Corporation (Nanophase). Nanophase was not able to scale up easily the gas-condensation approach described in the Siegel patent. Thus, a variation on the gas-condensation approach was developed,

called Physical Vapor Synthesis Approach. While this new approach is suitable for the production of commercial quantities of powders, the particle size distributions for Physical Vapor Synthesis are considerably **broader** than those obtained by the gas condensation approach. Applicants enclosed with an earlier amendment an advertisement article by Quinton Ford of Nanophase and pages down-loaded from the Nanophase web site that confirm this conclusion. These are attached in Appendix D. Therefore, the nanoscale particles needed to form the dispersions claimed by Applicants' claim were not commercially available from Nanophase.

With respect to claim 15, the gas condensation approach and the Physical Vapor Synthesis Approach both produce particle size distributions that are gaussian in character. Gaussian distributions inherently have a long extending tail. Part of this tail can be seen in the distribution in the Siegel et al. reference enclosed. Thus, these approaches will result in particles with a diameter that is five times larger than the average particle size. Therefore, the Rostoker patent does not anticipate Applicants' claim 15.

In conclusion, none of the cited references teach or suggest the narrow particle size distribution of aluminum oxide nanoparticles as disclosed and claimed by Applicants. Applicants respectfully request the withdrawal of the rejection of claims 1-16 and 19-20 under 35 U.S.C. §103(a) as being unpatentable over either the Sakatani patent alone or in view of the Ueda patent, the Ueda patent alone, the Atsugi patent alone or in view of the Ueda patent, the Rosenblum patent alone or in view of the Ueda patent, the Zipperian patent alone or in view of the Ueda patent, the Rostoker '130 patent alone or in view of the Ueda patent, the Rostoker '194 patent alone or in view of the Ueda patent, or the Neville patent alone or in view of the Ueda patent.

IV. Rejection of Claims 17-18 Over Shimo

The Examiner rejected claims 17 and 18 under 35 U.S.C. §103(a) as being unpatentable over U.S. Patent 5,064,517 to Shimo (the Shimo patent). The Examiner cited the Shimo patent for disclosing Applicants' claimed invention for the production of nanoscale aluminum oxide particles. Applicants have amended claim 17 to indicate that the reactants are flowed through the reaction chamber. In view of the amendment of claim 17 and the following comments, Applicants respectfully assert that the claims are clearly patentable over the Shimo patent.

The Shimo patent describes a process wherein gaseous reactants are placed within a reaction chamber. See, for example, column 2, lines 50-54 and column 7, lines 64-69. The reaction is initiated by irradiating the reactants with light, and the product particles are collected from the walls of the chamber. See, for example, column 8, lines 45-48 and column 9, lines 12-15. The Shimo patent does not teach or suggest reacting a **flowing** reactant stream. Thus, the Shimo patent does not disclose the first element of Applicants' claimed method, as amended. Since the reaction of a flowing reactant stream is absent from the prior art reference, the Shimo patent does not render Applicants' claims obvious. Applicants respectfully request withdrawal of the rejection of claims 17 and 18 under 35 U.S.C. §103(a) as being unpatentable over the Shimo patent.

V. Rejection of Claims 17 and 18 Over A Combination of References

The Examiner rejected claims 17 and 18 under 35 U.S.C. §103(a) as being unpatentable over either 1) the Sugoh patent, 2) the Ota patent, 3) the Arai patent, 4) the Moser patent, 5) the Helble patent, 6) the Sakatani patent, 7) the Ueda patent, 8) the Atsugi patent, 9) the Rosenblum patent, 10) the Zipperian patent, 11) the Rostoker '130 patent, 12) the Rostoker '194 patent, or 13 the Neville patent, as applied to claim 1, and further in view of

the Shimo patent. The Examiner argues that it would have been obvious to manufacture the aluminum oxide particles described by the references cited against claim 1 using the method disclosed by the Shimo patent. Applicants have amended claim 17 to indicate that the reactants are flowing when the reaction takes place. Applicants respectfully request reconsideration of the rejection of claims 17 and 18 based on the amendment of claim 17 and the following comments.

As noted above, the Shimo patent does not teach or suggest, Applicants' claimed method. Therefore, it is irrelevant whether or not the Shimo patent can be used to produce the materials disclosed in the other cited references. The cited references alone or in combination do not teach or suggest Applicants' claimed method, as amended. Therefore, the combination of references do not render claims 17 and 18 obvious. Applicants respectfully request withdrawal of the rejection of claims 17 and 18 under 35 U.S.C. §103(a) as being unpatentable over the references cited against claim 1 further in view of the Shimo patent.

VI. Double Patenting Over 08/961,735

The Examiner rejected claims 1-3, 5-16 and 19-20 under the judicially created doctrine of obviousness-type double patenting over claims 1-3, 5-9 and 11-16 of copending Application 08/961,735 (the '735 application). The claims in the '735 patent are directed to general polishing compositions incorporating nanoscale particles with very uniform particle size distributions. The claims are not directed to aluminum oxide particles.

Since the existence of highly uniform aluminum oxide particles is not obvious over the prior art, claims directed to the highly uniform particle sizes cannot and are not obvious over claims directed to general polishing compositions. The highly uniform aluminum oxide particles was first described in Applicants'

present specification. Therefore, they are not obvious over the previously filed case, let alone over the claims of the previously filed case. Applicants respectfully request withdrawal of the rejection of claims 1-3, 5-16 and 19-20 under the judicially created doctrine of obviousness-type double patenting over claims 1-3, 5-9 and 11-16 of the '735 application.

VII. Double Patenting Over 09/433,202

The Examiner in the Final Office Action suggested that a terminal disclaimer be filed over copending application 09/433,202. The Examiner did not present any arguments to support this assertion. The Examiner indicated that a double patent rejection was not made such that a final Office Action could be issued.

Applicants believe that such an approach is manifestly unfair. This was pointed out in the Amendment dated May 1, 2000. In any case, Applicants do not believe that a rejection over 09/433,202 is before them.

CONCLUSIONS AND REQUEST FOR RELIEF

Applicants submit that claims 1-3 and 5-22 are unobvious over the prior art of record. Applicants believe that the Examiner has failed to establish prima facie unpatentability of any of the claims. To the extent that the Examiner has provided a prima facie showing of unpatentability, Applicants have provided adequate evidence to establish patentability over the issues of record. Thus, Applicants respectfully request the reversal of the rejections of claims 1-3 and 5-22 and the allowance of claims 1-3 and 5-22.

Respectfully submitted,

WESTMAN, CHAMPLIN & KELLY, P.A.

By: Peter S. Dardi

Peter S. Dardi, Ph.D., Reg. No. 39,650
Suite 1600 - International Centre
900 Second Avenue South
Minneapolis, Minnesota 55402-3319
Phone: (612)334-3222 Fax: (612)334-3312

PSD:nw

OIPE
SEP 0 5 2000
PATENT & TRADEMARK OFFICE
JC119

Appendix A

WHAT IS CLAIMED IS:

1. A collection of particles comprising aluminum oxide, the collection of particles having an average diameter of primary particles from about 5 nm to about 500 nm and less than about one in 10^6 particles have a diameter greater than about three times the average diameter of the collection of particles.

2. The collection of particles of claim 1 wherein the collection of particles have an average diameter from about 5 nm to about 25 nm.

3. The collection of particles of claim 1 wherein the aluminum oxide has a crystalline structure of γ-Al_2O_3.

5. The collection of particles of claim 1 wherein the collection of particles includes less than about one in 10^6 particles with a diameter greater than about two times the average diameter.

6. The collection of particles of claim 1 wherein the collection of particles have a distribution of particle sizes such that at least about 95 percent of the particles have a diameter greater than about 40 percent of the average diameter and less than about 160 percent of the average diameter.

7. The collection of particles of claim 1 wherein the collection of particles have a distribution of particle sizes such that at least about 95 percent of the particles have a diameter greater than about 60 percent of the average diameter and less than about 140 percent of the average diameter.

RECEIVED
SEP - 7 2000
TECHNOLOGY CENTER R3700

8. The collection of particles of claim 1 wherein the collection of particles have a distribution of particle sizes such that at least about 99 percent of the particles have a diameter

greater than about 40 percent of the average diameter and less than about 160 percent of the average diameter.

9. A polishing composition comprising a dispersion of aluminum oxide particles of claim 1.

10. The polishing composition of claim 9 wherein the aluminum oxide has a crystalline structure of γ-Al_2O_3.

11. The polishing composition of claim 9 wherein the polishing composition comprises from about 0.05 percent by weight to about 15 percent by weight aluminum oxide particles.

12. The polishing composition of claim 9 wherein the polishing composition comprises from about 1.0 percent by weight to about 10 percent by weight aluminum oxide particles.

13. The polishing composition of claim 9 wherein the dispersion is an aqueous dispersion.

14. The polishing composition of claim 9 wherein the dispersion is a nonaqueous dispersion.

15. The polishing composition of claim 9 further comprising abrasive particles comprising silicon carbide, metal oxides other than aluminum oxide, metal sulfides or metal carbides.

16. The polishing composition of claim 9 further comprising colloidal silica.

17. A method for producing a collection of aluminum oxide particles having an average diameter from about 5 nm to about 500 nm, the method comprising:

flowing a molecular stream through a reaction chamber, the molecular stream comprising an aluminum precursor, an oxidizing agent, and an infrared absorber; and

pyrolyzing the flowing molecular stream in a reaction chamber, where the pyrolysis is driven by heat absorbed from a continuous wave laser beam.

18. The method of claim 17 wherein the aluminum oxide particles have an average diameter from about 5 nm to about 100 nm.

19. A collection of particles comprising aluminum oxide, the collection of particles having an average diameter from about 5 nm to about 500 nm and a distribution of particle sizes such that at least about 95 percent of the particles have a diameter greater than about 40 percent of the average diameter and less than about 160 percent of the average diameter.

20. The collection of particles of claim 19 wherein the aluminum oxide has a crystalline structure of γ-Al_2O_3.

21. The collection of particles of claim 19 wherein the collection of particles have a distribution of particle sizes such that at least about 99 percent of the particles have a diameter greater than about 40 percent of the average diameter and less than about 160 percent of the average diameter.

22. The collection of particles of claim 19 wherein the collection of particles have a distribution of particle sizes such that at least about 95 percent of the particles have a diameter greater than about 60 percent of the average diameter and less than about 140 percent of the average diameter.

Appendix C

Declaration and Resume of Dr. Nobuyuki Kambe

IN THE UNITED STATES PATENT AND TRADEMARK OFFICE

Applicant : Kumar et al.	
Applic No.: 09/136,483	
Filed : August 19, 1998	Group Art Unit: 1755
For : ALUMINUM OXIDE PARTICLES	Examiner: M. Marcheschi
Docket No.: N19.12-0016	

DECLARATION UNDER 37 C.F.R. §1.132

BOX AF
Assistant Commissioner for Patents
Washington, D.C. 20231

I HEREBY CERTIFY THAT THIS PAPER IS BEING SENT BY U.S. MAIL, FIRST CLASS, TO THE ASSISTANT COMMISSIONER FOR PATENTS, WASHINGTON, D.C. 20231, THIS
01 DAY OF May, 2000.
Peter S. Dardi
PATENT ATTORNEY

I, Nobuyuki Kambe, hereby declare as follows:

1. I am presently Vice President, Market Development at NanoGram Corporation.

2. I am a founder of NanoGram Corporation, and I have been a Vice President at NanoGram since it was founded in 1996. I have a Bachelor of Science degree and a Master of Science degree in Instrumentation Engineering from Keio University and a Ph.D. in Electrical Engineering from Massachusetts Institute of Technology in 1982.

3. Prior to my employment at NanoGram, I was Senior Managing Director with the International Center for Materials Research (ICMR), a consortium of prominent Japanese companies working jointly on the development of advanced materials. My duties at ICMR included instituting a research and development program in functional polymers and a research and a program in nanopaticles, which was the predecessor of NanoGram. Prior to working with ICMR, I held several positions with Nippon Telephone and Telegraph including Senior Research Scientist and Senior Manager.

4. I have considerable experience in advanced materials research and in particular on nanoparticles and nanomaterials. During my employment with NanoGram, I have worked closely with materials development at NanoGram, and I have also worked extensively with outside companies, consultants and academic researchers toward the development of particular markets and new areas for research related to nanoparticles.

5. I am very familiar with various approaches for producing nanoscale particles, characterization of these particles and the public availability of nanoscale particles with various properties. A successful founder of a technology driven company working in the area of nanoparticles is required to have such knowledge.

6. I am an inventor on the above referenced patent application.

7. I have read all of the references cited by the patent Examiner in the Office Action mailed on February 29, 2000. None of the particle synthesis approaches described in these references is capable of producing nanoparticles having the narrow particle size distribution of the claims pending in the present patent application. Furthermore, I am aware of no approaches that are available to separate nanoscale particles having an average particle size less than about 500 nm to produce a collection of particles with the claimed narrow particle size distribution. In addition, since the approaches described in the cited patents are not capable of producing nanoparticles with narrow particle size distributions, a person of ordinary skill in the art would not have thought, as of our filing date, that the claimed collections of particle would be obvious over the disclosure provided in these references.

8. I am aware of no methods other than the process described in our above noted patent application for producing aluminum oxide nanoparticles having an average particle size less than about 500 nm with the narrow particle size distributions specified in our

pending claims.

9. I declare that all statements made herein that are of my own knowledge are true and that all statements that are made on information and belief are believed to be true; and further that these statements were made with the knowledge that willful false statements and the like so made are punishable by fine or imprisonment, or both, under Section 1001 of Title 18 of the United States Code and that such willful false statements may jeopardize the validity of the application or any patent issued thereon.

Date: May 1, 2000 By: _____

Nobuyuki Kambe, Ph.D.

NOBUYUKI KAMBE

840 Hobart Avenue
Menlo Park, CA 94025 USA
Tel. 1-650-322-6832
E-mail kambe@nanogram.com

EDUCATION

1976 - 1982 Massachusetts Institute of Technology Cambridge, MA
Doctor of Philosophy in Electrical Engineering

- Dissertation in graphite intercalation materials and their structural behavior
- Visiting researcher at National Magnet Laboratory

1974 - 1976 Keio University Tokyo, Japan
Master of Science, Instrumentation Engineering

- Observation of novel phase transition in ultra-thin Au film over C film

1970 - 1974 Keio University Tokyo, Japan
Bachelor of Science, Instrumentation Engineering

- Percolation model over the surface of insulators

PROFESSIONAL EXPERIENCE

1996 - Present NanoGram Corporation Fremont, CA
Vice President, Market Development

- Identification, development and planning of new business opportunities for NanoGram particles

1994 - 1996 International Center for Materials Research Kawasaki, Japan
Senior Managing Director

- Creation of functional polymer R&D
- Creation of nanoparticle R&D at Lexington, KY as precursor of NanoGram

1981 - 1994 Nippon Telegraph & Telephone (NTT) Tokyo, Japan
1991 – 1994 Senior Manager at Corporate HQ

- Strategic corporate planning of new businesses for all NTT technologies
- Completion of technology management course at Japan Productivity Ctr

1989 – 1991 Senior Research Scientist and Supervisor at Basic Res. Lab.

- Nonlinear optical materials: synthesis, MBE (molecular beam epitaxy) machine build-up, nonlinear optics measurements
- NTT Basic Res. Lab. Director Award

1984 – 1989 Stuff Research Scientist

- Semiconductor superlattice laser devices: GaAs & GaSb-type, device fabrication process development
- Layered semiconductors: GaSe & InSe-type, synthesis, MBE, electron diffraction and spectroscopy, TEM
- Total renovation of high-power x-ray lab: planning and completion of 4 rotor-flex machine facility

1982 – 1989 Research Scientist

- Photosensitive materials: synthesis, optical characterization, nonlinear optical measurements

PATENTS AND PUBLICATIONS

Research interests include electronic and optical properties of low dimensional materials, graphite intercalation compounds, MBE-grown semiconductor thin films and new functional polymers and nanoparticle ceramics.

Ten (10) patents in nanomaterials.

Author of twenty publications and three books.

LANGUAGES

Japanese (mother tongue)

English (fluent)

REFERENCES

- Prof. Millie Dresselhaus, Institute Professor at MIT [617-253-6864]
- Mr. William Hecht, CEO at MIT Alumni Association [617-253-8204]
- Dr. Noriyoshi Osumi, VP at NTT America [650-903-0660]
- Dr. Rikuo Takano, Executive Director at Mitsubishi Materials [011-81-422-72-2435]
- Dr. Tatsuo Izawa, Executive Director at NTT [011-81-462-40-5000]
- Dr. Tomoaki Yamada, Fellow at NTT Basic Res. Lab. [011-81-462-40-3350]

Appendix D

Supporting Materials

1. CRC Handbook of Chemistry and Physics, Pages
2. U.S. Patent 5,320,800 to Siegel et al.
3. Siegel et al., J. de Physique C5: Supplement 10 681-686 (October 1988).
4. Quinton Ford of Nanophase
5. Pages from Nanophase Web Site

CRC Handbook of Chemistry and Physics

A Ready-Reference Book of Chemical and Physical Data

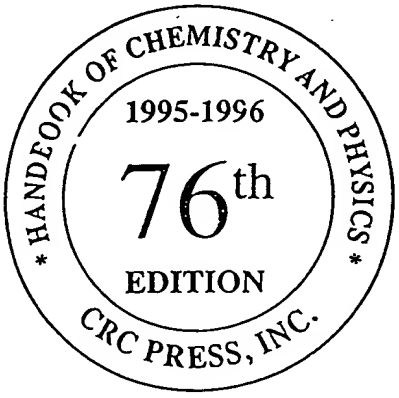

Editor-in-Chief

David R. Lide, Ph.D.

Former Director, Standard Reference Data
National Institute of Standards and Technology

Associate Editor

H. P. R. Frederikse, Ph.D.
(Retired)
Ceramics Division
National Institute of Standards and Technology

CRC Press
Boca Raton New York London Tokyo

LIST OF ABBREVIATIONS

Ac	acetyl
acc	acetone
acid	acid solutions
alk	alkaline solutions
amorp	amorphous
anh	anhydrous
aq	aqueous
blk	black
brn	brown
bz	benzene
chl	chloroform
col	colorless
conc	concentrated
cry	crystals, crystalline
cub	cubic
cyhex	cyclohexane
dec	decomposes
dil	dilute
diox	dioxane
eth	ethyl ether
EtOH	ethanol
exp	explodes, explosive
flam	flammable
gl	glass, glassy
grn	green
hc	hydrocarbon solvents
hex	hexagonal
hp	heptane
hx	hexane
hyd	hydrate
hyg	hygroscopic
i	insoluble in
liq	liquid
MeOH	methanol
mono	monoclinic
octahed	octahedral
oran	orange
orth	orthorhombic
os	organic solvents
peth	petroleum ether
pow	powder
prec	precipitate
pur	purple
py	pyridine
reac	reacts with
refrac	refractory
rhom	rhombohedral
s	soluble in
silv	silvery
sl	slightly soluble in
soln	solution
sp	sublimation point
stab	stable
subl	sublimes
temp	temperature
tetr	tetragonal
thf	tetrahydrofuran
tol	toluene
tp	triple point
trans	transition, transformation
tricl	triclinic
trig	trigonal
unstab	unstable
viol	violet
visc	viscous
vs	very soluble in
wh	white
xyl	xylene
yel	yellow

REFERENCES

1. Phillips, S.L., and Perry, D.L., *Handbook of Inorganic Compounds*, CRC Press, Boca Raton, FL, 1995.
2. Trotman-Dickenson, A.F., Executive Editor, *Comprehensive Inorganic Chemistry*, Vol. 1-5, Pergamon Press, Oxford, 1973.
3. Greenwood, N.N., and Earnshaw, A., *Chemistry of the Elements*, Pergamon Press, Oxford, 1984.
4. Budavari, S., Editor, *The Merck Index, Eleventh Edition*, Merck & Co., Rahway, NJ, 1989.
5. *GMELIN Handbook of Inorganic and Organometallic Chemistry*, Springer-Verlag, Heidelberg.
6. Chase, M.W., Davies, C.A., Downey, J.R., Frurip, D.J., McDonald, R.A., and Syverud, A.N.; *JANAF Thermochemical Tables, Third Edition, J. Phys. Chem. Ref. Data*, Vol. 14, Suppl. 1, 1985.
7. Donnay, J.D.H., and Ondik, H.M., *Crystal Data Determinative Tables, Third Edition, Volumes 2 and 4, Inorganic Compounds*, Joint Committee on Powder Diffraction Standards, Swarthmore, PA, 1973.
8. Lide, D.R., and Kehiaian, H.V., *CRC Handbook of Thermophysical and Thermochemical Data*, CRC Press, Boca Raton, FL, 1994.
9. *Kirk-Othmer Concise Encyclopedia of Chemical Technology*, Wiley-Interscience, New York, 1985.
10. *Dictionary of Inorganic Compounds*, Chapman & Hall, New York, 1992.
11. Massalski, T.B., Editor, *Binary Alloy Phase Diagrams*, American Society for Metals, Metals Park, Ohio, 1986.
12. *Landolt-Börnstein, Numerical Data and Functional Relationships in Science and Technology, Sixth Edition, III/4, Caloric Quantities of State*, Springer-Verlag, Heidelberg, 1961.
13. Deer, W.A., Howie, R.A., and Zussman, J., *An Introduction to the Rock-Forming Minerals, 2nd Edition*, Longman Scientific & Technical, Harlow, Essex, 1992.
14. Carmichael, R.S., *Practical Handbook of Physical Properties of Rocks and Minerals*, CRC Press, Boca Raton, FL, 1989.
15. Dinsdale, A.T., "SGTE Data for Pure Elements", *CALPHAD*, 15, 317-425, 1991.
16. Madelung, O., *Semiconductors: Group IV Elements and III-IV Compounds*, Springer-Verlag, Heidelberg, 1991.
17. Daubert, T.E., Danner, R.P., Sibul, H.M., and Stebbins, C.C., *Physical and Thermodynamic Properties of Pure Compounds: Data Compilation*, extant 1994 (core with 4 supplements), Taylor & Francis, Bristol, PA.

PHYSICAL CONSTANTS OF INORGANIC COMPOUNDS (continued)

No.	Name Formula	CAS RN Mol. Wt.	Physical Form	mp/°C den/g cm^{-3}	bp/°C Other Data	Solubility
39	Aluminum metaphosphate $Al(PO_3)_3$	32823-06-6 263.898	col powder; tetr	≈1525 2.78		i H_2O
40	Aluminum oxide Al_2O_3	1344-28-1 101.961	wh powder; hex	2054 3.97	≈3000 a,c,e,f	i H_2O, os; sl alk
41	Aluminum oxyhydroxide AlO(OH)	14457-84-2 59.989	ortho cry	3.44	f	i H_2O; s acid, alk
42	Aluminum palmitate $Al(C_{15}H_{31}COO)_3$	555-35-1 793.244	wh-yel powder			i H_2O, EtOH; s peth
43	Aluminum perchlorate nonahydrate $Al(ClO_4)_3·9H_2O$	14452-39-2 487.470	wh hyg cry	82 dec 2.0		
44	Aluminum phosphide AlP	20859-73-8 57.956	grn or yel cub cry	2550 2.40	a	reac H_2O
45	Aluminum selenide Al_2Se_3	1302-82-5 290.84	yel-brown powder	960 3.437		reac H_2O
46	Aluminum silicate Al_2SiO_5	12183-60-1 162.046	gray-grn cry	3.145	f	
47	Aluminum silicate dihydrate $Al_2O_3·2SiO_2·2H_2O$	1332-58-7 258.161	wh-yel powder; trid	2.59		i H_2O, acid, alk
48	Aluminum stearate $Al(C_{18}H_{35}O_2)_3$	637-12-7 877.406	wh powder	115 1.070		i H_2O, EtOH, eth; s alk
49	Aluminum sulfate $Al_2(SO_4)_3$	1004-01-3 342.154	wh cry	dec 1040		s H_2O; i EtOH
50	Aluminum sulfate octadecahydrate $Al_2(SO_4)_3·18H_2O$	7784-31-8 666.429	col monocl cry	dec 86 1.69	f	s H_2O
51	Aluminum sulfide Al_2S_3	1302-81-4 150.161	yel-gray powder	1100 2.02	a	
52	Aluminum telluride Al_2Te_3	12043-29-7 436.76	gray-blk hex cry	≈895 4.5		
53	Aluminum thiocyanate $Al(CNS)_3$	538-17-0 201.233	yel powder			s H_2O; i EtOH, eth
54	Americium Am	7440-35-9 243	silv metal; hex or cub	1176 12	2011 a,c	s acid
55	Americium(III) oxide Am_2O_3	12254-64-7 534	tan hex cry	11.77		s acid
56	Americium(III) bromide $AmBr_3$	14933-38-1 483	wh orth cry	6.85		s H_2O
57	Americium(III) chloride $AmCl_3$	13464-46-5 349	pink hex cry	500 5.87		
58	Americium(III) fluoride AmF_3	13708-80-0 300	pink hex cry	1393 9.53		
59	Americium(III) iodide AmI_3	13813-47-3 624	yel ortho cry	≈950 6.9		
60	Americium(IV) fluoride AmF_4	15947-41-8 319	tan monocl cry	7.23		
61	Americium(IV) oxide AmO_2	12005-67-3 275	blk cub cry	dec >1000 11.68		s acid
62	Ammonia NH_3	7664-41-7 17.031	col gas	-77.74 0.747 g/L	-33.33 a,b,c,d,e	vs H_2O; s EtOH, eth
63	Ammonium acetate $NH_4C_2H_3O_2$	631-61-8 77.084	wh hyg cry	114 1.073		vs H_2O
64	Ammonium azide NH_4N_3	12164-94-2 60.059	ortho cry; flam	160 1.346	exp a,e	s H_2O
65	Ammonium benzoate $NH_4C_7H_5O_2$	1863-63-4 139.154	wh cry or powder	198 1.26		s H_2O; sl EtOH
66	Ammonium bimalate $NH_4OOCCH_2CH(OH)COOH$	5972-71-4 151.119	ortho cry	160 1.15		s H_2O; sl EtOH
67	Ammonium borate tetrahydrate $(NH_4)_2B_4O_7·4H_2O$	12228-87-4 263.377	tetr cry			s H_2O; i EtOH
68	Ammonium bromide NH_4Br	12124-97-9 97.943	wh hyg tetr cry	542 dec 2.429	396 sp a,e	s H_2O, EtOH, ace; sl eth
69	Ammonium caprylate $NH_4C_8H_{15}O_2$	5972-76-9 161.245	hyg monocl cry	≈75		reac H_2O; s EtOH; i chl, bz
70	Ammonium carbamate NH_2COONH_4	1111-78-0 78.071	cry powder			vs H_2O; s EtOH
71	Ammonium carbonate $(NH_4)_2CO_3$	506-87-6 96.086	col cry powder	dec 58		
72	Ammonium cerium(III) sulfate tetrahydrate $NH_4Ce(SO_4)_2·4H_2O$	21995-38-0 422.342	monocl cry			s H_2O
73	Ammonium cerium(IV) nitrate $(NH_4)_2Ce(NO_3)_6$	16774-21-3 548.222	red-oran cry			vs H_2O
74	Ammonium chlorate NH_4ClO_3	10192-29-7 101.490	wh cry	102 exp 1.80		s H_2O
75	Ammonium chloride NH_4Cl	12125-02-9 53.492	col cub cry	520 tp (dec) 1.519	338 sp a,b,e	s H_2O
76	Ammonium chromate $(NH_4)_2CrO_4$	7788-98-9 152.071	yel cry	dec 185 1.90		s H_2O; sl ace, MeOH; i EtOH

JOURNAL DE PHYSIQUE
Colloque C5, supplément au n°10, Tome 49, octobre 1988

STRUCTURE AND PROPERTIES OF NANOPHASE TiO_2

R.W. SIEGEL, H. HAHN[1], S. RAMASAMY[2], L. ZONGQUAN[3], L. TING[4] and R. GRONSKY*

Materials Science Division, Argonne National Laboratory, Argonne, IL 60439, U.S.A.
National Center for Electron Microscopy, Lawrence Berkeley Laboratory, University of California, Berkeley, California, U.S.A.

Résumé - Echantillons de TiO_2 (rutile) nanophasé de grains ultrafins ont été synthétisés par la méthode de condensation dans un gaz, suivie ensuite par compaction en-situ, et étudiés par microscopie électronique en transmission, par microdureté de Vickers, et par spectroscopie d'annihilation positronique en fonction de température de frittage. La densité des échantillons augmente rapidement au-dessus de 500°C avec seulement une légère croissance de grains. La dureté obtenue par cette méthode, effectuée aux températures 400-600°C plus basses que la température de frittage conventionnel et sans avoir besoin des additives de frittage, est comparable on supérieure à celle des échantillons de gros grains.

Abstract - Ultrafine-grained, nanophase samples of TiO_2 (rutile) were synthesized by the gas-condensation method and subsequent in-situ compaction, and then studied by transmission electron microscopy, Vickers hardness measurements, and positron annihilation spectroscopy as a function of sintering temperature. The nanophase compacts densified rapidly above 500°C, with only a small increase in grain size. The hardness values obtained by this method are comparable to or greater than coarser-grained compacts, but at temperatures 400 to 600°C lower than conventional sintering temperatures and without the need for sintering aids.

1. INTRODUCTION

The gas-condensation method [1-3] for the production of small particles in the size range of 1 to 50 nm has recently enabled the synthesis of a new class of ultrafine-grained materials by the in-situ compaction and sintering of these particles [4]. The resulting nanophase materials, which may contain crystalline, quasicrystalline, or amorphous phases, can be metals, ceramics, or composites with rather different and improved properties than normal coarse-grained polycrystalline materials. The work so far done on these new materials and their potential for the future have been recently reviewed [5,6]. Some advantages of nanophase ceramics should be: (i) Their small particle size during synthesis should allow for increased sinterability at lower temperatures and smaller residual pore sizes owing to a combination of high driving forces and short diffusion distances, avoiding the need for sintering aids. (ii) The exceptional physical and chemical control available in the gas-condensation method lets the particle surfaces be maintained clean allowing subsequent high grain-boundary purity and thus negligible interfacial phase formation. (iii) The large fraction

---

[1] Present address: Materials Research Laboratory, University of Illinois, Urbana, Illinois USA.
[2] Permanent address: Department of Nuclear Physics, University of Madras, Madras, India.
[3] Permanent address: Institute of Solid State Physics, Academia Sinica, Hefei PRC.
[4] Permanent address: Institute of Low Energy Nuclear Physics, Beijing Normal University, Beijing PRC.

of atoms residing in interfaces, almost one-half in the case of a 5 nm grain size, may allow for new atomic arrangements and thus novel and improved ceramic properties. Such properties may include, for example, mechanical properties which might be improved through higher grain-boundary purity and the absence of brittle phases therein or small grain sizes allowing for more efficient deformation mechanisms and more effective crack dissipation.

In order to explore the feasibility of creating nanophase ceramics with such improved properties, ultrafine-grained nanophase TiO_2 (rutile) samples were synthesized in the present work by the gas-condensation method and then studied by a variety of techniques as a function of sintering temperature. The desirability of small and uniform particle size for obtaining quality ceramics has been well documented for ceramics in general [7] and for TiO_2 specifically [8,9]. Nanophase ceramics, with their high grain-boundary purity and very small and rather uniform particle size, are expected to sinter at lower temperatures than normally available ceramics with larger particle sizes, and to exhibit improved properties [6]. Consequently, for comparison with the nanophase samples, coarser-grained samples were also synthesized from commercial powders and similar measurements were carried out.

2. EXPERIMENTAL PROCEDURE

The ultra-high vacuum chamber used for the preparation of nanophase TiO_2 by the gas-condensation method has been described elsewhere [6]. Titanium (99.7% pure) was evaporated from a resistance-heated tungsten boat at temperatures between 1550°C and 1650°C into a 0.3-0.7 kPa helium atmosphere over a period of 15 to 30 min. The small Ti particles formed by condensation in the He-gas were deposited on the cold-finger of the production chamber, and subsequently oxidized by the introduction of about 2 kPa of oxygen into the chamber. The particles were then compacted at 1.4 GPa at room temperature, resulting in a TiO_2 nanophase compact of 9 mm diameter by about 0.2 mm thick with a mean grain diameter of 12 nm.

For comparison with the nanophase TiO_2, samples were also synthesized from commercial TiO_2 powder, which was ball-milled using NiO balls to an average grain size of 1.3 μm, with a maximum grain size of 2.5 μm. Three samples were made from this commercial powder. The first was compacted at 1.4 GPa at room temperature without any sintering aid, as a direct comparison with the nanophase sample, while the second was compacted at the same pressure, but using a 5% aqueous solution of polyvinyl alcohol (pva) as a sintering aid. The third sample was compacted at 0.1 GPa with the same pva solution, this method being essentially the conventional one for the preparation of such a ceramic. The densities of the green pellets ranged from 55 to 70% of theoretical density.

Grain-size distributions were determined in the nanophase samples by transmission electron microscopy (TEM), and in the coarser-grained samples by scanning electron microscopy (SEM). Vickers microhardness was measured at room temperature, using a load of 15 g and an indentation time of 25 s, on the as-compacted samples and after sintering successively for one-half hour at temperatures up to 1400°C. Complementary positron annihilation spectroscopy (PAS) lifetime and Doppler-broadening measurements were also made in order to monitor sample porosity as a function of sintering up to 900°C. In addition, high-resolution electron microscopy (HREM) observations of grain and grain-boundary structures were also carried out on selected nanophase samples using the Atomic Resolution Microscope at the National Center for Electron Microscopy, LBL. An operating voltage of 1 MeV was chosen to provide better penetration of some of the thicker particles while retaining resolution at the 0.16 nm level. No attempt was made to orient the individual particles under the electron beam; instead, the samples were scanned for large thin areas and imaged in through-focus series bracketing the minimum contrast [10] condition.

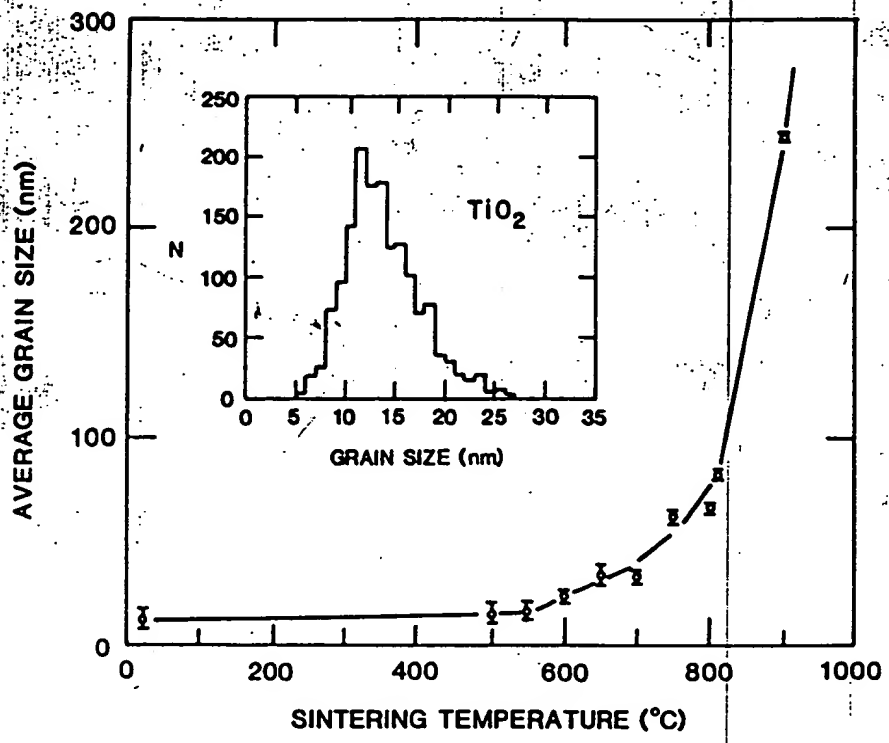

Figure 1. Average grain size of nanophase TiO_2 (rutile) as a function of sintering temperature determined by TEM. The sintering anneals were one-half hour in duration at each successive temperature. The grain-size distribution for the as-compacted sample is shown in the inset.

3. RESULTS AND DISCUSSION

The results of the grain-size determinations using TEM on the nanophase TiO_2 as a function of sintering temperature are presented in Figure 1. It can be seen that the grain-size distribution for the as-compacted sample is rather narrow and typical of the particle-size distribution produced in the gas-condensation method [2]. The distribution appears to remain unchanged by the Ti oxidation and subsequent compaction processes. It can also be readily seen that the average grain size increases very little up to about 550°C, and only rather slowly with sintering temperature up to about 800°C, at which temperature grain growth becomes fairly rapid. A similar grain-size stability against temperature has been found for nanocrystalline iron with an initial average grain size of 6 nm [11].

Figure 2 shows a high-resolution electron micrograph from a rather typical region of the nanophase TiO_2 sample sintered for one-half hour at 500°C. The grains here are seen to be essentially equiaxed with relatively planar boundaries. The grain boundaries in the as-compacted sample, on the other hand, appeared to be significantly less planar than this, but detailed atomic structural studies of these nanophase boundaries have not yet been completed. The lattice fringes seen in Figure 2 are those representative of the atomic planes of rutile, as confirmed by both electron and X-ray diffraction patterns on all of these samples.

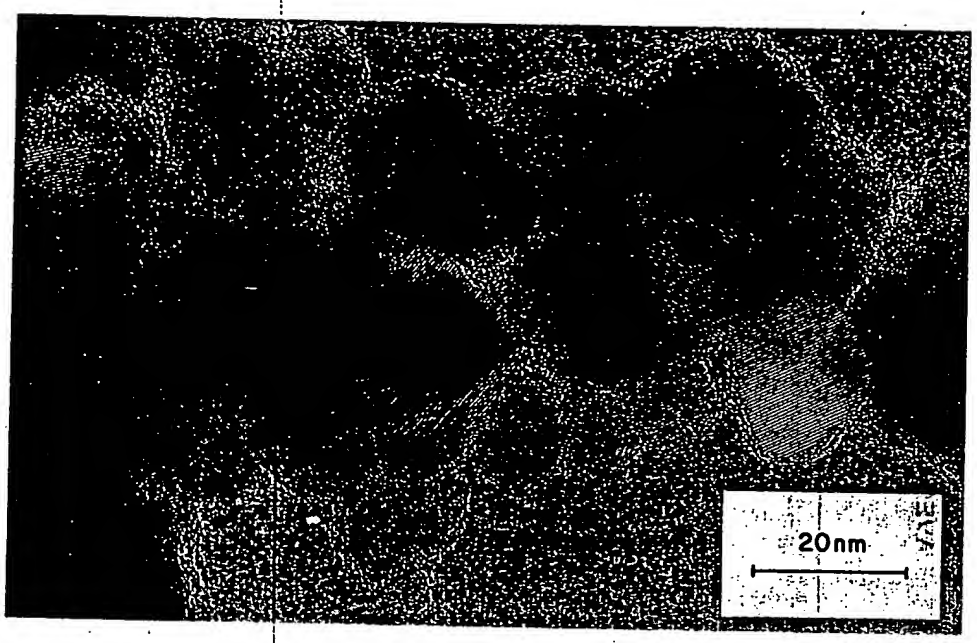

Figure 2. High-resolution transmission electron micrograph of nanophase TiO_2 (rutile) after sintering for one-half hour at 500°C. The sample was prepared for TEM observation by fracturing the sintered compact, which gave rise to the open areas seen in the micrograph.

The Vickers microhardness measured at room temperature is shown in Figure 3 as a function of sintering temperature for three different TiO_2 (rutile) samples, the nanophase sample with 12 nm initial average grain size compacted at 1.4 GPa, and two samples with 1.3 μm initial average grain size compacted at 1.4 GPa and 0.1 GPa. The latter sample, prepared essentially in accord with standard ceramic processing methods, was the only one of these three which was sintered with the aid of pva. The results for a fourth sample prepared in a similar manner with pva, but compacted at 1.4 GPa, are not shown in Figure 3; they are very similar to those for the 1.3 μm, 0.1 GPa sample, but shifted to lower temperatures by about 150°C. It can be readily seen from these microhardness measurements that the nanophase TiO_2 sinters at considerably lower (between 400 and 600°C) temperatures than the commercial 1.3 μm powder with the aid of pva, yielding comparable or greater microhardness values. For reference, the Vickers microhardness of a single crystal of TiO_2 measured under identical conditions is 1036 ± 66 kgf/mm^2. Preliminary fracture toughness studies on these samples, made by measuring the crack lengths emanating from microindentations at higher loads, appear to confirm the similar or better mechanical properties of the nanophase TiO_2 in comparison with the coarser-grained material and single-crystal TiO_2 (rutile) as well. Without the aid of pva, the commercial powders are seen to sinter rather poorly and exhibit inferior mechanical properties, as expected.

Although it seems apparent from the microhardness measurements that densification of the nanophase sample was taking place upon sintering above 500°C, PAS measurements were also carried out in order to monitor this densification more directly. The results, which will be published elsewhere by the present authors in a more complete account of this study of nanophase TiO_2, show in their simple two-state behavior that both the 12 nm, 1.4 GPa nanophase sample and the 1.3 μm, 1.4 GPa commercial-powder sample (see Figure 3) began densifying rapidly above 500°C, but that the nanophase sample did so more rapidly with increasing

temperat
density
which a
indicate
grained

The resu
compacts,
densify
hardness
of single
to 600°C
sintering
of nanoph
results o
nanophase

VICKERS MICROHARDNESS (kgf/mm^2) 160 120 80 400 0

Figure 3.
temperature
temperatures
grain size
grained comp
(diamonds) a
commercial p

temperature than the coarser-grained sample, resulting in a smaller void or pore density at 900°C. As might have been expected, the PAS lifetime measurements, which are also sensitive to varying pore sizes when they are small, clearly indicate smaller pore sizes in the nanophase sample relative to the coarser-grained sample at all the sintering temperatures investigated by PAS.

The results of these first investigations on nanophase TiO_2 indicate that these compacts, although already rather well bonded on compaction at room temperature, densify rapidly above 500°C, with only a small increase in grain size. The hardness values obtained by this method are comparable to or greater than those of single-crystal TiO_2 or coarser-grained compacts, but at temperatures some 400 to 600°C lower than conventional sintering temperatures and without the need for sintering aids. Much work still needs to be done regarding the characterization of nanophase ceramics and the elucidation of their full potential. However, the results of this first study appear to hold considerable promise for the future of nanophase ceramics.

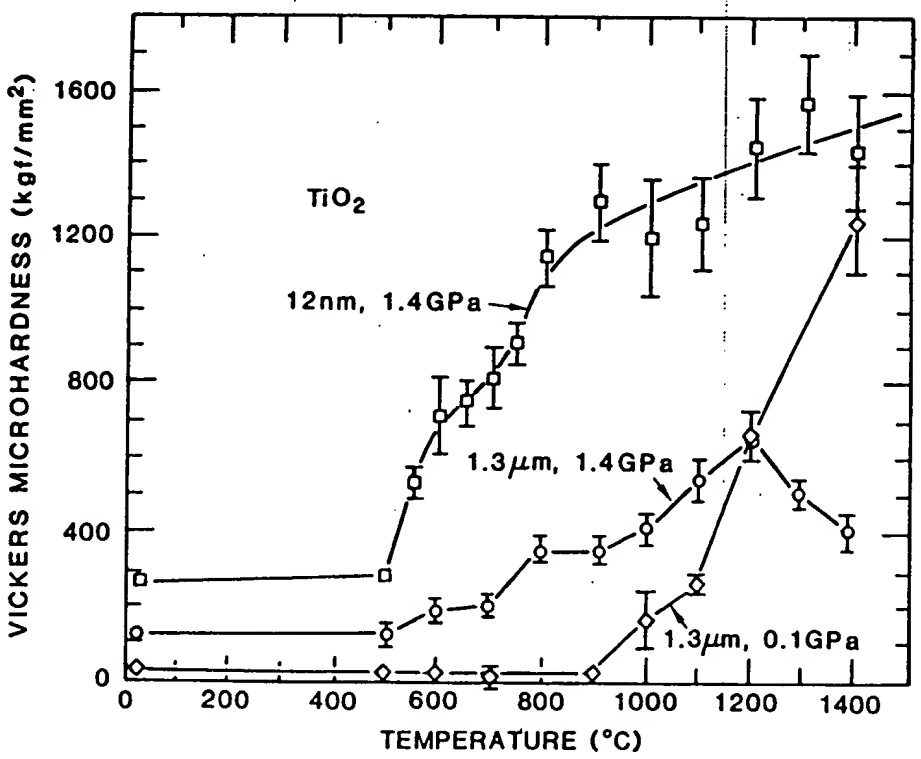

Figure 3. Vickers microhardness in kgf/mm^2 of TiO_2 (rutile) measured at room temperature as a function of one-half hour sintering at successively increased temperatures. Results for a nanophase sample (squares) with an initial average grain size of 12 nm compacted at 1.4 GPa are compared with those for coarser-grained compacts with 1.3 μm initial average grain size sintered at 0.1 GPa with (diamonds) and at 1.4 GPa without (circles) the aid of polyvinyl alcohol from commercial powder.

ACKNOWLEDGEMENT

This work was supported by the U. S. Department of Energy, BES-Materials Sciences, under Contracts W-31-109-Eng-38 at ANL and DE-AC03- 76SF00098 at LBL.

REFERENCES

[1] K. Kimoto, Y. Kamiya, M. Nonoyama, and R. Uyeda, Jap. J. Appl. Phys. 2, 702 (1963).

[2] C. G. Granqvist and R. A. Buhrman, J. Appl. Phys. 47, 2200 (1976).

[3] A. R. Thölén, Acta Metall. 27, 1765 (1979).

[4] H. Gleiter, in **Deformation of Polycrystals: Mechanisms and Microstructures**, N. Hansen et al., eds., Risø National Laboratory, Roskilde (1981) p.15; see also these Proceedings.

[5] R. Birringer, U. Herr, and H. Gleiter, Trans. Jap. Inst. Met. 27, Suppl., 43 (1986).

[6] R. W. Siegel and H. Hahn, in **Current Trends in the Physics of Materials**, M. Yussouff, ed., World Scientific Publ. Co., Singapore (1987) p. 403.

[7] H. K. Bowen, Mater. Sci. Eng. 44, 1 (1980).

[8] E. A. Barringer and H. K. Bowen, J. Amer. Ceram. Soc. 65, C-199 (1982).

[9] B. Fegley, Jr., E. A. Barringer, and H. K. Bowen, J. Amer. Ceram. Soc. 67, C-113 (1984).

[10] R. Gronsky, in **Treatise on Materials Science and Technology Series: Experimental Techniques**, Vol. 19 B, H. Herman, ed., Academic Press, New York (1983) p. 225.

[11] E. Hort, Diploma Thesis, Universität des Saarlandes, Saarbrücken (1986).

Manufacturing Nanocrystalline Materials by Physical Vapor Synthesis

By Quinton Ford, Director of Marketing, Industrial Products, Nanophase Technologies Corp., Burr Ridge, Ill.

A CONTINUOUS PROCESS BASED ON GAS-PHASE CONDENSATION CAN PRODUCE NANOCRYSTALLINE PARTICLES IN ECONOMICAL QUANTITIES.

During the past decade, a great deal of research and development has been focused on fabricating and characterizing nanocrystalline materials. Within the industry, nanocrystalline materials are commonly defined as crystalline materials that have an average particle or grain size of less than 100 nanometers (0.1 micron). A deliberate distinction is made between nanocrystalline materials and submicron crystalline materials, which have an average particle or grain size of less than 1 micron.

The relative percentage of interfacial atoms to total atoms in a material increases dramatically with decreasing size below 100 nanometers (see Figure 1). The resultant properties of nanocrystalline materials thus have a much greater dependence on the contributions of interfacial atoms (those atoms on the surface of a particle or in the grain boundaries of a consolidated material) than submicron materials. Some unconventional mechanical, chemical, electrical, optical and magnetic properties exhibited by nanocrystalline materials are attributed to this greater dependence on the contributions of interfacial atoms.

PROCESSING METHODS

A wide range of techniques have been developed to fabricate nanocrystalline materials. The most commonly practiced of these are gas-phase condensation, sol-gel chemistry, spray pyrolysis and hydrothermal processing. The challenge with all techniques is to successfully scale production to commercial volumes of nanocrystalline materials with properties and economies that allow their use in mainstream applications. One of the first techniques to be so scaled, physical vapor synthesis, is based on the principles of gas-phase condensation.

In the 1980s, gas-phase condensation was demonstrated to be capable of fabricating a wide range of ceramic and metallic nanocrystalline particles. Gas-phase condensation involves the evaporation of precursor materials in reduced-pressure, inert environments. After evacuating a chamber, inert gas is introduced to create the reduced-pressure environment. The precursor material is then evaporated using any of a variety of energy sources.

Atoms of evaporated precursor collide with the cooler atoms of the inert backfill gas. These cooler gas atoms cause the evaporated precursor to condense and solidify as nanocrystalline particles of the precursor. If reactive gas is used for backfill instead of inert gas, the evaporated precursor and gas react, condense and solidify as nanocrystalline particles of the formed compound.

The cooling of the gas is caused by convective currents that are created within the chamber by the temperature gradient between the energy source and a

Figure 1

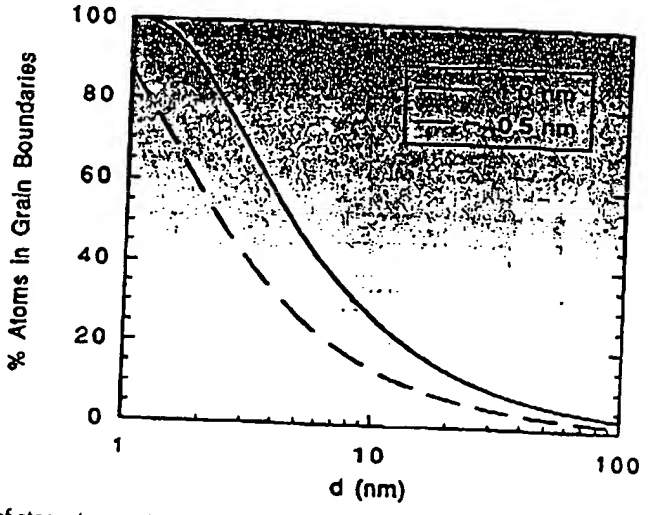

Percentage of atoms in grain boundaries of nanocrystalline material as a function of average grain size assuming grain boundary thickness range of 0.5 to 1 nanometer. (From R.W. Siegel, "Cluster-Assembled Nanophase Materials", *Annu. Rev. Mater. Sci.* 21, 559-578, 1991)

Figure 2

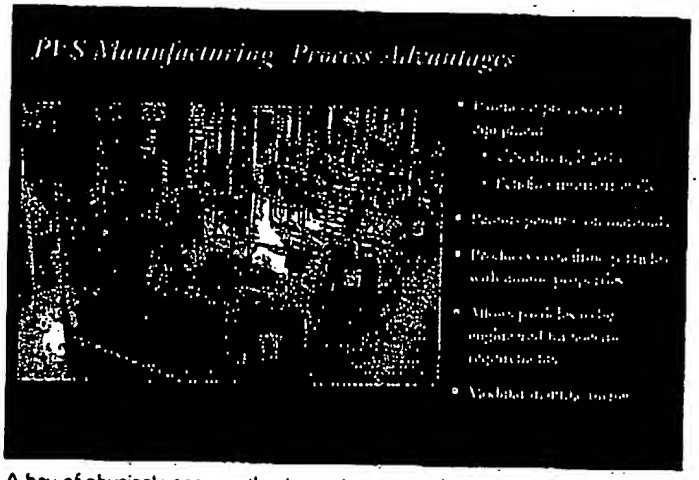

A bay of physical vapor synthesis production machines is readied.

Figure 3

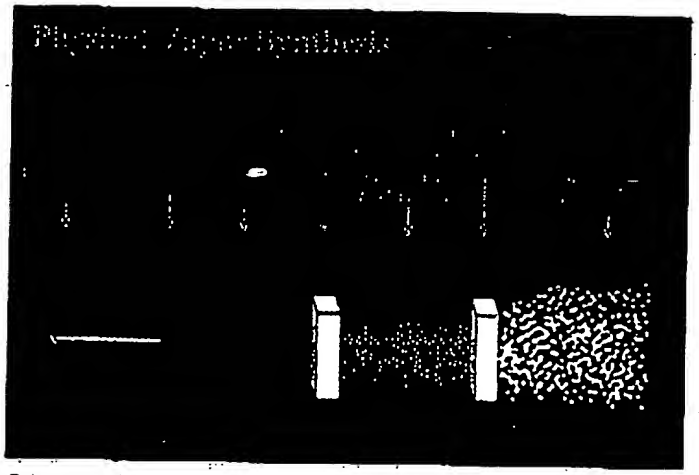

Schematic of the physical vapor synthesis technique.

Using Physical Vapor Synthesis Materials in Polishing Slurries

One commercial application of physical vapor synthesis materials is as an abrasive component for polishing slurries used in the production of semiconductors. Current trends in semiconductor design include decreasing line widths and increasing numbers of metal and dielectric layers. These design trends present significant issues during photolithography steps unless the layers to be imaged are planar across the entire wafer. A process referred to as chemical mechanical planarization (CMP) is gaining widespread acceptance within the industry to polish the sputtered metal and dielectric layers on the semiconductor wafers to a highly planar state.

Aluminum oxide produced by physical vapor synthesis is incorporated into slurry for planarizing tungsten metal layers. The slurry is prepared by introducing the aluminum oxide powder to water, adding mechanical energy to break down agglomerates, and extracting particles comprising the upper end of the particle size distribution. Oxidizing chemicals are later blended with the abrasive slurry just prior to use.

Slurry containing aluminum oxide produced by physical vapor synthesis has been evaluated as superior to other slurries in defectivity and microscratching of tungsten surfaces. The concurrent removal rates and uniformities are comparable to those of other slurries. Consequently, cost of ownership can be lowered by the overall performance of slurry containing physical vapor synthesis aluminum oxide.

Cerium oxide produced by physical vapor synthesis is currently being evaluated as an additive to slurries for planarization of dielectric layers. Such slurries generally contain silica as the sole abrasive component. Initial tests indicate that adding a small percentage of cerium oxide to silica-based slurries can increase removal rates to four times the rates of slurries containing no cerium oxide. No concurrent degradation of defectivity, microscratching or uniformity have been detected.

cooled collection surface. These convective currents carry the nanocrystalline particles to the collection surface, where they are later harvested. The collection surface is typically the outer surface of a metal tube through which liquid nitrogen is passed.

IMPROVING OUTPUT

Nanocrystalline particles produced via gas-phase condensation are equiaxed, nonporous, free of residual surface chemicals, and have a narrow particle size distribution. However, the reduced-pressure conditions and dependence on natural convection limit the technique to a low-rate batch process. Practically-sized systems can produce only tens of grams of nanocrystalline materials per day, resulting in economies that are not feasible for most applications.

In the early 1990s, scientists at Nanophase Technologies developed a patented technique based on the principles of gas-phase condensation. This technique produces particles with similar attributes to those produced through gas-phase condensation, while eliminating the need for reduced-pressure conditions and the dependence on natural convection. The technique, named physical vapor synthesis, operates as a continuous process and at significantly increased rates compared to gas phase condensation.

A single physical vapor synthesis production machine is capable of delivering tens of kilograms of nanocrystalline materials per day. This provides economies that are feasible for a large

Figure 4

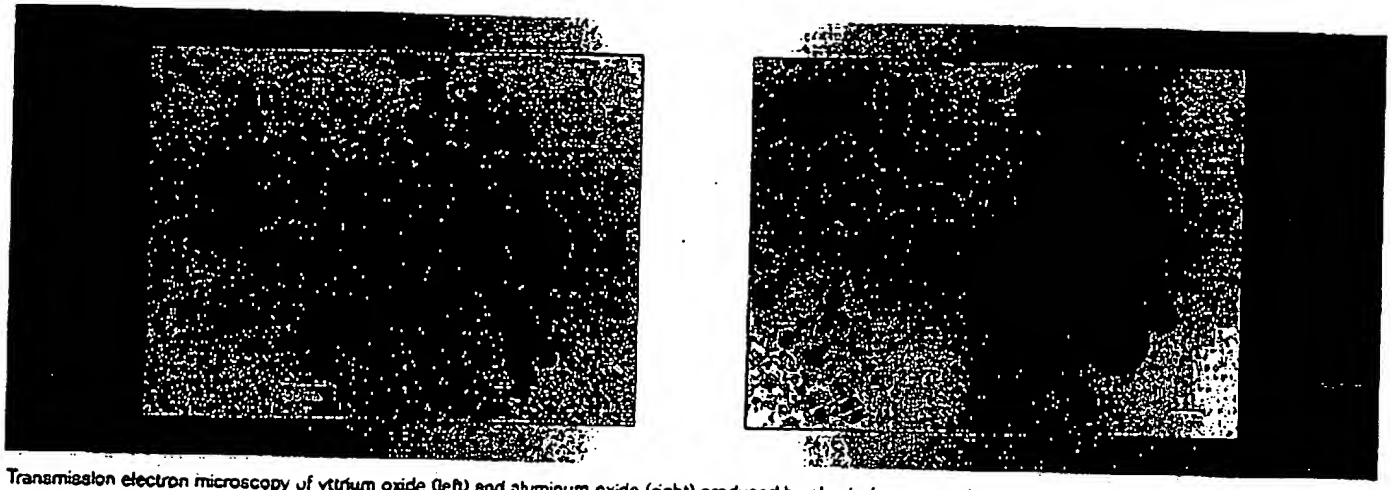

Transmission electron microscopy of yttrium oxide (left) and aluminum oxide (right) produced by physical vapor synthesis.

number of applications. The technique has already been successfully scaled to a production capacity exceeding 100 tons per year, and additional capacity can be added in a modular fashion as needed (see Figure 2).

COOLING REQUIRED

In physical vapor synthesis (Figure 3), precursor material is introduced at a controlled rate into a chamber. Within the chamber, a plasma arc is formed between a nonconsumable electrode and the consumable precursor. The precursor, typically a high-purity metal rod, passes through the plasma arc and is melted and vaporized.

A quench and/or reactive gas is introduced to the chamber. Atoms of evaporated precursor collide with the cooler atoms of the quench gas. The evaporated precursor condenses and solidifies as nanocrystalline particles of the precursor. If a reactive gas is also present, it reacts with the evaporated precursor, causing nanocrystalline particles of the resultant compound to be formed upon condensation and solidification.

After the nanocrystalline particles are solidified, their temperature is still elevated. The particles must be cooled to minimize agglomeration. Additional gas is turbulently introduced to accelerate cooling of the particles. The gas propels the particles into a collector housing. The collector housing contains filter media that allows the gas to exit but traps the weakly agglomerated nanocrystalline particles. The nanocrystalline particles collect on the filter media in the collector housing and are periodically harvested.

Advantages of Physical Vapor Synthesis

- Economical
- Narrow particle size distribution
- Continuous process
- Particle size control
- Nonporous, equiaxed particles
- High-purity materials
- Wide range of oxides

PRODUCT CHARACTERISTICS

Numerous nanocrystalline oxides and noble metals have been successfully fabricated using physical vapor synthesis. These include aluminum oxide, titanium dioxide, zinc oxide, iron oxide, cerium oxide, yttrium oxide, copper oxide, magnesium oxide, manganese oxide, indium-tin oxide, palladium, silver, gold and platinum.

Non-noble metals are also of commercial interest in nanocrystalline form. However, in this size regime, the surfaces of these particles are highly reactive and will oxidize when exposed to air. In the case of some metals, this oxidation causes violent combustion. Several methods to stabilize particles are under development and are expected to allow eventual commercialization of these metals. Additionally, fabrication of such materials as nanocrystalline carbides and nitrides will be attempted with modifications to the current physical vapor synthesis practices.

A metastable phase of a material generally results from physical vapor synthesis due to the high process temperatures and rapid solidification. Particle morphologies vary with material, although they are commonly equiaxed. Aluminum oxide particles produced appear perfectly spherical when imaged by SEM or TEM (see Figure 4).

PARTICLE SIZE CONTROL

Physical vapor synthesis provides sufficient control to allow concurrent adjustment of the specific surface area and the average particle size of production materials. Specific surface areas can be varied from approximately 30 to 90 m^2/g as desired. This corresponds to average particle sizes ranging from approximately 10 to 100 nanometers. Based on close correlation between average particle sizes measured from TEM images and calculated from BET specific surface areas, physical vapor synthesis particles are virtually nonporous.

More important than the average particle size in most applications is the particle size distribution, specifically the upper end of the distribution. Physical vapor synthesis materials have lognormal distributions, with one endpoint at a few nanometers and another between 300 and 500 nanometers (see Figure 5). Less than 1% of the particles are above 150 nanometers.

Figure 5

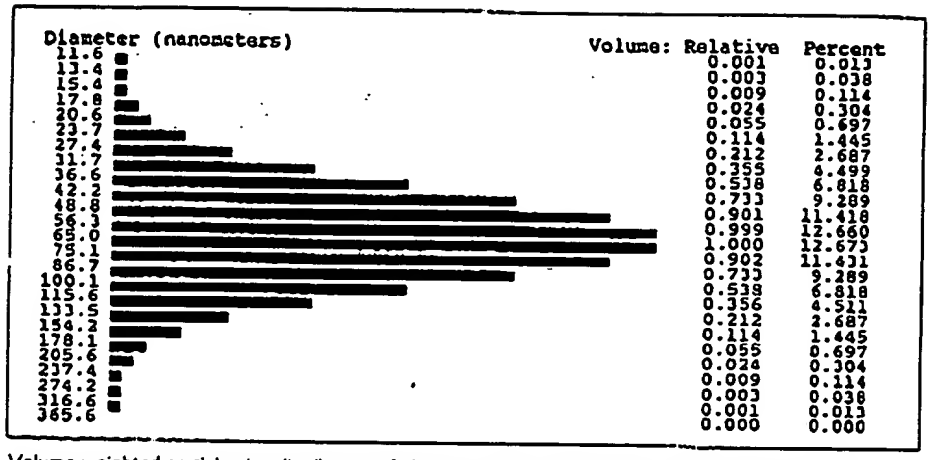

Volume-weighted particle size distribution of aluminum oxide produced by physical vapor synthesis.

When the particles are collected from physical vapor synthesis, they are weakly agglomerated up to tens of microns. The agglomerates can be broken down to the particle size distributions described above by such techniques as ultrasonication and media milling. Further refinement of these particle size distributions is also possible, eliminating particles above a specific size.

The overall purity of physical vapor synthesis nanocrystalline particles approximates the purity of the precursor material. Consequently, precursors commensurate with the overall purity requirements of the application are used. Specific impurities of concern for a given application can be engineered to desired levels.

APPLICATIONS

Applications for oxide particles produced by physical vapor synthesis have already been commercialized and include abrasives in polishing slurries for semiconductors, anti-fungal agents for health care and additives to increase the wear resistance of polymers. Additional applications for oxide and noble metal particles are also being developed. These include transparent conductive coatings, precious metal catalysts and additives to provide various functionalities to polymers. ❑

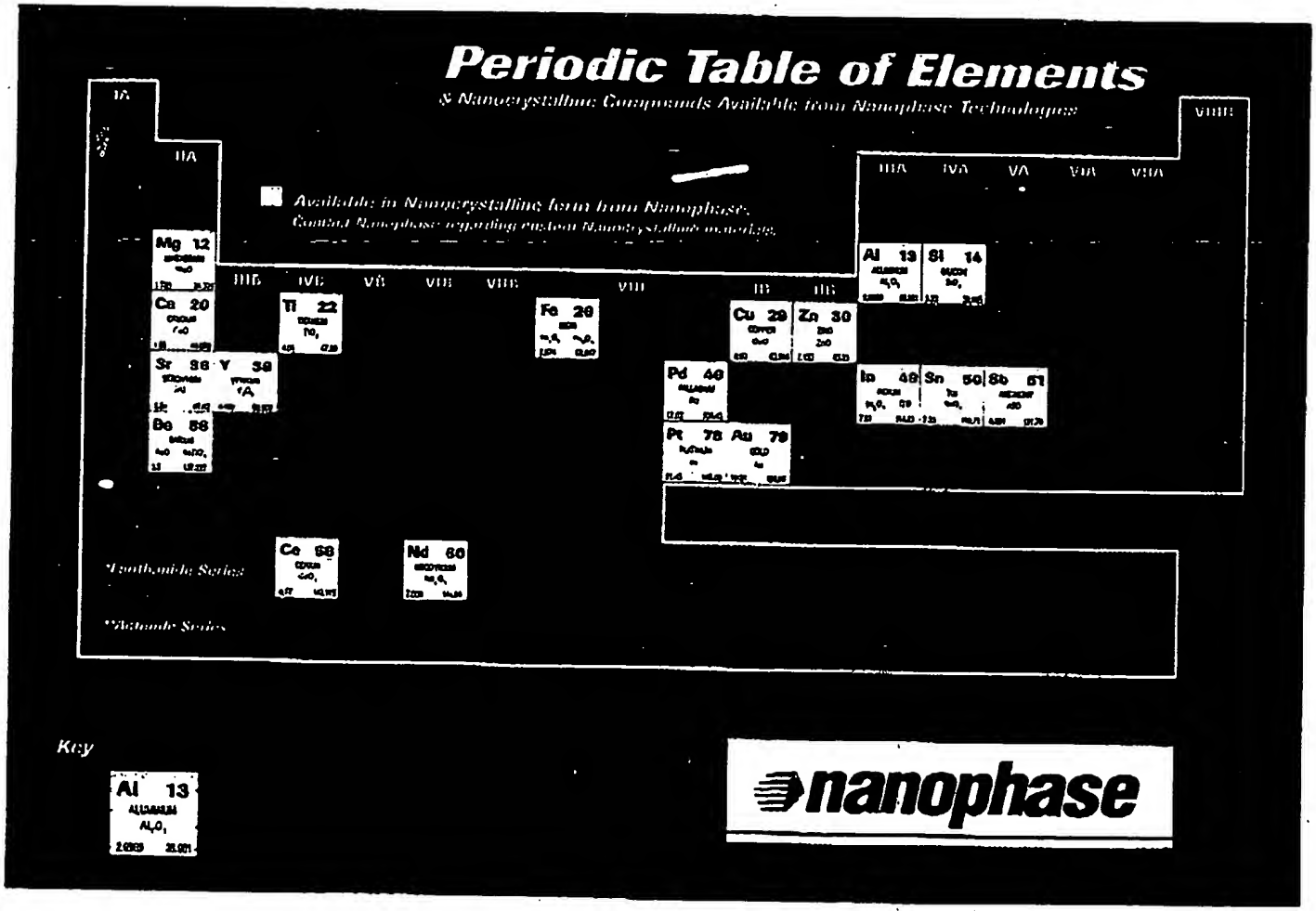

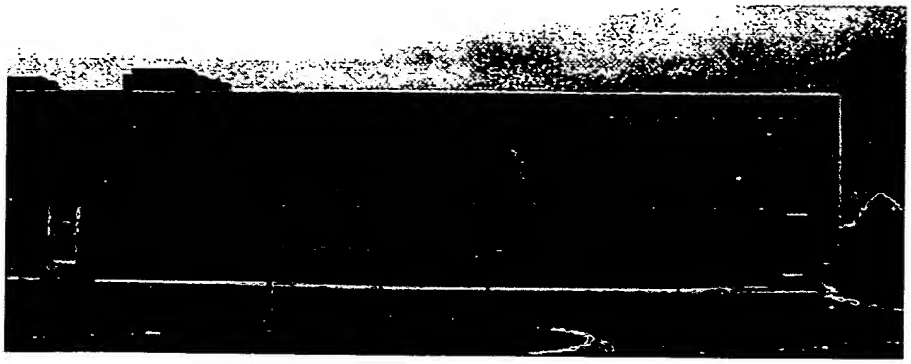

Nanophase Technologies Corporation is the world's leader in the development, production, and marketing of *nanocrystalline* materials for a wide range of industrial applications.

This web site is designed to provide information on our company, our technologies, our products, and applications for our *nanocrystalline* materials . We hope that you will visit this site often.

Corporate History

The origin of Nanophase can be traced back to research performed during the 1980s at Argonne National Laboratory, a U.S. Department of Energy facility. Interested in studying the properties of *nanocrystalline* materials, researchers at Argonne conceived a unique process to fabricate them. This process, commonly referred to today as *gas phase condensation*, could produce small quantities of materials with unique characteristics. Besides their sizes being measured in *nanometers*, the particles were of high purity, had no residual surface contaminants, were spherical, and were *non-porous*.

Convinced that these materials were commercially important and that *gas phase condensation* could be scaled to produce them in large quantities at reasonable cost, Argonne scientist Dr. Richard Siegel founded Nanophase in 1989. At that time, *gas phase condensation* could produce only a few grams of *nanocrystalline* material per day at a cost of approximately $1,000 per gram.

Several years of effort by scientists at Nanophase resulted in the development of a new process based generally on the principles of *gas phase condensation*, but with significantly improved fabrication rates and economies. This process, named Physical Vapor Synthesis (PVS) now allows Nanophase to produce tons of materials per year with costs as low as a few pennies per gram. PVS is patented and was recognized with an R&D 100 Award in 1995 as one of the year's most technologically significant new developments.

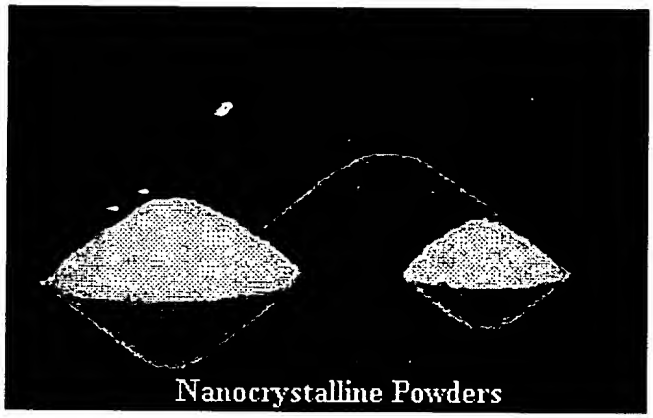

Nanocrystalline Powders

NanoTek® Aluminum Oxide

Product Code: 0100

Molecular Formula	Al_2O_3
Purity	99.5+%
Average Particle Size	27 - 56 nm (from SSA)
Specific Surface Area	30 - 60 m^2/g (BET)
Morphology	Spherical
Crystal Phase	Gamma
Distribution	2 - ~400 nm (by laser scattering, Horiba LA-910)
Refractive Index	1.7
Appearance	White to off white powder
Bulk Density	0.10 g/cc
True Density	3.6 g/cc

Pricing

Unit Size	Price
25g	$19.00
50g	$27.00
100g	$39.00
250g	$64.00
500g	$85.00
1kg	$135.00
2kg	$200.00
>2kg	Quote

Physical Vapor Synthesis (PVS)

Nanophase primarily employs its patented Physical Vapor Synthesis (PVS) process to produce *nanocrystalline* particles. PVS utilizes a plasma to heat a selected metal *precursor* in open atmosphere. As the temperature rises, the metal's atoms boil off into a stream of flowing gas, creating a *vapor*.

Collisions with atoms of a gas that is introduced to the process cool the metal atoms so that the *vapor condenses* into liquid molecular clusters. Cooling continues, freezing these molecular clusters into solid particles of *nanometric* size. The flowing gas transports the particles to a collection vessel. The presence of oxygen allows oxygen atoms to intermingle with metal atoms forming *nanocrystalline metal oxides* such as aluminum oxide and titanium dioxide.

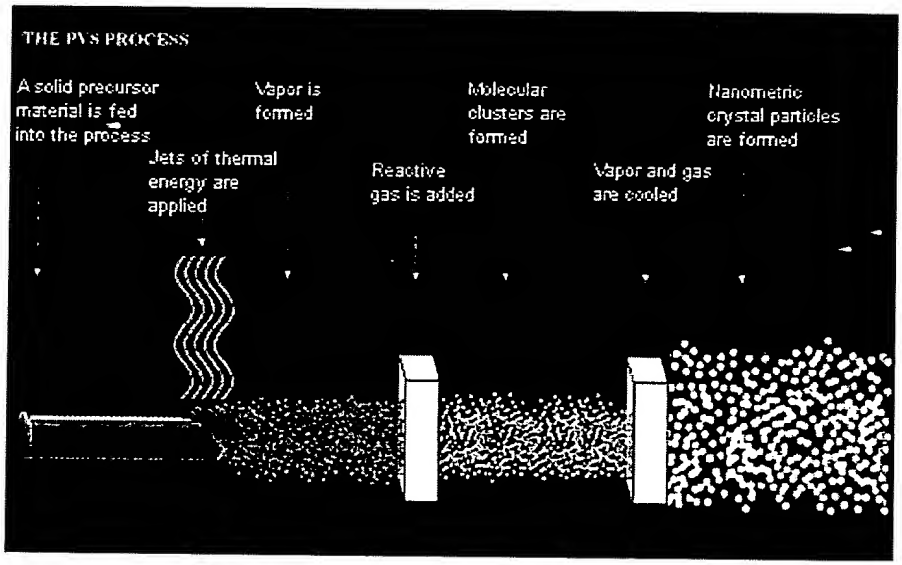

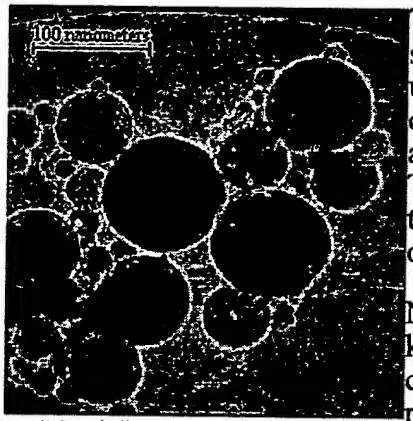

TEM of NanoTek Aluminum Oxide produced using PVS

The resultant powder consists of weakly *agglomerated* particles of spherical *morphology*. Purity of the powders is primarily dependent upon the purity of the *precursor* material. There are no residual chlorides or sulfides present on the surfaces of the particles as there are with materials produced by certain other combustion techniques. The clean nature of these surfaces enable treatments to be applied to tailor these materials for applications requiring *dispersion* in a variety of fluids.

Nanophase developed PVS from the general principles of a process known as *gas phase condensation*. *Gas phase condensation* is conducted under high vacuum conditions which limit it to producing research scale quantities of nanocrystalline materials. It typically employs a resistive heat source to generate a gas phase of the *precursor* material. Cooling of this gas phase to cause condensation and freezing to form nanocrystalline particles is accomplished using a liquid-nitrogen cooled collection surface. The materials produced by *gas phase condensation* are similar in *morphology*, purity, and size to those produced via PVS.

Gas phase condensation is practiced by many research scientists around the world as a means of fabricating materials for their experiments. Nanophase's patented PVS process is the only known method by which commercial quantities of these materials can be produced.

Appendix D

Supporting Materials

1. CRC Handbook of Chemistry and Physics, Pages
2. U.S. Patent 5,320,800 to Siegel et al.
3. Siegel et al., J. de Physique C5: Supplement 10 681-686 (October 1988).
4. Quinton Ford of Nanophase
5. Pages from Nanophase Web Site

CRC Handbook of Chemistry and Physics

A Ready-Reference Book of Chemical and Physical Data

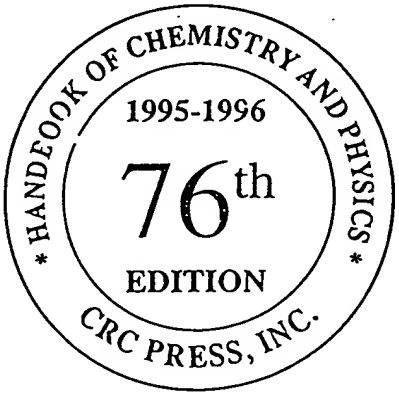

Editor-in-Chief

David R. Lide, Ph.D.

Former Director, Standard Reference Data
National Institute of Standards and Technology

Associate Editor

H. P. R. Frederikse, Ph.D.
(Retired)
Ceramics Division
National Institute of Standards and Technology

CRC Press
Boca Raton New York London Tokyo

LIST OF ABBREVIATIONS

Ac	acetyl
ace	acetone
acid	acid solutions
alk	alkaline solutions
amorp	amorphous
anh	anhydrous
aq	aqueous
blk	black
brn	brown
bz	benzene
chl	chloroform
col	colorless
conc	concentrated
cry	crystals, crystalline
cub	cubic
cyhex	cyclohexane
dec	decomposes
dil	dilute
diox	dioxane
eth	ethyl ether
EtOH	ethanol
exp	explodes, explosive
flam	flammable
gl	glass, glassy
grn	green
hc	hydrocarbon solvents
hex	hexagonal
hp	heptane
hx	hexane
hyd	hydrate
hyg	hygroscopic
i	insoluble in
liq	liquid
MeOH	methanol
mono	monoclinic
octahed	octahedral
oran	orange
orth	orthorhombic
os	organic solvents
peth	petroleum ether
pow	powder
prec	precipitate
pur	purple
py	pyridine
reac	reacts with
refrac	refractory
rhom	rhombohedral
s	soluble in
silv	silvery
sl	slightly soluble in
soln	solution
sp	sublimation point
stab	stable
subl	sublimes
temp	temperature
tetr	tetragonal
thf	tetrahydrofuran
tol	toluene
tp	triple point
trans	transition, transformation
tricl	triclinic
trig	trigonal
unstab	unstable
viol	violet
visc	viscous
vs	very soluble in
wh	white
xyl	xylene
yel	yellow

REFERENCES

1. Phillips, S.L., and Perry, D.L., *Handbook of Inorganic Compounds*, CRC Press, Boca Raton, FL, 1995.
2. Trotman-Dickenson, A.F., Executive Editor, *Comprehensive Inorganic Chemistry*, Vol. 1-5, Pergamon Press, Oxford, 1973.
3. Greenwood, N.N., and Earnshaw, A., *Chemistry of the Elements*, Pergamon Press, Oxford, 1984.
4. Budavari, S., Editor, *The Merck Index, Eleventh Edition*, Merck & Co., Rahway, NJ, 1989.
5. *GMELIN Handbook of Inorganic and Organometallic Chemistry*, Springer-Verlag, Heidelberg.
6. Chase, M.W., Davies, C.A., Downey, J.R., Frurip, D.J., McDonald, R.A., and Syverud, A.N.; *JANAF Thermochemical Tables, Third Edition*, *J. Phys. Chem. Ref. Data*, Vol. 14, Suppl. 1, 1985.
7. Donnay, J.D.H., and Ondik, H.M., *Crystal Data Determinative Tables, Third Edition, Volumes 2 and 4, Inorganic Compounds*, Joint Committee on Powder Diffraction Standards, Swarthmore, PA, 1973.
8. Lide, D.R., and Kehiaian, H.V., *CRC Handbook of Thermophysical and Thermochemical Data*, CRC Press, Boca Raton, FL, 1994.
9. *Kirk-Othmer Concise Encyclopedia of Chemical Technology*, Wiley-Interscience, New York, 1985.
10. *Dictionary of Inorganic Compounds*, Chapman & Hall, New York, 1992.
11. Massalski, T.B., Editor, *Binary Alloy Phase Diagrams*, American Society for Metals, Metals Park, Ohio, 1986.
12. *Landolt-Börnstein, Numerical Data and Functional Relationships in Science and Technology, Sixth Edition, II/4, Caloric Quantities of State*, Springer-Verlag, Heidelberg, 1961.
13. Deer, W.A., Howie, R.A., and Zussman, J., *An Introduction to the Rock-Forming Minerals, 2nd Edition*, Longman Scientific & Technical, Harlow, Essex, 1992.
14. Carmichael, R.S., *Practical Handbook of Physical Properties of Rocks and Minerals*, CRC Press, Boca Raton, FL, 1989.
15. Dinsdale, A.T., "SGTE Data for Pure Elements", *CALPHAD*, 15, 317-425, 1991.
16. Madelung, O., *Semiconductors: Group IV Elements and III-IV Compounds*, Springer-Verlag, Heidelberg, 1991.
17. Daubert, T.E., Danner, R.P.; Sibul, H.M., and Stebbins, C.C., *Physical and Thermodynamic Properties of Pure Compounds: Data Compilation*, extant 1994 (core with 4 supplements), Taylor & Francis, Bristol, PA.

PHYSICAL CONSTANTS OF INORGANIC COMPOUNDS (continued)

No.	Name Formula	CAS RN Mol. Wt.	Physical Form	mp/°C den/g cm^{-3}	bp/°C Other Data	Solubility
39	Aluminum metaphosphate $Al(PO_3)_3$	32823-06-6 263.898	col powder; tetr	≈1525 2.78		i H_2O
40	Aluminum oxide Al_2O_3	1344-28-1 101.961	wh powder; hex	2054 3.97	≈3000 a,c,e,f	i H_2O, os; sl alk
41	Aluminum oxyhydroxide AlO(OH)	14457-84-2 59.989	ortho cry	3.44	f	i H_2O; s acid, alk
42	Aluminum palmitate $Al(C_{15}H_{31}COO)_3$	555-35-1 793.244	wh-yel powder			i H_2O, EtOH; s peth
43	Aluminum perchlorate nonahydrate $Al(ClO_4)_3·9H_2O$	14452-39-2 487.470	wh hyg cry	82 dec 2.0		
44	Aluminum phosphide AlP	20859-73-8 57.956	grn or yel cub cry	2550 2.40	a	reac H_2O
45	Aluminum selenide Al_2Se_3	1302-82-5 290.84	yel-brown powder	960 3.437		reac H_2O
46	Aluminum silicate Al_2SiO_5	12183-80-1 162.046	gray-grn cry	3.145	f	
47	Aluminum silicate dihydrate $Al_2O_3·2SiO_2·2H_2O$	1332-58-7 258.161	wh-yel powder; tricl	2.59		i H_2O, acid, alk
48	Aluminum stearate $Al(C_{18}H_{35}O_2)_3$	637-12-7 877.406	wh powder	115 1.070		i H_2O, EtOH, eth; s alk
49	Aluminum sulfate $Al_2(SO_4)_3$	1004-01-3 342.154	wh cry	dec 1040		s H_2O; i EtOH
50	Aluminum sulfate octadecahydrate $Al_2(SO_4)_3·18H_2O$	7784-31-8 666.429	col monocl cry	dec 86 1.69	f	s H_2O
51	Aluminum sulfide Al_2S_3	1302-81-4 150.161	yel-gray powder	1100 2.02	a	
52	Aluminum telluride Al_2Te_3	12043-29-7 436.76	gray-blk hex cry	≈895 4.5		
53	Aluminum thiocyanate $Al(CNS)_3$	538-17-0 201.233	yel powder			s H_2O; i EtOH, eth
54	Americium Am	7440-35-9 243	silv metal; hex or cub	1176 12	2011 a,c	s acid
55	Americium(III) oxide Am_2O_3	12254-64-7 534	tan hex cry	11.77		s acid
56	Americium(III) bromide $AmBr_3$	14933-38-1 483	wh orth cry	6.85		s H_2O
57	Americium(III) chloride $AmCl_3$	13464-46-5 349	pink hex cry	500 5.87		
58	Americium(III) fluoride AmF_3	13708-80-0 300	pink hex cry	1393 9.53		
59	Americium(III) iodide AmI_3	13813-47-3 624	yel ortho cry	≈950 6.9		
60	Americium(IV) fluoride AmF_4	15947-41-8 319	tan monocl cry	7.23		
61	Americium(IV) oxide AmO_2	12005-67-3 275	blk cub cry	dec >1000 11.68		s acid
62	Ammonia NH_3	7664-41-7 17.031	col gas	-77.74 0.747 g/L	-33.33 a,b,c,d,e	vs H_2O; s EtOH, eth
63	Ammonium acetate $NH_4C_2H_3O_2$	631-61-8 77.084	wh hyg cry	114 1.073		vs H_2O
64	Ammonium azide NH_4N_3	12164-94-2 60.059	ortho cry; flam	160 1.346	exp a,e	s H_2O
65	Ammonium benzoate $NH_4C_7H_5O_2$	1863-63-4 139.154	wh cry or powder	198 1.26		s H_2O; sl EtOH
66	Ammonium bimalate $NH_4OOCCH_2CH(OH)COOH$	5972-71-4 151.119	ortho cry	160 1.15		s H_2O; sl EtOH
67	Ammonium borate tetrahydrate $(NH_4)_2B_4O_7·4H_2O$	12228-87-4 263.377	tetr cry			s H_2O; i EtOH
68	Ammonium bromide NH_4Br	12124-97-9 97.943	wh hyg tetr cry	542 dec 2.429	396 sp a,e	s H_2O, EtOH, ace; sl eth
69	Ammonium caprylate $NH_4C_8H_{15}O_2$	5972-76-9 161.245	hyg monocl cry	≈75		reac H_2O; s EtOH; i chl, bz
70	Ammonium carbamate NH_2COONH_4	1111-78-0 78.071	cry powder			vs H_2O; s EtOH
71	Ammonium carbonate $(NH_4)_2CO_3$	506-87-6 96.086	col cry powder	dec 58		
72	Ammonium cerium(III) sulfate tetrahydrate $NH_4Ce(SO_4)_2·4H_2O$	21995-38-0 422.342	monocl cry			s H_2O
73	Ammonium cerium(IV) nitrate $(NH_4)_2Ce(NO_3)_6$	16774-21-3 548.222	red-oran cry			vs H_2O
74	Ammonium chlorate NH_4ClO_3	10192-29-7 101.490	wh cry	102 exp 1.80		s H_2O
75	Ammonium chloride NH_4Cl	12125-02-9 53.492	col cub cry	520 tp (dec) 1.519	338 sp a,b,e	s H_2O
76	Ammonium chromate $(NH_4)_2CrO_4$	7788-98-9 152.071	yel cry	dec 185 1.90		s H_2O; sl ace, MeOH; i EtOH

US005320800A

United States Patent [19]

Siegel et al.

[11] Patent Number: 5,320,800

[45] Date of Patent: Jun. 14, 1994

[54] NANOCRYSTALLINE CERAMIC MATERIALS

[75] Inventors: Richard W. Siegel, Hinsdale; G. William Nieman; Julia R. Weertman, both of Evanston, all of Ill.

[73] Assignees: ARCH Development Corporation, Chicago; Northwestern University, Evanston, both of Ill.

[21] Appl. No.: 86,387

[22] Filed: Jun. 30, 1993

Related U.S. Application Data

[63] Continuation of Ser. No. 622,244, Dec. 4, 1990, abandoned, and a continuation-in-part of Ser. No. 466,585, Dec. 5, 1989, Pat. No. 5,128,081.

[51] Int. Cl.[5] B22F 3/02

[52] U.S. Cl. 419/66; 148/514

[58] Field of Search 419/23, 66, 6, 19; 148/514; 75/245, 247; 428/547

[56] References Cited

U.S. PATENT DOCUMENTS

4,389,250	6/1983	Melton et al.	75/232
4,594,104	6/1986	Keybould	75/243
4,596,746	6/1986	Morishita et al.	428/458
4,654,229	3/1987	Morita et al.	427/180
4,683,118	7/1987	Hayashi et al.	419/23
4,909,840	3/1990	Schlump	75/232
5,049,355	9/1991	Gennari et al.	420/425

Primary Examiner—Behrend E. Harvey
Assistant Examiner—Ngoclan T. Mai
Attorney, Agent, or Firm—Reinhart, Boerner, Van Deuren, Norris & Rieselbach

[57] ABSTRACT

A method for preparing a treated nanocrystalline metallic material. The method of preparation includes providing a starting nanocrystalline metallic material with a grain size less than about 35 nm, compacting the starting nanocrystalline metallic material in an inert atmosphere and annealing the compacted metallic material at a temperature less than about one-half the melting point of the metallic material.

3 Claims, 9 Drawing Sheets

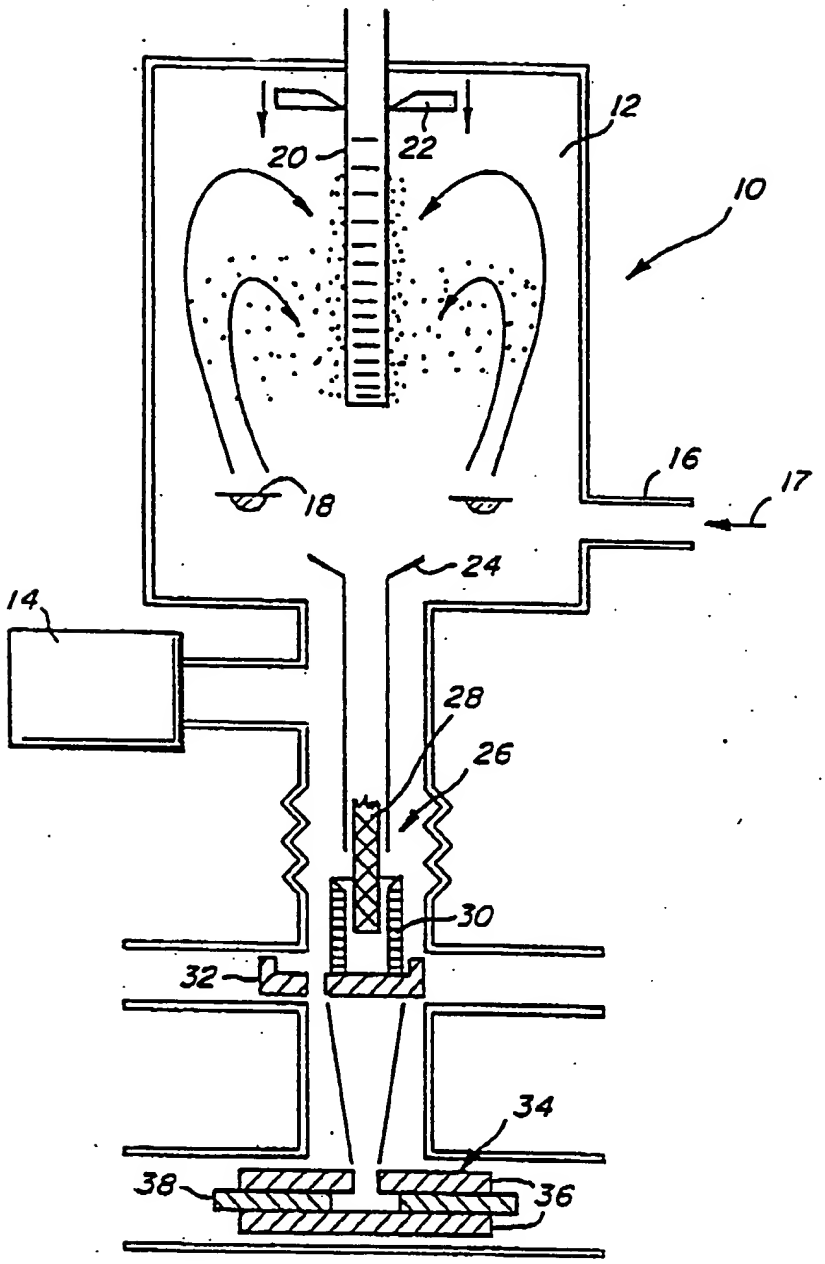

FIG. 1

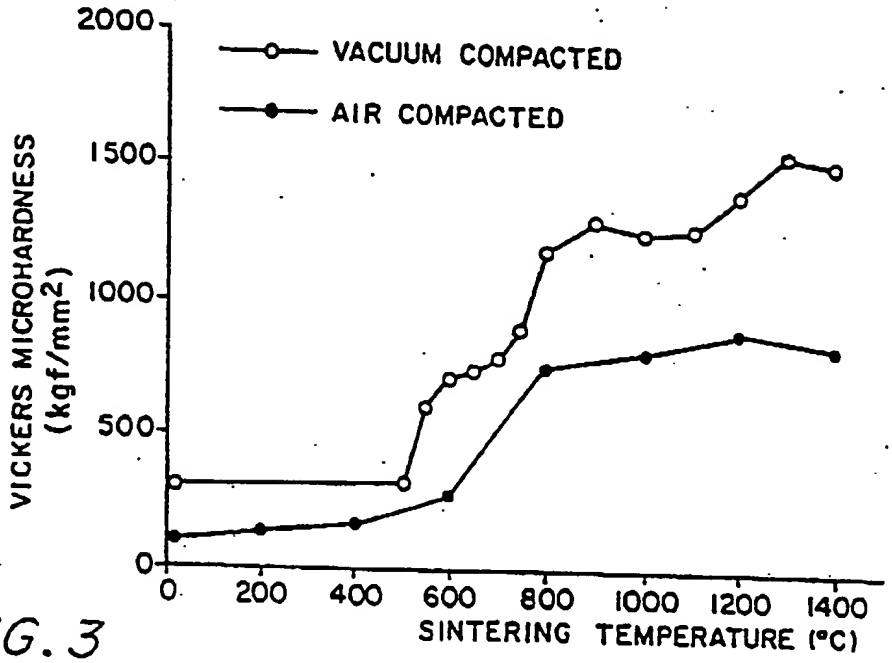
2000
1500
1000
500
0
VACUUM COMPACTED
AIR COMPACTED
VICKERS MICROHARDNESS (kgf/mm2)
0
200
400
600
800
1000
1200
1400
SINTERING TEMPERATURE (°C)

FIG. 3

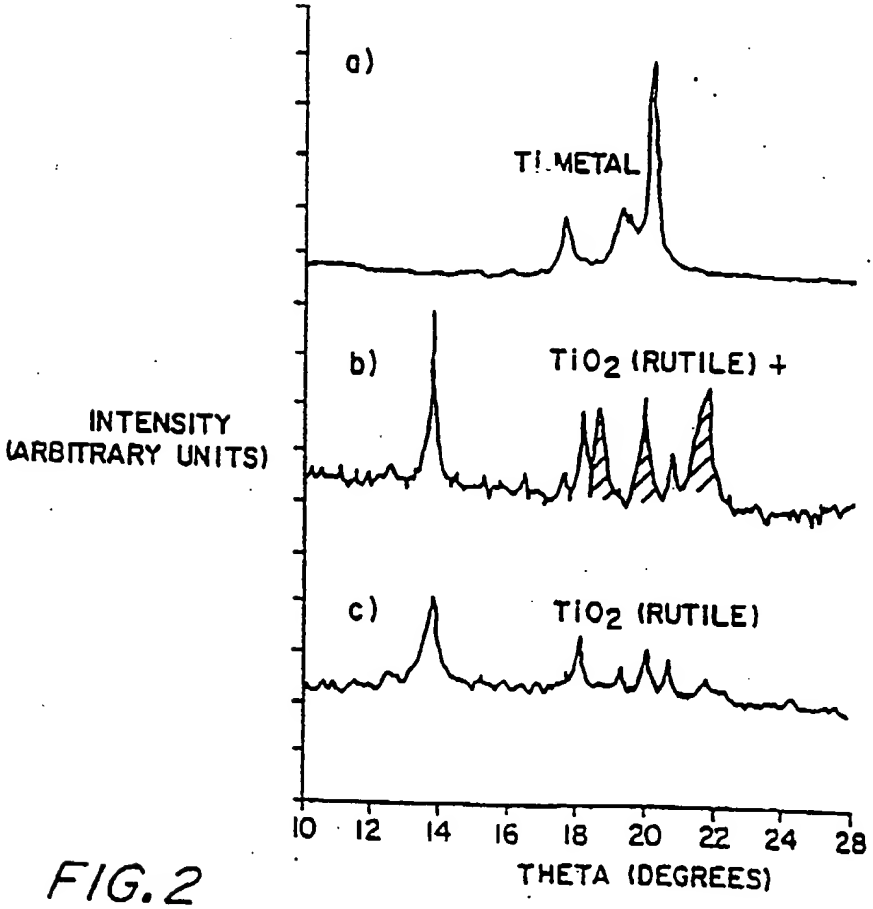
a)
Ti METAL
b)
TiO2 (RUTILE) +
c)
TiO2 (RUTILE)
INTENSITY (ARBITRARY UNITS)
10
12
14
16
18
20
22
24
28
THETA (DEGREES)

FIG. 2

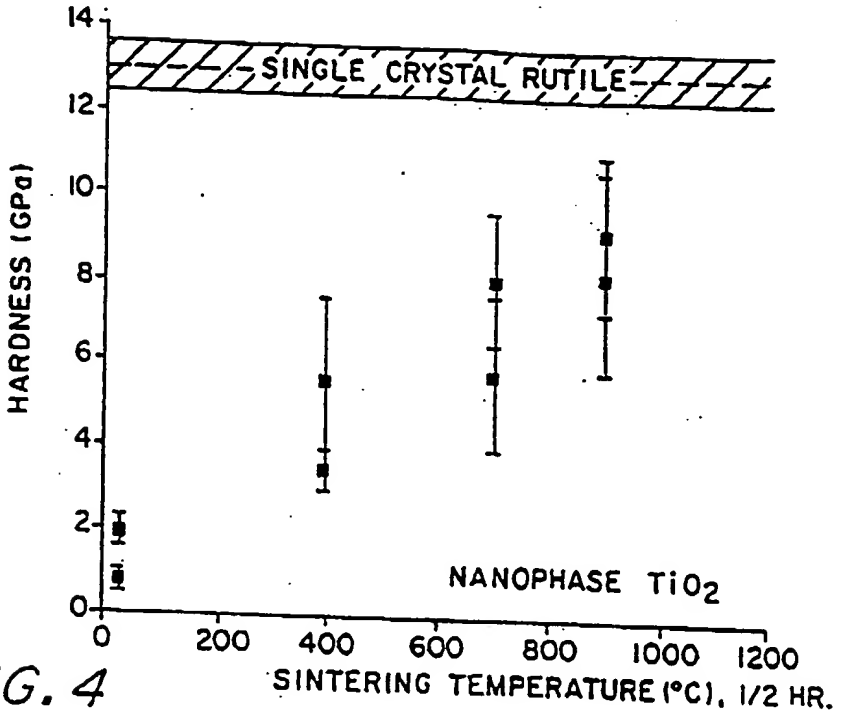
SINGLE CRYSTAL RUTILE
HARDNESS (GPa)
NANOPHASE TiO_2
SINTERING TEMPERATURE (°C), 1/2 HR.

FIG. 4

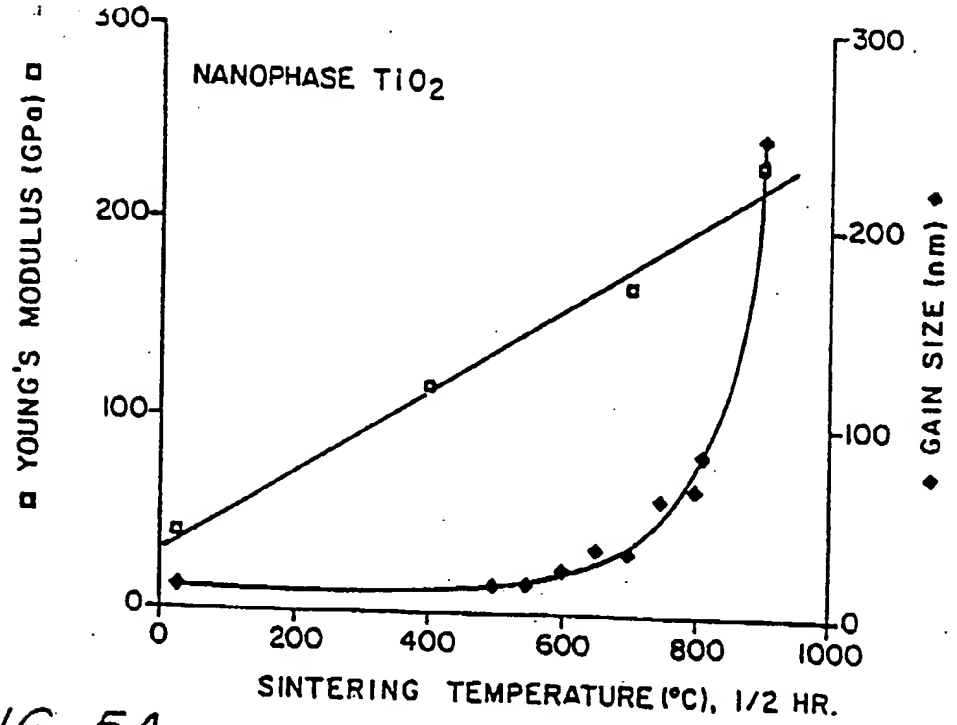
NANOPHASE TiO_2
□ YOUNG'S MODULUS (GPa) □
◆ GAIN SIZE (nm) ◆
SINTERING TEMPERATURE (°C), 1/2 HR.

FIG. 5A

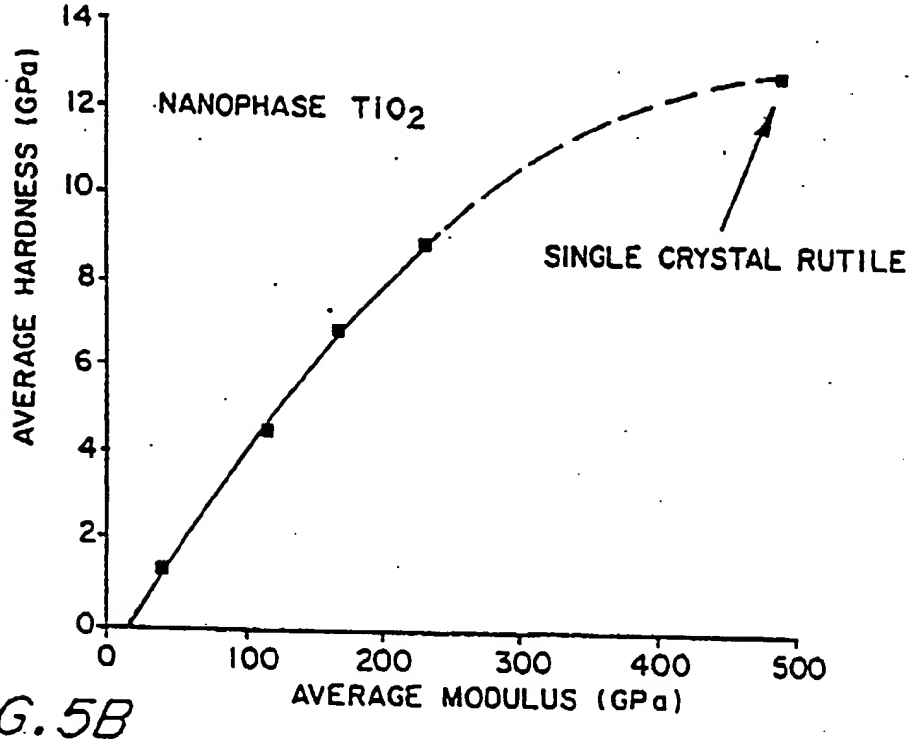
AVERAGE HARDNESS (GPa)
14
12
10
8
6
4
2
0
NANOPHASE TiO_2
SINGLE CRYSTAL RUTILE
0
100
200
300
400
500
AVERAGE MODULUS (GPa)

FIG. 5B

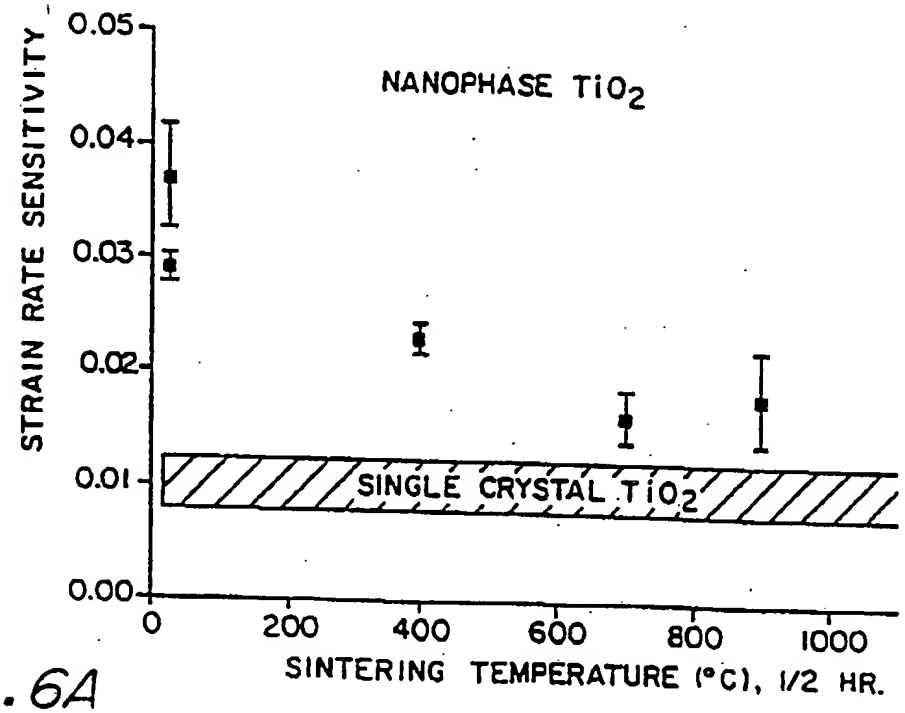
STRAIN RATE SENSITIVITY
0.05
0.04
0.03
0.02
0.01
0.00
NANOPHASE TiO_2
SINGLE CRYSTAL TiO_2
0
200
400
600
800
1000
SINTERING TEMPERATURE (°C), 1/2 HR.

FIG. 6A

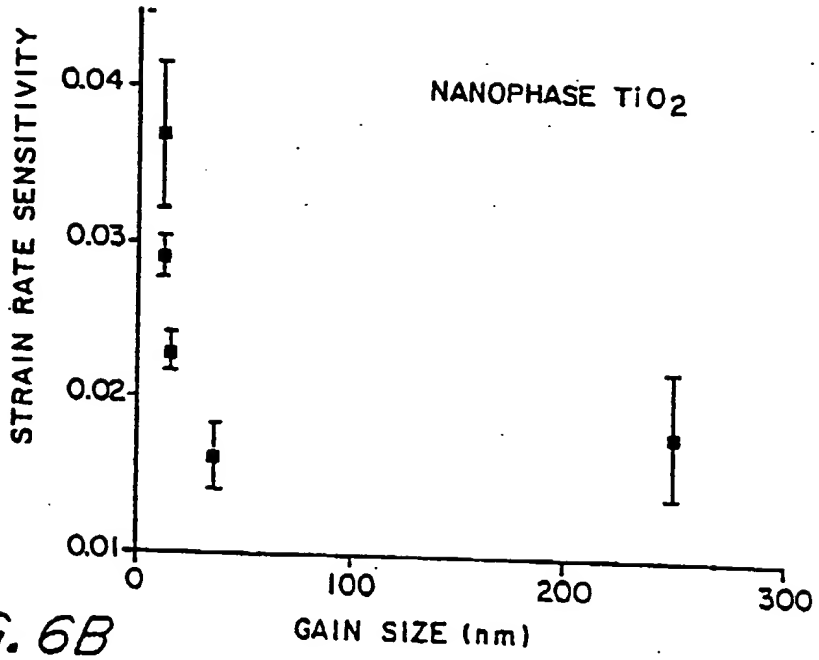
STRAIN RATE SENSITIVITY
0.04
0.03
0.02
0.01
NANOPHASE TiO_2
0
100
200
300
GAIN SIZE (nm)

FIG. 6B

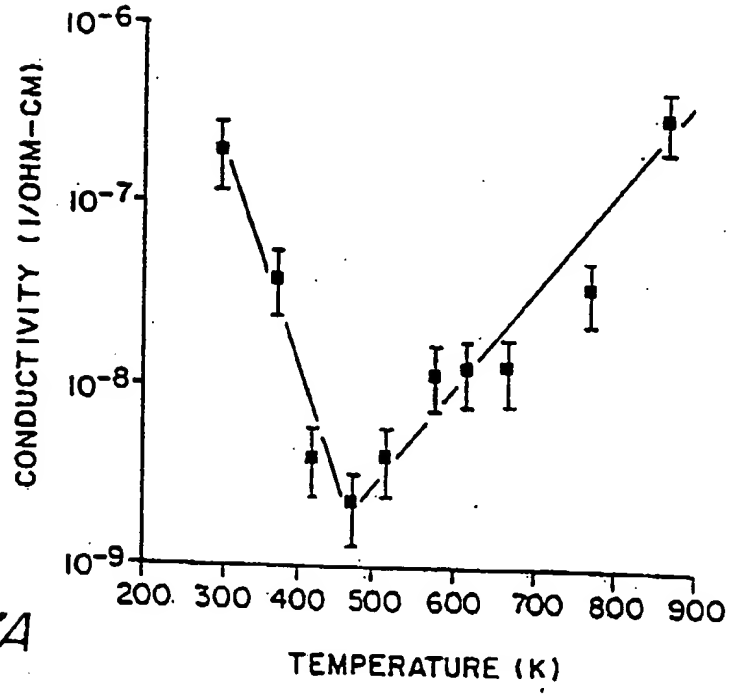
CONDUCTIVITY (1/OHM-CM)
10^{-6}
10^{-7}
10^{-8}
10^{-9}
200 300 400 500 600 700 800 900
TEMPERATURE (K)

FIG. 7A

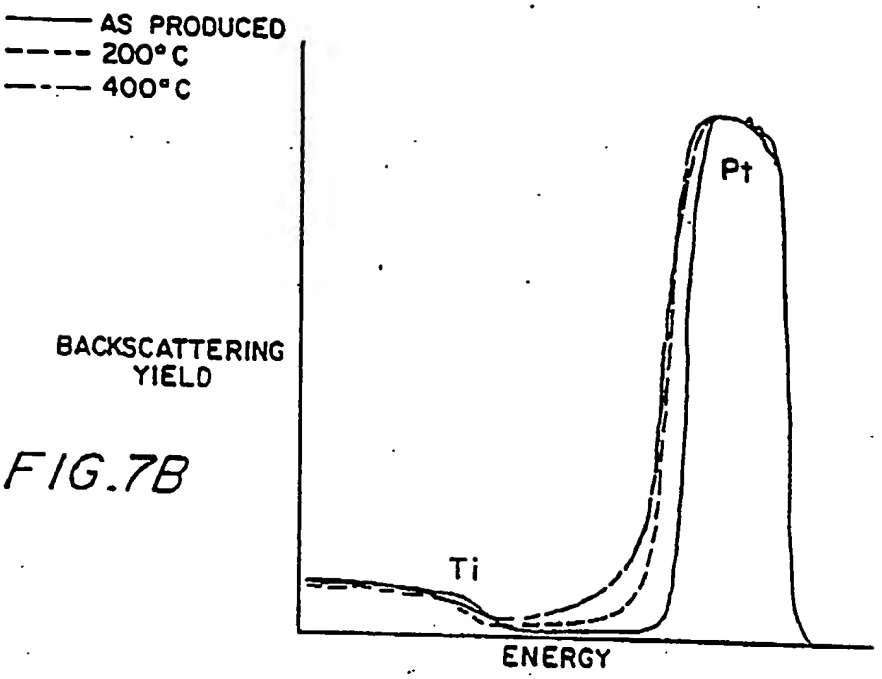

FIG. 7B

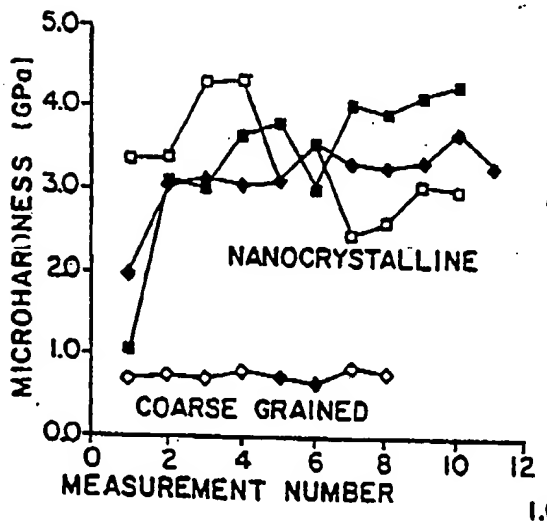

FIG. 8A

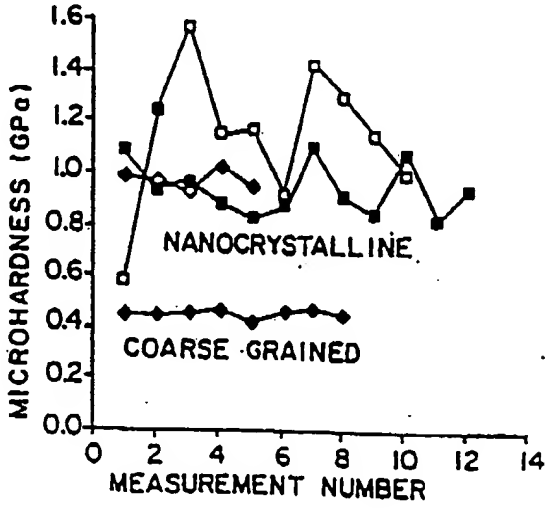

FIG. 8B

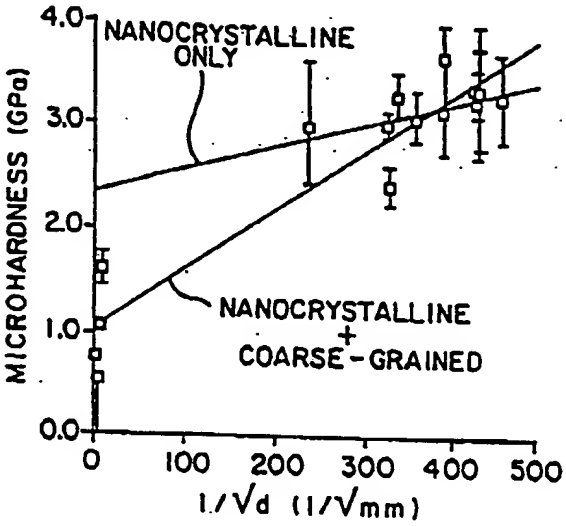

FIG.8C

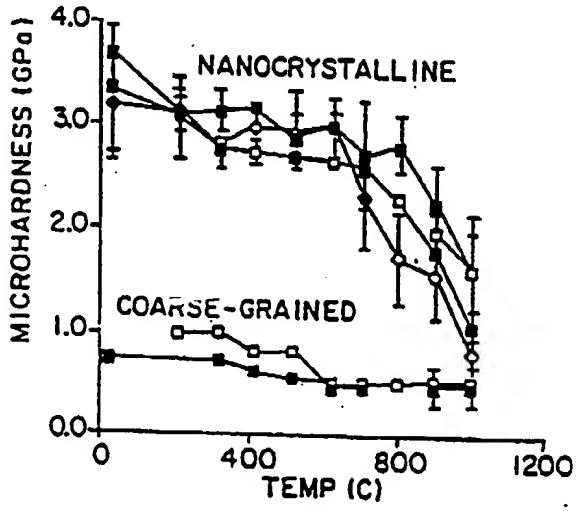

FIG.8D

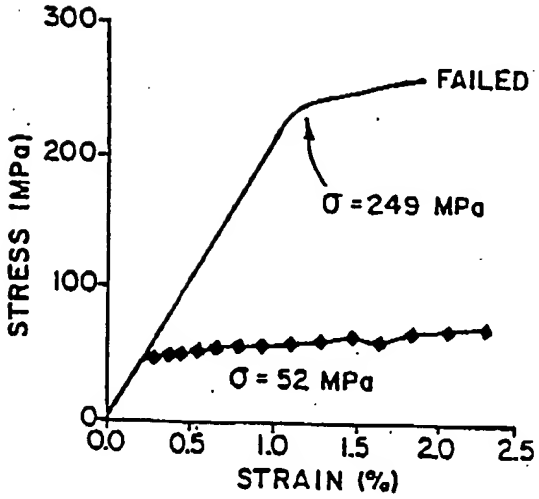

FIG.9A

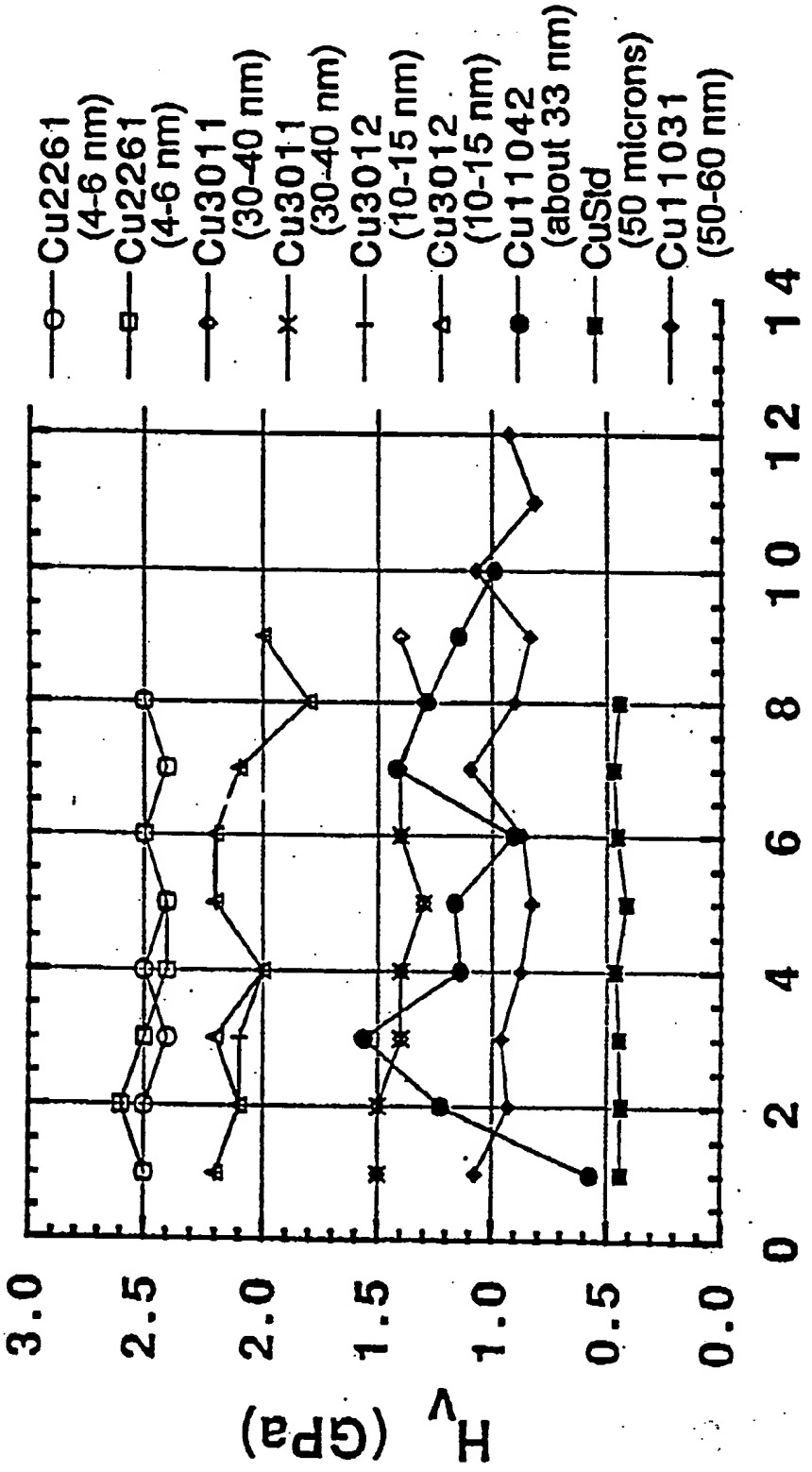
Cu2261 (4-6 nm)
Cu2261 (4-6 nm)
Cu3011 (30-40 nm)
Cu3011 (30-40 nm)
Cu3012 (10-15 nm)
Cu3012 (10-15 nm)
Cu11042 (about 33 nm)
CuStd (50 microns)
Cu11031 (50-60 nm)
3.0
2.5
2.0
1.5
1.0
0.5
0.0
H_v (GPa)
0
2
4
6
8
10
12
14
Measurement No.

FIG. 8E

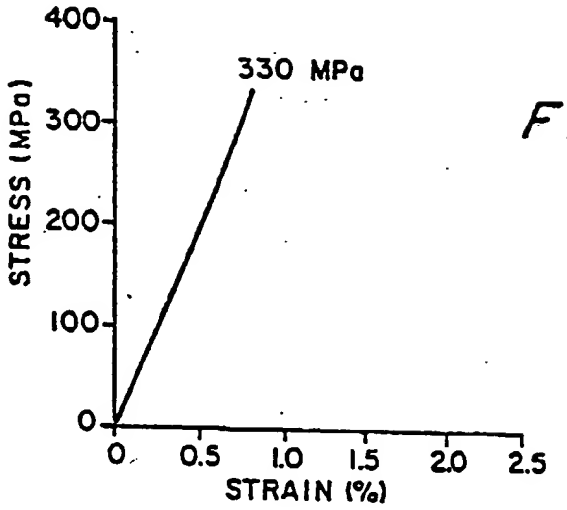

FIG.9B

FIG.9C

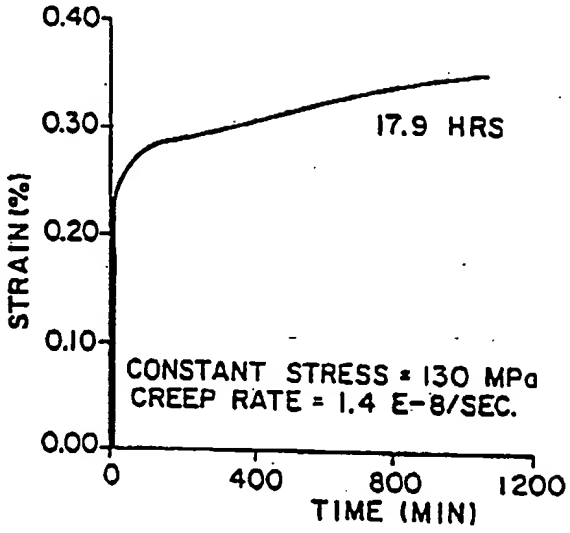

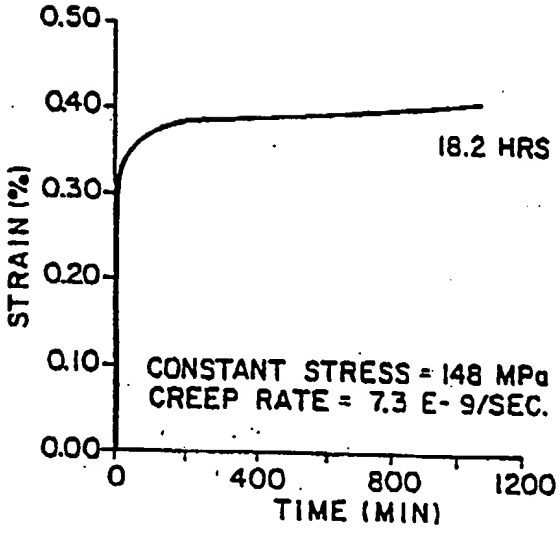

FIG.9D

NANOCRYSTALLINE CERAMIC MATERIALS

This invention was made with Government support under Contract No. W-31-109-ENG-38 awarded by the Department of Energy. The Government has certain rights in this invention.

This invention was made with Government support under Grant Number: NSF-DMF 8320157 awarded by the National Science Foundation. The Government has certain rights in this invention.

This is a continuation of Ser. No. 07/622,244, filed Dec. 4, 1990, now abandoned, and a continuation-in-part of Ser. No. 07/466,585, filed on Dec. 5, 1989, now U.S. Pat. No. 5,128,081.

The present invention is generally related to methods and products of manufacture and use of ultrafine-grained, or nanocrystalline, metallic materials. More particularly, the invention is related to methods of controlling the grain sizes, chemical phases produced, levels of porosity, and the electrical, mechanical, magnetic and chemical properties of nanocrystalline metallic materials.

Technological Progress is often based on the availability of new and improved materials which enable increasing the performance of new products or new methods of manufacture. For example, the discovery of the class of high temperature superconducting ceramics has given rise to numerous possible new products and new manufacturing methods. Frequently, progress in new material developments arises from the discovery of new chemical compounds or more sophisticated methods of manufacturing products, such as, new methods of miniaturization for use in integrated circuit manufacture. Recently, methods have been developed for controllably producing ultrafine-grained, or nanocrystalline, materials (typically, about 1–100 nm grain diameters). These new methods have made possible the production of new materials having substantially different physical and chemical properties than the large grained, or single crystal, counterparts having substantially the same chemical composition. Numerous traditional problems in areas such as ceramic materials can now be addressed using these new nanocrystalline materials to control and modify materials properties.

It is therefore an object of the invention to Provide improved methods and products of manufacture of nanocrystalline materials.

It is another object of the invention to provide a novel method of preparing a product nanocrystalline material using variable gas pressure atmospheres.

It is a further object of the invention to provide an improved method of manufacturing any electronic components encompassing different nanocrystalline or nanophase materials.

It is an additional object of the invention to provide a new method of preparation and product nanocrystalline metallic material.

It is also an object of the invention to provide new nanocrystalline and nanophase materials for magnetic materials applications.

It is another object of the invention to provide novel products of metallic nanocrystalline Pd and Cu.

It is a still another object of the invention to provide an improved method of using nanocrystalline metallic materials.

It is yet another object of the invention to provide a novel method of producing a nanocrystalline metallic material having predetermined sintering characteristics.

It is still an additional object of the invention to provide an improved method of mechanical processing of a nanocrystalline metallic material, while controlling mechanical properties by adjustment of grain size.

It is yet another object of the invention to provide a method of manufacturing nanocrystalline zinc oxygen compounds for use in varistors.

It is still another object of the invention to provide new forms of nanocrystalline titanium oxide sensors.

Further objects and advantages of the invention together with the organization and manner of operation thereof, will become apparent from the following detailed description of the invention when taken in conjunction with the accompanying drawings and nonlimiting examples.

BRIEF DESCRIPTION OF THE DRAWINGS

FIG. 1 shows one form of apparatus used for producing nanocrystalline materials;

FIG. 2 illustrates X-ray plots of nanocrystalline (nanophase) material compacted using 1.4 GPa at ambient temperatures and FIG. 2A is for titanium evaporated in 60 Pa of helium and compacted without any exposure to oxygen; FIG. 2B is for titanium evaporated in 60 Pa of helium and exposed to oxygen prior to compaction and the shaded peaks arise from an unidentified phase or phases of titanium and oxygen; and FIG. 2C is for titanium evaporated in 500 Pa of helium followed by exposure to oxygen to produce rutile;

FIG. 3 illustrates Vickers microhardness of 12 nm average grain size rutile measured at room temperature; the specimens have undergone cycles of half hour sintering at successively higher temperatures in air; open circles illustrate results for vacuum compacted material with no exposure to air and closed circles illustrate results for air compacted materials;

FIG. 4 shows nanoindenter-derived hardness of nanocrystalline (nanophase) rutile as a function of sintering temperature compared with nanoindenter hardness for a single crystal rutile wherein hardness is tested at two sites for each sample;

FIG. 5A illustrates Young's modulus data and grain growth for nanocrystalline (nanophase) rutile at different sintering temperatures and

FIG. 5B shows the correspondence between hardness and Young's modulus in nanocrystalline (nanophase) rutile and single crystal rutile;

FIG. 6A illustrates strain rate sensitivities of nanocrystalline (nanophase) rutile with the range of strain rate sensitivities measured for single crystal rutile shown by the gray band, and FIG. 6B shows strain rate sensitivity versus grain size in nanocrystalline (nanophase) rutile wherein grain size was determined from the data of FIG. 5A; and

FIG. 7A shows the range of conductivity of Pt doped nanocrystalline rutile and FIG. 7B illustrates the spatial distribution of the Pt in the rutile based on Rutherford back scattering analysis;

FIG. 8A shows microhardness of three representative nanocrystalline Pd samples and a coarse-grained Pd sample; low measurement 1 is from a low-compacted rim; FIG. 8B shows microhardness of two nanocrystalline Cu samples and a coarse-grained Cu sample; data includes two traverses of one sample; low measurement 1 is from a low-compacted rim; FIG. 8C shows micro-

hardness of eleven nanocrystalline Pd samples and four coarse-grained Pd samples versus $1/\sqrt{d}$; FIG. 8D shows microhardness of three nanocrystalline Pd samples and two coarse-grained Pd samples as a function of annealing temperature; all the samples were annealed for 100 minutes in 0.16 Pa vacuum; and FIG. 8E shows Vickers microhardness of six nanocrystalline Cu samples and a coarse-grained Cu sample.

FIG. 9A shows a stress-strain curve for a nanocrystalline (average grain size 7 nm) sample and a coarse grained (100 μm grain size) Pd sample. $\dot{\epsilon} \approx 2 \times 10^{-5}/s$; FIG. 9B shows a stress-strain curve for a nanocrystalline (10 nm) Pd sample. $\dot{\epsilon} \approx 2 \times 10^{-5}/s$;

FIG. 9C shows a creep plot for constant stress, room temperature creep tests on a nanocrystalline (10 nm) Pd samples and FIG. 9D shows a creep plot for constant stress and room temperature creep tests on a nanocrystalline (10 nm) Pd sample.

DETAILED DESCRIPTION OF PREFERRED EMBODIMENTS

An apparatus for preparation of nanocrystalline or nanophase materials (hereinafter, "nanocrystalline" materials shall include crystalline, quasicrystalline and amorphous phases) is shown in FIG. 1 at 10. The apparatus 10 includes a vacuum chamber 12 wherein a vacuum (preferably, better than about 10^{-6} Pa) is achieved by any one of a variety of conventional pumping systems 14. In other forms of the invention the vacuum can be about 10^{-4} Pa and useful product materials are still obtained. After evacuation, the vacuum chamber 12 is back-filled through gas port 16 with selected gases 17, such as, inert gases, oxidizing gases (such as oxygen and air and mixtures of oxidizing and inert gases) which are utilized for carrying out various processing steps.

In the case of preparing oxides of titanium in the apparatus 10, initially a helium gas atmosphere is provided while a titanium metal source 18 (typically greater than 99.9% pure) is evaporated by conventional Joule heating. In other forms of the invention, the titanium can be removed from a source by other conventional means, such as electron beam, sputtering, RF or plasma heating, or laser beam irradiation. The evaporated titanium condenses into small particles in the helium atmosphere and is transported by convection currents to a liquid nitrogen cooled cold surface 20 where the condensed titanium accumulates. In other forms of the invention, forced gas flow can be used to assist in directly accumulating the material in a compaction device. Further, the material removed from the source can be deposited on an ambient temperature surface in a nanophase or nanocrystalline form.

In a preferred form of the invention, the accumulated titanium can be oxidized to form a nanocrystalline titanium oxide material. Further, in other forms of the invention, the titanium can be oxidized before or after removing the titanium from the cold surface 20. The resulting phases of titanium oxide and their properties depend on the gases used and the chosen point of oxidation in the manufacturing process. In further embodiments to be described hereinafter, various nanocrystalline metals produced in an apparatus such as 10, can be subjected to a generically oxidizing atmospheres, such as C, S, N, F, or Cl to form nanocrystalline materials.

Once sufficient nanocrystalline titanium oxide material has accumulated on the cold surface 20, a scraping device 22 (typically a ring of "Teflon"—a trademark of Du Pont Corp) removes the titanium oxide material. The removed titanium oxide falls into funnel 24 and is collected in a low pressure compaction unit 26. This low pressure compaction unit 26 includes a piston 28, an anvil portion 30 and a slide section 32. Further compaction of the nanocrystalline titanium oxide material can be carried out by using a high pressure compaction unit 34, including sleeve 36 and piston 38. All of the collection and compaction steps can be performed in a highly controlled vacuum or gas atmosphere depending on the properties desired for the resulting nanocrystalline end product.

During typical manufacture of nanocrystalline materials, the evaporation pressure (or the background partial pressure from "removal" of the desired chemical species from a source) is roughly 5–50 Pa. In the case of evaporating the titanium source 18, the pressure is about 10 Pa while the helium gas pressure is controlled to select the desired phase of titanium oxide. For example, in order to reliably attain the rutile phase of nanocrystalline oxide in the illustrated apparatus 10, the helium gas pressure is maintained above about 500 Pa. In order to ultimately produce an amorphous titanium oxide material, the helium gas pressure is kept between about 10–500 Pa when collecting titanium on the cold surface 20. A coarse grained titanium (and ultimately oxidized to rutile) is achieved by using helium gas pressures below about 10 Pa within the apparatus 10.

If oxygen gas is rapidly introduced to the vacuum chamber 12 after evaporation of titanium in 500 Pa of helium gas pressure, the resulting oxidized phase is a nanocrystalline rutile with a nominal particle size of about 12 nm. The powdered, uncompacted rutile material has a characteristics bluish white color. On the other hand, as stated hereinbefore if the helium pressure in the vacuum chamber 12 is between about 10–500 Pa, an amorphous titanium oxide phase is formed. Electron energy loss spectroscopy confirms that the amorphous material contains substantial oxygen. Also, in general the titanium material collected on the cold surface 20 is gray in color when using a helium gas atmosphere pressure below about 500 Pa. This color remains the same before and after oxidation when using oxygen gas. Other factors determining the final phases of titanium oxide include the order in which oxidation takes place, and the type of gas (for example, helium, oxygen or air) present during compaction of the collected titanium powder material. If the original powder material is produced using helium pressures greater than about 500 Pa, the nanocrystalline material is still the same phase (for example, rutile if the powders have been exposed to oxygen and titanium metal if no oxygen or air exposure has occurred). However, if the powders are amorphous after air or oxygen exposure and the helium pressure is about 10–500 Pa helium pressure, the result is a bulk crystalline titanium oxide powder. The nature of the crystalline phase, however, depends on whether or not the powder material was exposed to oxygen prior to compaction. Powder material compacted in vacuum in the apparatus 10 without prior exposure to oxygen contained only crystalline titanium metal with a grain size of 20–50 nm. This is significantly larger than the grain size obtained if a 500 Pa helium pressure is used in the apparatus 10, even though a lower pressure level is generally expected to result in a smaller grain size. If, however, the powder titanium oxide material is exposed to oxygen, and the oxygen gas is subsequently removed prior to scraping powders from the cold surface 20, the compacted titanium oxide powder material undergoes a

further oxidation reaction upon exposure to air. The resulting titanium oxide material is a mixture of rutile and at least one other oxide phase (see FIG. 2).

Control of gas atmosphere conditions in the vacuum chamber 12 can allow the manufacture of titanium oxide material made up of different phases have different physical, chemical and electronic properties. For example, not only can one selectively generate a generally desired chemical phase, but one can control certain chemistry of the powder materials. This latter point can be illustrated for the case of nanocrystalline titanium oxide. In FIG. 3 there is shown a comparison of the microhardness sintering behavior of nanocrystalline titanium oxide powder with and without exposure to air prior to an initial low pressure powder compaction. Not only does the vacuum consolidated material begin sintering at lower temperatures than air consolidated material, but also the ultimate hardness obtained is greater than the air compacted material. The ability to control such characteristics as hardness and sinterability, in addition to the phases present, allows the manufacture of product materials having predetermined physical, chemical and electronic properties. Such controlled variability of characteristics arises from the different chemical phases produced and the surface chemical states being present as a consequence of varying the gas pressures experienced by the nanocrystalline material and the other general processing conditions, such as the compaction conditions. These features enable assembly of a component having portions with different chemical compositions and different structures. The assembled component can involve various generic nanocrystalline materials, such as, for example, composites of titanium oxides, zinc oxides, magnesium oxides, aluminum oxides and metals as well.

Further useful characteristics of nanocrystalline materials include controllable porosity in ceramic, metallic or composite materials. For example, nanocrystalline titanium was prepared in the manner described hereinbefore by evaporating the titanium from resistance heated tungsten boats at temperatures of 1550°–1650° C. into a 300–700 Pa helium atmosphere. The titanium material collected on the cold surface 20 was oxidized to titanium oxide (rutile) by rapid introduction of 2000 Pa of oxygen. The resulting rutile material was scraped from the cold surface 20, compacted and then specimens were sintered in air at 550° C. at times of 15 minutes, 30 minutes, 1 hour, 2 hours, 4 hours, 8 hours and 23 hours. Characterization of rutile grain size and void content were performed by small angle neutron scattering in the Argonne National Laboratory IPNS facility, and it was concluded that the rutile grain size was in the typical nanometer size range. The grains were separated by 0.5 nm boundaries which contained voids with the grain boundary rutile having a density of about 60–70%.

The level of density can thus be controlled by sintering and compacting to achieve a desired degree of microscopic and/or atomistic density ranging from the as produced state up to substantially theoretical density. Such control allows freedom to fix, for example, (1) the diffusion properties of a material, (2) the hardness, (3) strain rate sensitivity and (4) surface area and surface chemical states. Regarding diffusion properties, the substantial increase in grain boundary surface area and void or pore content in nanocrystalline materials also enhances diffusion properties. Such properties are important, for example, for (1) electrical and optical properties, (2) and (3) mechanical and wear properties and (4) catalytic properties, respectively. See the Examples for further amplifying information on these properties.

Based on the measurements shown in FIG. 4, the hardness of nanocrystalline rutile shows a steady, substantially linear increase with sintering temperature. This tread indicates that sintering and densification processes are taking place even at quite low temperatures. Such a result is believed to be unexpected since previous studies have indicated that density changes do not begin to occur until about 600° C. Nevertheless, it should be remembered that the first stage of sintering involves formation of inter-particle necks without a concurrent decrease in pore volume. Thus, at relatively low sintering temperatures, such as less than 600° C., the interconnections between particles would lend strength to the ceramic while not affecting the overall density. At these same temperatures, increases occur in Young's modulus; and changes in strain sensitivity are also observed (see FIGS. 5 and 6) further supporting the conclusion that microstructural changes are occurring. Enhanced diffusion at these low temperatures is also confirmed by the substantially improved diffusivity of platinum (see FIG. 7) into nanocrystalline rutile at temperatures as low as about 150°–200° C. (also see Example 6). Diffusion at such low temperatures is believed to occur along the surfaces of microscopically fine pores typically found in nanocrystalline rutile, but it is not inconceivable that self-diffusion can also proceed by a similar route at low temperatures.

As illustrated in FIG. 5, Young's modulus does not reach the single crystal value but obtains about 47% of that value at 900° C. sintering temperature. The modulus appears to rise almost linearly with sintering temperature, indicating that some degree of sintering is occurring even at the lowest temperatures of the study. The independent measure of hardness and modulus in FIGS. 5A and 5B support the proposition that densification processes are indeed occurring in a monotonic manner. Consequently, while densification may be occurring at temperatures below 600° C., grain growth is relatively slow at these same temperatures (see FIG. 5A); and catastrophic, substantial grain growth does not occur until about 875° C. Therefore, one can consolidate these powders into a substantially dense ceramic state, while maintaining the nanocrystalline Particle size. As can be seen in FIG. 5A one can keep the grain size to less than about sixty to seventy nm at sintering temperatures of 800° C. for one half hour. In a conventional manner one can utilize known relationships of time-temperature-transformation to establish different temperatures and time combinations which will avoid catastrophic grain growth.

As shown in FIGS. 6A and 6B, the nanocrystalline rutile shows extremely high strain rate sensitivities indicating a potential for excellent room temperature ductility. The degree of strain rate exhibited is not found in conventional ceramic materials. This may arise for a number of possible reasons, none of which limit the scope of the claims presented hereinafter. These possibilities include increased grain boundary sliding activity, perhaps derived from the significant porosity (which is up to about 25% for an as compacted sample), and the ultrafine grain size should enhance grain boundary sliding activity.

In other forms of the invention one can carry out conventional chemical oxidation reactions to convert any metal into its oxidized state. Any oxidizable metal

which can be deposited on the cold surface 20, or entrained in the condensing gas, can be converted by generic oxidation into its oxidized form. Such generic oxidation reactions can thus, for example, involve gas atmospheres of halogens, carburizing atmospheres such as CH_4, nitriding atmospheres such as N and NH_4 and sulphurizing atmospheres such as S or H_2S. The conventional nature of such generic oxidation reactions is illustrated in such texts as, *College Chemistry*, L. Pauling, W. H. Freeman and Co., San Francisco, 1957. It has long been known that generic oxidation-type reactions between elements well separated on the electronegativity scale (see Linus Pauling's *College Chemistry*), form well bonded compounds. Thus, the illustrated oxidation reactions already used in synthesizing nanophase ceramics are readily generalized to a wide range of other compounds, such as BN, formed from constituents sufficiently separated on the electronegativity scale by a fully analogous process to that already used.

While preferred embodiments of the present invention have been illustrated and described it will be understood that changes and modifications can be made within without departing from the invention in its broader aspects. Various features of the invention are defined in the following nonlimiting examples and the claims.

EXAMPLES

Example 1

Titanium dioxide has been prepared using titanium metal (99.9% purity) evaporated to form small titanium particles which are condensed in selected helium gas atmospheres described in the specification. The titanium is collected on a cold surface 20 and then oxidized by introducing approximately 2000 Pa oxygen rapidly into the vacuum chamber 12. During collection of the titanium particles on the cold surface 20, adequate quantities are built up before the material is oxidized and removed, or consolidated. Once adequate material is accumulated on the cold surface 20, it is warmed to room temperature and then spontaneously converted to titanium oxide by the oxygen atmosphere. Additional runs were made in which the cold surface 20 was not warmed to room temperature, and the same results were achieved. The rate of oxygen introduction into the chamber has been found to play a role in the form of oxides obtained. For example, bleeding oxygen slowly into the chamber results in the formation of a mixture of rutile and other oxides phases compared to rutile only for rapid introduction of oxygen. Following oxidation, the vacuum chamber 12 is evacuated again, and the titanium oxide powder is collected and consolidated under various atmospheric conditions, such as vacuum and selectively with oxygen and/or air. The resulting material has a log-normal grain size distribution with a typical mean grain size of approximately 12 nm. For oxides of aluminum and magnesium, which are extremely reactive with oxygen, a thin protective amorphous coating can be formed under certain conditions, and this layer can prevent complete oxidation of the metal. Because of this it has been necessary to perfect variations on the basic technique to form nanocrystalline oxides of highly reactive metals, such as, aluminum and magnesium. These techniques will be described in additional examples hereinafter.

Example 2

In the case of preparation of nanocrystalline aluminum oxide, nanocrystalline aluminum powders are first produced in substantially the same manner as titanium in Example 1, although it is unnecessary to include any helium atmosphere. After the nanocrystalline aluminum is collected on the cold surface 20, it is then annealed in air at 1000° C. for at least one to two hours. This treatment results in transformation of the nanocrystalline aluminum powders (likely with a very thin oxide coating) to the thermodynamically stable alpha phase of aluminum oxide. Little increase in particle size occurs during the annealing process, and the final average particle size obtained is about 18 nm.

Example 3

Nanocrystalline magnesium oxide has been produced by directly subliming the oxide by Joule heating of MgO in tungsten boats heated to 1600° C. in a 200 Pa atmosphere of helium. The nanocrystalline material which is collected on the cold surface 20 is oxygen deficient, but is fully converted to nanocrystalline MgO by oxygen subsequently introduced into the vacuum chamber 12. The MgO as produced has an approximate grain size of about 5 nm, but it has been determined not to be pure single phase MgO due to contamination by sublimation of tungsten oxide phases from the tungsten boat used to hold the MgO. Such a composite, however, can have well defined and desirable applications. Production of uncontaminated MgO can be obtained by careful electron beam evaporation, laser beam ablation or high rate sputtering. Details of preparation of substantially stoichiometric, pure MgO using an oxidizing atmosphere are set forth in Example 9.

Example 4

The production of nanocrystalline zinc oxygen is similar to that of MgO. As in the case of MgO, ZnO has a high vapor pressure at temperatures well below the melting point, and it is thus possible to produce nanocrystalline powders of zinc oxides by Joule heating. Nanocrystalline zinc oxide material with grain sizes of roughly 6 to 15 nm have been produced by subliming coarse grained ZnO from graphite boats at temperatures of 1400° C. in a 10^{-6} Pa vacuum. X-ray diffraction measurements reveal that the as produced and consolidated samples not only include ZnO, but some significant quantities of Zn metal are also produced. This result is observed even if the powder has been exposed to oxygen prior to compaction. In some cases only Zn is observed in X-ray scans, but some amorphous oxide phase also is present in the samples (chemical analysis has shown that these materials typically contain 40 at.% oxygen) Annealing of the material in air at 300° C. for 3 hours has been found to successfully convert any remaining Zn metal to ZnO. The end product was examined by X-ray diffractrometry scans. It was noted that material which is only lightly compacted at very low pressures (less than roughly 0.5 GPa) transforms much more easily to ZnO than material which has been compacted at 1.4 Pa. The higher pressure compaction results in some Zn metal remaining even after several hours at 600° C. (above the melting point of Zn metal and presumably the Zn is passivated by ZnO). Other methods of producing a substantially stoichiometric ZnO using oxidizing atmospheres are set forth in Example 10.

Example 5

Raman microprobe studies were carried out on nanocrystalline titanium oxides and oxidation induced spectral changes were observed. Raman measurements can show that both rutile and anatase phases were present in the examples. The anatase phase could be completely removed from the specimen by annealing at temperatures above about 600°–750° C. for two hours in air. The spectrum showed the as compacted material contained the anatase phase peak which disappeared after the anneal. That is, the 144 cm^{-1} and 154 cm^{-1} peaks of anatase diminished, leaving only the rutile lines. In addition, it was noted that the phase transformation (anatase to rutile) temperatures and times were reduced in these nanocrystalline materials. Further, the oxygen deficiency present in the nanocrystalline titanium oxide is removed by the annealing operation in air, as revealed by the sharpening and shifting of the rutile and anatase lines in the Raman spectrum.

Example 6

Pt was diffused into nanocrystalline rutile Prepared in accordance with Example 1. A 100 nm Pt layer was deposited by evaporation onto the rutile and annealed at 200° C. for two hours and then at 400° C. for another two hours. The conductivity of the doped rutile is illustrated in FIG. 7A, and the spatial distribution of the Pt in the doped rutile is clearly shown by the Rutherford back scattering data shown in FIG. 7B.

Example 7

The apparatus 10 shown in FIG. 1 has also been used to prepare nanocrystalline Pd and Cu. Mean grain size can be controlled in a known manner by the conditions of atom removal, such as by the evaporation temperature and by the inert gas atmosphere pressure. The powder produced is compacted under 1.4 Pa uniaxial pressure in vacuum (typically 10^{-6} Pa) to form samples for mechanical testing. In particular mechanical properties have been improved by reducing the mean grain size to less than 10 nm. The Archimedes method in ethyl phthalate was used to measure densities of a compacted specimen. These densities ranged from 82% to 96% of the coarse grained standard and were reproducible within 2%. Pd samples averaged 5–10 nm grain size and Cu was 25–35 nm.

Vickers microhardness measurements were made on as-compacted and polished samples using a one hundred g load applied for twenty seconds. Measurements were made on the nanocrystalline Pd samples, two nanocrystalline Cu samples, and several coarse grained Pd/Cu samples. Three nanocrystalline and two coarse-grained palladium samples were annealed in vacuum (0.13 Pa) for 100 minutes at each temperature, incremented by 100° C. from 200° through 100° C. Microhardness was measured on unpolished surfaces of small fragments (0.2 mm×2 mm×4 mm), derived from the original pellets, at room temperature after each anneal. The small size of the samples used did not permit grain size determination by X-ray diffraction after each anneal. Grain size and hardness of a single sample were determined prior to and following vacuum annealing at 500° C. for 100 minutes in order to estimate the hardness change and grain growth due to annealing.

Microhardness results on as-compacted palladium samples show a four fold increase in hardness for ten nanocrystalline Pd samples compared to coarse-grained (100 μm) Pd (FIG. 8A), and a doubling in hardness for two nanocrystalline Cu samples over coarse-grained (50 μm) Cu (FIG. 8B). Measurements on low-compacted rims yield much lower hardness values, as shown. The magnitude of the increase in hardness of the nanocrystalline samples over that of the coarse-grained samples agrees with data for increase in yield strength determined by uniaxial tensile tests on the same samples. Hardness for the as-compacted nanocrystalline Pd samples ranged from 4.3 GPa to 2.3 GPa with a mean of 3.1±0.5 GPa. Mean microhardness for a coarse-grained Pd sample (100 μm) was 0.74±0.05 GPa. Microhardness determined for a set of samples polished to 0.25 μm gave a mean hardness of 2.9±0.1 GPa. Microhardness for a 25 nm grain size Cu sample was 1.2±0.2 GPa (1.2±0.1 GPa for the polished sample), and was 0.9±0.04 GPa for a 35 nm grain size sample (1.0±0.09 GPa for the polished sample). Mean microhardness for a coarse-grained (50 μm) Cu sample was determined to be 0.45±0.04 GPa. Polishing was observed to dramatically reduce variance in the measured hardness without affecting the mean hardness.

For pyramidal indenters, hardness (H_v) of metals is empirically related to the yield stress (σ_y) by the relation $H_v/\sigma_y=3$. If the Hall-Petch relationship persists to nanocrystalline grain sizes (d), then

$$H_v=H_{vo}+k_H d^{-\frac{1}{2}},$$

where k_{Hv} and H_{vo} are constants. The present investigation of the relationship between Vickers microhardness and crystalline size shows that [1] the increase in hardness as a function of $d^{-\frac{1}{2}}$ is smaller for the group of nanocrystalline samples alone than for coarse-grained and nanocrystalline samples taken together; and [2] the large variance in the data results in a considerable uncertainty in the slope, k_{Hv} (FIG. 8C). The best-fit straight line through the data points for eleven nanocrystalline Pd samples, two originally nanocrystalline samples coarsened at 1000° C., and for two coarse-grained Pd samples is H_v=1030 MPa+6 (MPa/mm) $d^{-\frac{1}{2}}$. The best-fit straight line though only the nanocrystalline data is H_v=2236 MPa+2.5 (MPa$\sqrt{}$mm) $d^{-\frac{1}{2}}$. The uncertainty in these lines due to scatter in the nanocrystalline data is apparent. Possibly more reliable values for H_{vo} and k_{Hv} are obtained by plotting mean microhardness of polished samples or maximum hardness of as-compacted samples as a function of $d^{-\frac{1}{2}}$. Values of H_{vo}, k_{Hv} are 834 MPa, 5 MPa mm for polished, as-compacted samples and 755 MPa, 8 MPa mm for the maximum hardness data. Mean microhardness for each of 11 Pd samples ranging in grain size from 5 to 18 nm shows a small apparent increase in hardness with decrease in grain size, but the mean of the standard deviations of the samples (441 MPa) is large enough to make all of these hardness values overlap. Microhardness measurements on the two nanocrystalline Cu samples indicate the 25 nm Cu is harder than the 35 nm Cu, but these data, too, overlap statistically.

Failure to define clearly the dependence of microhardness on nanocrystalline grain size results, in part, from the fact that changes in indentation diagonal length due to grain size-related hardness differences are of the same order of magnitude as the uncertainties in the measurements. For example, a Vickers hardness of 4.9 GPa results in a diagonal length of ≃19.1 μm. A hardness of 3.4 GPa corresponds to a diagonal length of ≃23.0 μm. Processing flaws much larger than the mean

grain size, such as pores and cracks, are probably responsible for reducing and homogenizing hardness values. The measured microhardness is a net hardness, representing both grain strength as well as flaw strength, so the lower stress necessary to crush or propagate such flaws will tend to reduce the hardness of the sample. Hardness values for the <10 nm size samples span a very large range. The maximum hardness values (≈4.9 GPa) could represent the hardness of relatively flaw-free material; the lower hardness (≈2.45 GPa), of flaw-rich material. Thus, the measured bulk sample hardness could be much lower than the hardness due to grain size reduction. However, ultimate hardness may be partly ameliorated by inherent softening due to grain boundary sliding.

Microhardness also was investigated as a function of annealing temperature, and results are shown graphically in FIG. 8D. Two nanocrystalline Pd samples show small mean hardness drops during the initial 200° C. anneal. However, the standard samples and the third nanocrystalline sample do not change mean hardness in this range, and hardness variation is large. Mean hardness of nanocrystalline Pd decreases slowly for temperatures between 200 (0.26 T_m) and 700° C. (0.53 T_m), then declines rapidly at a rate of approximately −50 MPa/100° C., as determined by the average slope of the mean H_v vs temperature data for three samples. The standard samples decrease in hardness slowly between 300° C. and 600° C., then show little change. The standard deviation in the hardness measurements of the nanocrystalline samples is much larger than that of the standard grain size samples. For a sample annealed in vacuum only at 500° C. for 100 minutes the mean grain size increased from 8 to 18 nm while microhardness was 3.1±0.3 GPa and 3.0±0.6 GPa, respectively. Grains observed optically after the 1000° C. heat treatment range widely in size with a mean value of approximately 16 μm. The hardness data for the samples in FIG. 8D and for the sample annealed only at 500° C. therefore indicate that hardness decrease corresponds to grain coarsening. Further, this effect occurs mainly above 0.5 T_m.

The apparent drop in mean hardness from the as-compacted values after the 200° C. anneal in the two nanocrystalline samples could arise from the annealing out of strains introduced by the compaction process, since large internal stresses resulting from compaction would increase the hardness. Alternatively, it may indicate that some annealing of intra-grain defects has occurred, reducing sites that could inhibit dislocation motion. Sintering of coarse porosity would increase the hardness, as shown by annealing studies on nanocrystalline TiO_2.

Nanocrystalline Pd samples (5–10 nm grain size) evaluated by Vickers microhardness measurements therefore show a surprising four fold increase in hardness over coarse-grained samples (100 μm), and nanocrystalline Cu samples (25–35 nm) likewise show a rather surprising doubling of hardness over coarse-grained Cu (50 μm). Increases in yield strength of the same magnitude were found in tensile tests on the same samples.

When microhardness data are plotted against $d^{-\frac{1}{2}}$, a much flatter slope is found for nanocrystalline samples alone than for coarse-grained and nanocrystalline samples combined. Study of microhardness versus annealing temperature suggests that grain growth is slow in the nanocrystalline samples up to a temperature of approximately 0.5 T_m, since mean microhardness changes very little. At higher temperatures a decrease in hardness is interpreted to be the effect of grain growth. Interpretation of the small slope of the H_v vs $d^{-\frac{1}{2}}$ data for nanocrystalline samples, as well as the small decrease of the mean microhardness data with annealing up to 0.5 T_m, is made more difficult due to statistical variability and inhomogeneity of hardness, which mask small variations. It is likely that microhardness is strongly influenced by microstructural processing flaws that control the upper limit of hardness of the samples until the point at which grain size becomes comparable to flaw size. It is possible that as particle size decreases to the size of several dislocation core diameters, "normal" dislocation processes responsible for Hall-Petch effects in larger grains no longer operate, or that grain boundary sliding becomes active.

Example 8

In the area of tensile strength and creep properties, uniaxial tensile tests and constant load creep tests were performed at room temperature on nanocryst-lline Pd prepared in the apparatus 10. It is know that metals with mean grain sizes in the micrometer size range show a well-defined dependence of yield stress and flow stress on grain size. For found to follow the Hall-Petch relation,

$$\sigma_y = \sigma_o + kd^{-\frac{1}{2}}$$

where σ_o is the friction stress, and k is a constant representing the stress to propagate dislocation activity into an adjacent grain. At low homologous temperatures, the Coble relation for the creep rate $\dot{\epsilon}$,

$$\dot{\epsilon} = \frac{B\sigma\delta\Omega D_b}{d^3 kT}$$

gives the predominant diffusional creep rate, where B is a constant, σ is applied stress, δ is the boundary thickness, Ω is the atomic volume, and D_b is the boundary diffusion coefficient. Thus, in nanocrystalline materials creep rates are enhanced by a factor of 10^9 over those for micrometer grain size materials. A reported increase in diffusivity in nanocrystalline Cu over the normal grain boundary value would further enhance the creep rate.

Pure Pd powders were prepared by inert-gas condensation and consolidated in a vacuum of approximately 1×10^{-6} Pa using a uniaxial pressure of 1.4 GPa to form 9 mm diameter disks 185–460 m thick. Precision density measurements on this as-compacted Pd, using the Archimedes method in ethyl phthalate, gave densities ranging from 86% to 96% of a coarse-grained standard. Measured densities for a sample were reproducible within 2%. Samples were prepared for mechanical testing by electric discharge machining dogbone-shaped specimens 8 mm long with gauge sections of 2–3.5 mm. Mechanical polishing was used in an attempt to reduce or remove surface flaws, but the amount of polishing possible varied with the sample thickness. Samples were tested at room temperature in uniaxial tension using load control on a miniaturized servo-electric test apparatus, built to test these small specimens. The instrument uses a 445N capacity load cell to monitor load provided by a 110N force load source, and an LVDT with a 0.13 mm displacement capacity and 0.4 μm sensitivity to monitor displacement.

We report here the results of two room temperature tensile tests (FIGS. 9A and B) and of two room temperature creep tests (FIGS. 9C and D) on samples of nanocrystalline Pd. For comparison, tensile test is reported for a sample of coarse-grained Pd(FIG. 9A). Note that measurements for the coarse-grained sample are affected by the large sizes of the grains with respect to the sample thickness and width, while the nanocrystalline sample tests give bulk-sample properties. The strain rate for all tensile test samples was approximately 2×10^{-5}/s. FIG. 9A shows results of tensile tests on a sample with a mean grain size of 7 nm and a coarse-grained sample. The nanocrystalline sample was polished using 6 μm silicon carbide to a thickness of 165 μm; the coarse-grained sample was polished to a thickness of 230 μm using 1 μm silicon carbide. The apparent 2% offset yield stress of the 7 nm Pd sample is five times larger than that of the coarse-grained sample. The nanocrystalline sample failed at a strain of 1.75% while the coarse grained sample did not fail before exceeding the displacement range of the LVDT. Fracture of the nanocrystalline sample of FIG. 9A occurred on an inclined surface composed of very flat plateaus and ledges. In contrast, FIG. 9B shows the stress-strain behavior of a 10 nm grain size Pd sample. This sample was polished with 0.25 μm diamond paste to a thickness of 190 μm, reducing the size of the remaining flaws below those in the previous sample. The sample in FIG. 9B showed no indication of yielding up to 330 MPa, the maximum capacity of the machine. The results in FIGS. 9A and B show the large increase in yield strength for nanocrystalline Pd samples relative to coarse-grained Pd. They also indicate a strong flaw size sensitivity, typical of many strong materials. Comparison of FIGS. 9A and B suggest that the yield stress for the 7 nm nanocrystalline sample is the critical stress for crack propagation and thus is an apparent yield stress. A large increase in hardness and a significant flaw sensitivity were also found in previous microhardness tests on these same samples.

The experimental values of Young's modulus for the three tensile samples vary from sample to sample and are far lower than the true modulus for Pd (122 GPa). In addition to the usual inaccuracy in measurement of this modulus from stress-strain cures, the displacement sensitivity of the LVDT prohibits accurate measurement of very small strains. The influence of bulk and surface flaws can also lower the apparent modulus.

Calculations using known data of the diffusion (Coble) creep rate for 10 nm grain size Cu predict a diffusion creep rate at 298K under a stress of 100 MPa of $\geq 1\times10^{-5}$/s. To investigate the Possibility of appreciable diffusional creep in nanocrystalline Pd, room temperature creep tests were performed. A 10 nm grain size sample was polished to a gage thickness of 450 μm using 0.25 μm diamond paste prior to tensile testing. The sample was placed under a constant stress of 130 MPa for a duration of 17.9 hours. Temperature was not monitored, but it is unlikely to have varied by more than a few degrees during the test. The creep rate measured is 1.4×10^{-8}/s, and data for the test are shown in FIG. 9C. A second creep test on the same nanocrystalline Pd sample is shown in FIG. 9D. This test was run using a load of 148 MPa for a duration of 18.2 hours. The creep rate measured in the second test is 7.3×10^{-9}/s. Both creep rates are near the resolution of the test equipment. The observed creep rate of this Pd sample is three orders of magnitude smaller than that which might have been expected on the basis of conventional data. Negligibly small creep rates were also found from creep test on nanocrystalline copper.

Example 9

Nanocrystalline MgO was prepared in a manner similar to Example 3 except a mixture of helium and oxygen was used in the vacuum chamber 12. The MgO was sublimed from a tungsten boat with a base vacuum of about 10^{-6} torr. The temperature of the boat was about 1600°-1750° C., and the oxygen partial pressure was about 60-70 Pa and the helium pressure was about 650 Pa. During the evaporation, approximately 5 to 250 Pa of oxygen was injected every few minutes. The fully oxidized MgO which had accumulated on the cold surface 20 was then scraped and material collected in the vacuum chamber 12 at about 7×10^{-7} torr. In order to insure correct MgO stoichiometry an additional 6500 Pa of oxygen was quickly injected, and this resulted in a strong exothermic reaction evidenced by a noticeable optical flash. In preparation of another nanocrystalline MgC specimen, the procedure was substantially the same except after scraping the collected material from the cold surface 22, and before compaction, the powder was exposed to O_2. The same general exothermic reaction occurred, accompanied by a flash of light. X-ray diffraction analysis showed the resulting products in both cases was MgO with some WO_x contamination. The WO_x contamination can be removed by use of other more focused evaporation techniques, such as laser ablation of MgO.

Example 10

Additional nanocrystalline zinc oxygen specimens were prepared in a manner similar to Example 4, but an oxidizing gas pressure (O_2) was added to enhance the formation of stoichiometric ZnO. After collecting the nanocrystalline zinc oxygen compound on the cold surface 22, 1300 Pa of O_2 was let into the vacuum chamber 12. The collected material changed from a black to a gray color. Precompaction of a pellet was quite successful using the low pressure compaction unit 26. The pellet was subsequently pressed in the high pressure compaction unit 34. Further, nanocrystalline ZnO was prepared in substantially the same manner described above but some additional O_2 was added during sublimation (about 100 Pa every ten minutes over the half hour of collection of zinc oxygen). The collected material was noted to turn from black to gray in color. Variations of these oxidizing atmospheres were used, including smaller amounts of 13 Pa of O_2 every five ten minutes causing formation of gray zinc oxide material with no color change when about 4000 Pa of O_2 was let into the vacuum chamber at the end of the run.

Example 11

Nanocrystalline Al_2O_3 has also been produced using a mixture of O_2 and helium during collection of material on the cold surface 20 of the apparatus 10. During evaporation of aluminum from a BN boat the temperature ranged from about 1000° C. to 1100° C., the helium gas pressure was at about 600 Pa and the O_2 pressure was about 200 Pa. The resulting material collected on the cold surface 20 was scraped, and it was determined by X-ray diffraction to be a substantial amount of aluminum remained unconverted to Al_2O_3.

Example 12

MgO was prepared in substantially the same way as in Example 9, but the O_2 pressure was maintained at about 260 Pa and helium at 650 Pa throughout sublimation. The temperature of the source MgO material was maintained at about 1600°–1700° C. with tungsten boat about 100°–150° C. hotter than the MgO source. A reaction did occur between MgO and WO_x forming MgO/WO_x compound with no evidence of insufficient oxygen (X-ray diffraction results).

Example 13

Nanocrystalline Si was prepared by evaporating by Joule heating at about 1500°–1600° C. electronics grade Si from a W boat. Helium pressures in the vacuum chamber of 550 Pa and 13 Pa were used in two runs. Initially the materials collected on the cold surface 20 appeared lighter orange at thin layers, changing to orange and then black for thicker deposits. The Si prepared at higher pressure helium underwent an exothermic reaction (light flash) when exposed to oxygen but none occurred for the lower helium pressure run.

We claim:

1. A method of preparing a treated nanocrystalline metallic material, comprising the steps of:

providing a starting nanocrystalline metallic material having a mean grain size less than about 35 nm;

compacting said starting nanocrystalline metallic material in a selected inert atmosphere, said compacted metallic material having the mean grain size less than about 35 nm; and

annealing said compacted metallic material at a temperature less than about one-half of the melting point of said metallic material.

2. The method as defined in claim 1 wherein said nanocrystalline metallic material is selected from the group consisting essentially of noble metals, transition metals and mixtures thereof.

3. The method as defined in claim 2 wherein said nanocrystalline metallic material further includes silicon as an additive thereto.

* * * * *

JOURNAL DE PHYSIQUE
Colloque C5, supplément au n°10, Tome 49, octobre 1988

STRUCTURE AND PROPERTIES OF NANOPHASE TiO_2

R.W. SIEGEL, H. HAHN[1], S. RAMASAMY[2], L. ZONGQUAN[3], L. TING[4] and R. GRONSKY*

Materials Science Division, Argonne National Laboratory, Argonne, IL 60439, U.S.A.
National Center for Electron Microscopy, Lawrence Berkeley Laboratory, University of California, Berkeley, California, U.S.A.

Résumé - Echantillons de TiO_2 (rutile) nanophasé de grains ultrafins ont été synthétisés par la méthode de condensation dans un gaz, suivie ensuite par compaction en-situ, et étudiés par microscopie électronique en transmission, par microdureté de Vickers, et par spectroscopie d'annihilation positronique en fonction de température de frittage. La densité des échantillons augmente rapidement au-dessus de 500°C avec seulement une légère croissance de grains. La dureté obtenue par cette méthode, effectuée aux températures 400-600°C plus basses que la température de frittage conventionnel et sans avoir besoin des additives de frittage, est comparable on supérieure à celle des échantillons de gros grains.

Abstract - Ultrafine-grained, nanophase samples of TiO_2 (rutile) were synthesized by the gas-condensation method and subsequent in-situ compaction, and then studied by transmission electron microscopy, Vickers hardness measurements, and positron annihilation spectroscopy as a function of sintering temperature. The nanophase compacts densified rapidly above 500°C, with only a small increase in grain size. The hardness values obtained by this method are comparable to or greater than coarser-grained compacts, but at temperatures 400 to 600°C lower than conventional sintering temperatures and without the need for sintering aids.

1. INTRODUCTION

The gas-condensation method [1-3] for the production of small particles in the size range of 1 to 50 nm has recently enabled the synthesis of a new class of ultrafine-grained materials by the in-situ compaction and sintering of these particles [4]. The resulting nanophase materials, which may contain crystalline, quasicrystalline, or amorphous phases, can be metals, ceramics, or composites with rather different and improved properties than normal coarse-grained polycrystalline materials. The work so far done on these new materials and their potential for the future have been recently reviewed [5,6]. Some advantages of nanophase ceramics should be: (i) Their small particle size during synthesis should allow for increased sinterability at lower temperatures and smaller residual pore sizes owing to a combination of high driving forces and short diffusion distances, avoiding the need for sintering aids. (ii) The exceptional physical and chemical control available in the gas-condensation method lets the particle surfaces be maintained clean allowing subsequent high grain-boundary purity and thus negligible interfacial phase formation. (iii) The large fraction

---

[1] Present address: Materials Research Laboratory, University of Illinois, Urbana, Illinois USA.
[2] Permanent address: Department of Nuclear Physics, University of Madras, Madras, India.
[3] Permanent address: Institute of Solid State Physics, Academia Sinica, Hefei PRC.
[4] Permanent address: Institute of Low Energy Nuclear Physics, Beijing Normal University, Beijing PRC.

of atoms residing in interfaces, almost one-half in the case of a 5 nm grain size, may allow for new atomic arrangements and thus novel and improved ceramic properties. Such properties may include, for example, mechanical properties which might be improved through higher grain-boundary purity and the absence of brittle phases therein or small grain sizes allowing for more efficient deformation mechanisms and more effective crack dissipation.

In order to explore the feasibility of creating nanophase ceramics with such improved properties, ultrafine-grained nanophase TiO_2 (rutile) samples were synthesized in the present work by the gas-condensation method and then studied by a variety of techniques as a function of sintering temperature. The desirability of small and uniform particle size for obtaining quality ceramics has been well documented for ceramics in general [7] and for TiO_2 specifically [8,9]. Nanophase ceramics, with their high grain-boundary purity and very small and rather uniform particle size, are expected to sinter at lower temperatures than normally available ceramics with larger particle sizes, and to exhibit improved properties [6]. Consequently, for comparison with the nanophase samples, coarser-grained samples were also synthesized from commercial powders and similar measurements were carried out.

2. EXPERIMENTAL PROCEDURE

The ultra-high vacuum chamber used for the preparation of nanophase TiO_2 by the gas-condensation method has been described elsewhere [6]. Titanium (99.7% pure) was evaporated from a resistance-heated tungsten boat at temperatures between 1550°C and 1650°C into a 0.3-0.7 kPa helium atmosphere over a period of 15 to 30 min. The small Ti particles formed by condensation in the He-gas were deposited on the cold-finger of the production chamber, and subsequently oxidized by the introduction of about 2 kPa of oxygen into the chamber. The particles were then compacted at 1.4 GPa at room temperature, resulting in a TiO_2 nanophase compact of 9 mm diameter by about 0.2 mm thick with a mean grain diameter of 12 nm.

For comparison with the nanophase TiO_2, samples were also synthesized from commercial TiO_2 powder, which was ball-milled using NiO balls to an average grain size of 1.3 μm, with a maximum grain size of 2.5 μm. Three samples were made from this commercial powder. The first was compacted at 1.4 GPa at room temperature without any sintering aid, as a direct comparison with the nanophase sample, while the second was compacted at the same pressure, but using a 5% aqueous solution of polyvinyl alcohol (pva) as a sintering aid. The third sample was compacted at 0.1 GPa with the same pva solution, this method being essentially the conventional one for the preparation of such a ceramic. The densities of the green pellets ranged from 55 to 70% of theoretical density.

Grain-size distributions were determined in the nanophase samples by transmission electron microscopy (TEM), and in the coarser-grained samples by scanning electron microscopy (SEM). Vickers microhardness was measured at room temperature, using a load of 15 g and an indentation time of 25 s, on the as-compacted samples and after sintering successively for one-half hour at temperatures up to 1400°C. Complementary positron annihilation spectroscopy (PAS) lifetime and Doppler-broadening measurements were also made in order to monitor sample porosity as a function of sintering up to 900°C. In addition, high-resolution electron microscopy (HREM) observations of grain and grain-boundary structures were also carried out on selected nanophase samples using the Atomic Resolution Microscope at the National Center for Electron Microscopy, LBL. An operating voltage of 1 MeV was chosen to provide better penetration of some of the thicker particles while retaining resolution at the 0.16 nm level. No attempt was made to orient the individual particles under the electron beam; instead, the samples were scanned for large thin areas and imaged in through-focus series bracketing the minimum contrast [10] condition.

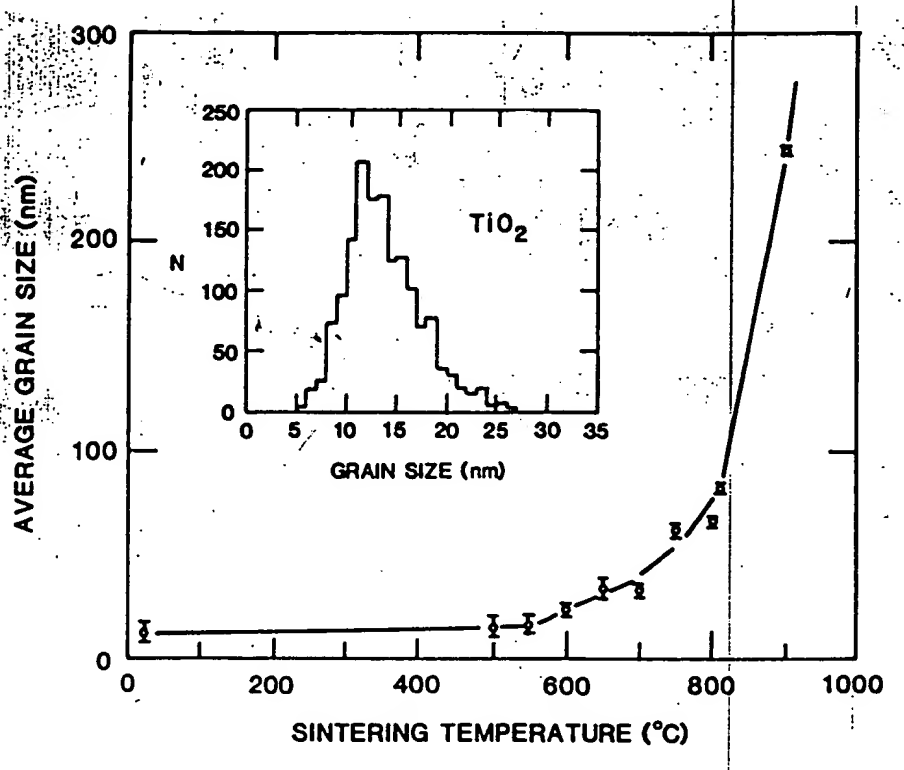

Figure 1. Average grain size of nanophase TiO_2 (rutile) as a function of sintering temperature determined by TEM. The sintering anneals were one-half hour in duration at each successive temperature. The grain-size distribution for the as-compacted sample is shown in the inset.

3. RESULTS AND DISCUSSION

The results of the grain-size determinations using TEM on the nanophase TiO_2 as a function of sintering temperature are presented in Figure 1. It can be seen that the grain-size distribution for the as-compacted sample is rather narrow and typical of the particle-size distribution produced in the gas-condensation method [2]. The distribution appears to remain unchanged by the Ti oxidation and subsequent compaction processes. It can also be readily seen that the average grain size increases very little up to about 550°C, and only rather slowly with sintering temperature up to about 800°C, at which temperature grain growth becomes fairly rapid. A similar grain-size stability against temperature has been found for nanocrystalline iron with an initial average grain size of 6 nm [11].

Figure 2 shows a high-resolution electron micrograph from a rather typical region of the nanophase TiO_2 sample sintered for one-half hour at 500°C. The grains here are seen to be essentially equiaxed with relatively planar boundaries. The grain boundaries in the as-compacted sample, on the other hand, appeared to be significantly less planar than this, but detailed atomic structural studies of these nanophase boundaries have not yet been completed. The lattice fringes seen in Figure 2 are those representative of the atomic planes of rutile, as confirmed by both electron and X-ray diffraction patterns on all of these samples.

Figure 2. High-resolution transmission electron micrograph of nanophase TiO_2 (rutile) after sintering for one-half hour at 500°C. The sample was prepared for TEM observation by fracturing the sintered compact, which gave rise to the open areas seen in the micrograph.

The Vickers microhardness measured at room temperature is shown in Figure 3 as a function of sintering temperature for three different TiO_2 (rutile) samples, the nanophase sample with 12 nm initial average grain size compacted at 1.4 GPa, and two samples with 1.3 μm initial average grain size compacted at 1.4 GPa and 0.1 GPa. The latter sample, prepared essentially in accord with standard ceramic processing methods, was the only one of these three which was sintered with the aid of pva. The results for a fourth sample prepared in a similar manner with pva, but compacted at 1.4 GPa, are not shown in Figure 3; they are very similar to those for the 1.3 μm, 0.1 GPa sample, but shifted to lower temperatures by about 150°C. It can be readily seen from these microhardness measurements that the nanophase TiO_2 sinters at considerably lower (between 400 and 600°C) temperatures than the commercial 1.3 μm powder with the aid of pva, yielding comparable or greater microhardness values. For reference, the Vickers microhardness of a single crystal of TiO_2 measured under identical conditions is 1036 ± 66 kgf/mm^2. Preliminary fracture toughness studies on these samples, made by measuring the crack lengths emanating from microindentations at higher loads, appear to confirm the similar or better mechanical properties of the nanophase TiO_2 in comparison with the coarser-grained material and single-crystal TiO_2 (rutile) as well. Without the aid of pva, the commercial powders are seen to sinter rather poorly and exhibit inferior mechanical properties, as expected.

Although it seems apparent from the microhardness measurements that densification of the nanophase sample was taking place upon sintering above 500°C, PAS measurements were also carried out in order to monitor this densification more directly. The results, which will be published elsewhere by the present authors in a more complete account of this study of nanophase TiO_2, show in their simple two-state behavior that both the 12 nm, 1.4 GPa nanophase sample and the 1.3 μm, 1.4 GPa commercial-powder sample (see Figure 3) began densifying rapidly above 500°C, but that the nanophase sample did so more rapidly with increasing

temperat
density
which ar
indicate
grained

The resu
compacts,
densify
hardness
of single
to 600°C
sintering
of nanoph
results o
nanophase

VICKERS MICROHARDNESS (kgf/mm^2) 160 120 80 400 0

Figure 3.
temperature
temperatures
grain size
grained comp
(diamonds) a
commercial p

temperature than the coarser-grained sample, resulting in a smaller void or pore density at 900°C. As might have been expected, the PAS lifetime measurements, which are also sensitive to varying pore sizes when they are small, clearly indicate smaller pore sizes in the nanophase sample relative to the coarser-grained sample at all the sintering temperatures investigated by PAS.

The results of these first investigations on nanophase TiO_2 indicate that these compacts, although already rather well bonded on compaction at room temperature, densify rapidly above 500°C, with only a small increase in grain size. The hardness values obtained by this method are comparable to or greater than those of single-crystal TiO_2 or coarser-grained compacts, but at temperatures some 400 to 600°C lower than conventional sintering temperatures and without the need for sintering aids. Much work still needs to be done regarding the characterization of nanophase ceramics and the elucidation of their full potential. However, the results of this first study appear to hold considerable promise for the future of nanophase ceramics.

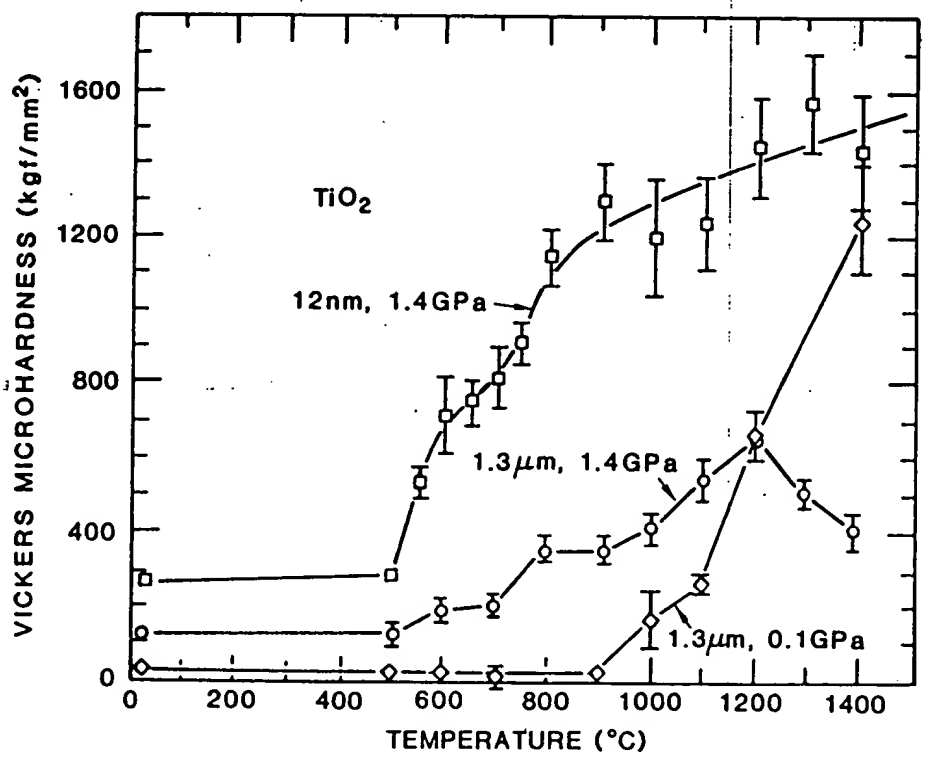

Figure 3. Vickers microhardness in kgf/mm² of TiO_2 (rutile) measured at room temperature as a function of one-half hour sintering at successively increased temperatures. Results for a nanophase sample (squares) with an initial average grain size of 12 nm compacted at 1.4 GPa are compared with those for coarser-grained compacts with 1.3 μm initial average grain size sintered at 0.1 GPa with (diamonds) and at 1.4 GPa without (circles) the aid of polyvinyl alcohol from commercial powder.

ACKNOWLEDGEMENT

This work was supported by the U. S. Department of Energy, BES-Materials Sciences, under Contracts W-31-109-Eng-38 at ANL and DE-AC03- 76SF00098 at LBL.

REFERENCES

[1] K. Kimoto, Y. Kamiya, M. Nonoyama, and R. Uyeda, Jap. J. Appl. Phys. 2, 702 (1963).

[2] C. G. Granqvist and R. A. Buhrman, J. Appl. Phys. 47, 2200 (1976).

[3] A. R. Thölén, Acta Metall. 27, 1765 (1979).

[4] H. Gleiter, in **Deformation of Polycrystals: Mechanisms and Microstructures**, N. Hansen et al., eds., Risø National Laboratory, Roskilde (1981) p.15; see also these Proceedings.

[5] R. Birringer, U. Herr, and H. Gleiter, Trans. Jap. Inst. Met. 27, Suppl., 43 (1986).

[6] R. W. Siegel and H. Hahn, in **Current Trends in the Physics of Materials**, M. Yussouff, ed., World Scientific Publ. Co., Singapore (1987) p. 403.

[7] H. K. Bowen, Mater. Sci. Eng. 44, 1 (1980).

[8] E. A. Barringer and H. K. Bowen, J. Amer. Ceram. Soc. 65, C-199 (1982).

[9] B. Fegley, Jr., E. A. Barringer, and H. K. Bowen, J. Amer. Ceram. Soc. 67, C-113 (1984).

[10] R. Gronsky, in **Treatise on Materials Science and Technology Series: Experimental Techniques**, Vol. 19 B, H. Herman, ed., Academic Press, New York (1983) p. 225.

[11] E. Hort, Diploma Thesis, Universität des Saarlandes, Saarbrücken (1986).

Manufacturing Nanocrystalline Materials by Physical Vapor Synthesis

By Quinton Ford, Director of Marketing, Industrial Products, Nanophase Technologies Corp., Burr Ridge, Ill.

A CONTINUOUS PROCESS BASED ON GAS-PHASE CONDENSATION CAN PRODUCE NANOCRYSTALLINE PARTICLES IN ECONOMICAL QUANTITIES.

During the past decade, a great deal of research and development has been focused on fabricating and characterizing nanocrystalline materials. Within the industry, nanocrystalline materials are commonly defined as crystalline materials that have an average particle or grain size of less than 100 nanometers (0.1 micron). A deliberate distinction is made between nanocrystalline materials and submicron crystalline materials, which have an average particle or grain size of less than 1 micron.

The relative percentage of interfacial atoms to total atoms in a material increases dramatically with decreasing size below 100 nanometers (see Figure 1). The resultant properties of nanocrystalline materials thus have a much greater dependence on the contributions of interfacial atoms (those atoms on the surface of a particle or in the grain boundaries of a consolidated material) than submicron materials. Some unconventional mechanical, chemical, electrical, optical and magnetic properties exhibited by nanocrystalline materials are attributed to this greater dependence on the contributions of interfacial atoms.

PROCESSING METHODS

A wide range of techniques have been developed to fabricate nanocrystalline materials. The most commonly practiced of these are gas-phase condensation, sol-gel chemistry, spray pyrolysis and hydrothermal processing. The challenge with all techniques is to successfully scale production to commercial volumes of nanocrystalline materials with properties and economies that allow their use in mainstream applications. One of the first techniques to be so scaled, physical vapor synthesis, is based on the principles of gas-phase condensation.

In the 1980s, gas-phase condensation was demonstrated to be capable of fabricating a wide range of ceramic and metallic nanocrystalline particles. Gas-phase condensation involves the evaporation of precursor materials in reduced-pressure, inert environments. After evacuating a chamber, inert gas is introduced to create the reduced-pressure environment. The precursor material is then evaporated using any of a variety of energy sources.

Atoms of evaporated precursor collide with the cooler atoms of the inert backfill gas. These cooler gas atoms cause the evaporated precursor to condense and solidify as nanocrystalline particles of the precursor. If reactive gas is used for backfill instead of inert gas, the evaporated precursor and gas react, condense and solidify as nanocrystalline particles of the formed compound.

The cooling of the gas is caused by convective currents that are created within the chamber by the temperature gradient between the energy source and a

Figure 1

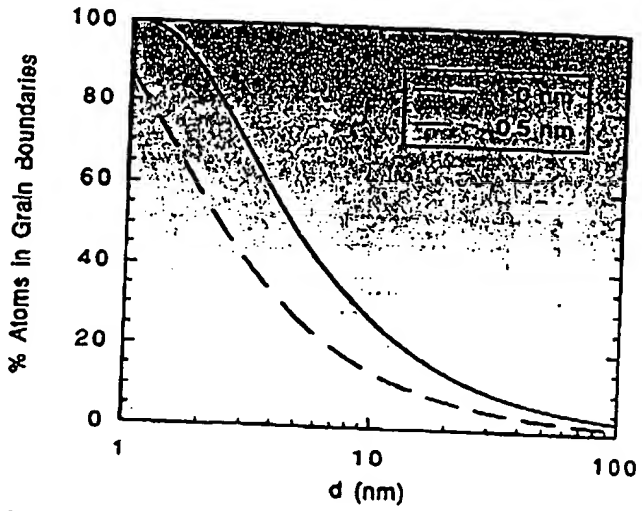

Percentage of atoms in grain boundaries of nanocrystalline material as a function of average grain size assuming grain boundary thickness range of 0.5 to 1 nanometer. (From R.W. Siegel, "Cluster-Assembled Nanophase Materials", *Annu. Rev. Mater. Sci.* 21, 559-578, 1991)

Figure 2

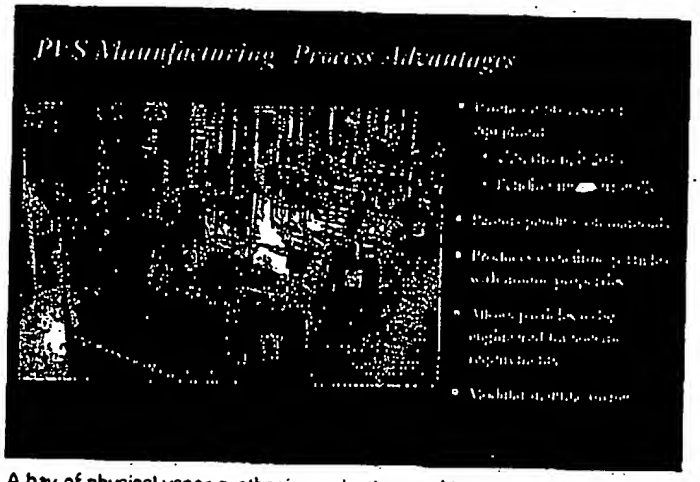

A bay of physical vapor synthesis production machines is readied.

Figure 3

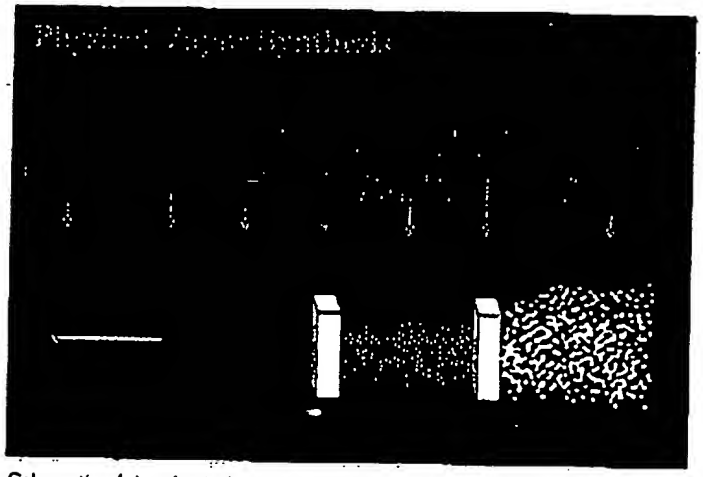

Schematic of the physical vapor synthesis technique.

Using Physical Vapor Synthesis Materials in Polishing Slurries

One commercial application of physical vapor synthesis materials is as an abrasive component for polishing slurries used in the production of semiconductors. Current trends in semiconductor design include decreasing line widths and increasing numbers of metal and dielectric layers. These design trends present significant issues during photolithography steps unless the layers to be imaged are planar across the entire wafer. A process referred to as chemical mechanical planarization (CMP) is gaining widespread acceptance within the industry to polish the sputtered metal and dielectric layers on the semiconductor wafers to a highly planar state.

Aluminum oxide produced by physical vapor synthesis is incorporated into slurry for planarizing tungsten metal layers. The slurry is prepared by introducing the aluminum oxide powder to water, adding mechanical energy to break down agglomerates, and extracting particles comprising the upper end of the particle size distribution. Oxidizing chemicals are later blended with the abrasive slurry just prior to use.

Slurry containing aluminum oxide produced by physical vapor synthesis has been evaluated as superior to other slurries in defectivity and microscratching of tungsten surfaces. The concurrent removal rates and uniformities are comparable to those of other slurries. Consequently, cost of ownership can be lowered by the overall performance of slurry containing physical vapor synthesis aluminum oxide.

Cerium oxide produced by physical vapor synthesis is currently being evaluated as an additive to slurries for planarization of dielectric layers. Such slurries generally contain silica as the sole abrasive component. Initial tests indicate that adding a small percentage of cerium oxide to silica-based slurries can increase removal rates to four times the rates of slurries containing no cerium oxide. No concurrent degradation of defectivity, microscratching or uniformity have been detected.

cooled collection surface. These convective currents carry the nanocrystalline particles to the collection surface, where they are later harvested. The collection surface is typically the outer surface of a metal tube through which liquid nitrogen is passed.

IMPROVING OUTPUT

Nanocrystalline particles produced via gas-phase condensation are equiaxed, nonporous, free of residual surface chemicals, and have a narrow particle size distribution. However, the reduced-pressure conditions and dependence on natural convection limit the technique to a low-rate batch process. Practically-sized systems can produce only tens of grams of nanocrystalline materials per day, resulting in economies that are not feasible for most applications.

In the early 1990s, scientists at Nanophase Technologies developed a patented technique based on the principles of gas-phase condensation. This technique produces particles with similar attributes to those produced through gas-phase condensation, while eliminating the need for reduced-pressure conditions and the dependence on natural convection. The technique, named physical vapor synthesis, operates as a continuous process and at significantly increased rates compared to gas phase condensation.

A single physical vapor synthesis production machine is capable of delivering tens of kilograms of nanocrystalline materials per day. This provides economies that are feasible for a large

Figure 4

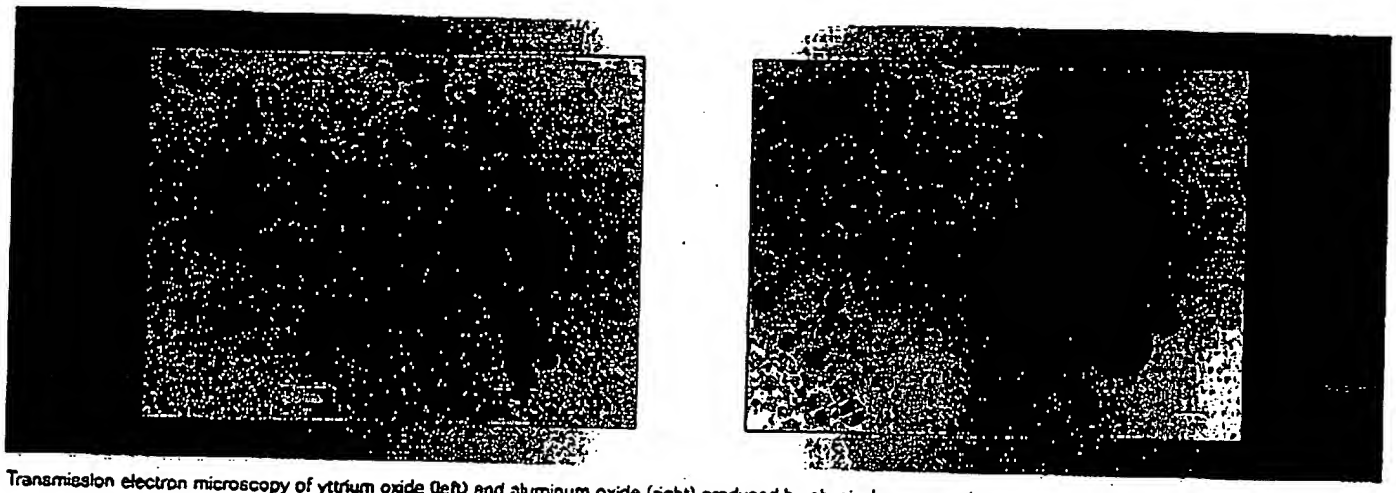

Transmission electron microscopy of yttrium oxide (left) and aluminum oxide (right) produced by physical vapor synthesis.

number of applications. The technique has already been successfully scaled to a production capacity exceeding 100 tons per year, and additional capacity can be added in a modular fashion as needed (see Figure 2).

COOLING REQUIRED

In physical vapor synthesis (Figure 3), precursor material is introduced at a controlled rate into a chamber. Within the chamber, a plasma arc is formed between a nonconsumable electrode and the consumable precursor. The precursor, typically a high-purity metal rod, passes through the plasma arc and is melted and vaporized.

A quench and/or reactive gas is introduced to the chamber. Atoms of evaporated precursor collide with the cooler atoms of the quench gas. The evaporated precursor condenses and solidifies as nanocrystalline particles of the precursor. If a reactive gas is also present, it reacts with the evaporated precursor, causing nanocrystalline particles of the resultant compound to be formed upon condensation and solidification.

After the nanocrystalline particles are solidified, their temperature is still elevated. The particles must be cooled to minimize agglomeration. Additional gas is turbulently introduced to accelerate cooling of the particles. The gas propels the particles into a collector housing. The collector housing contains filter media that allows the gas to exit but traps the weakly agglomerated nanocrystalline particles. The nanocrystalline particles collect on the filter media in the collector housing and are periodically harvested.

Advantages of Physical Vapor Synthesis

- Economical
- Narrow particle size distribution
- Continuous process
- Particle size control
- Nonporous, equiaxed particles
- High-purity materials
- Wide range of oxides

PRODUCT CHARACTERISTICS

Numerous nanocrystalline oxides and noble metals have been successfully fabricated using physical vapor synthesis. These include aluminum oxide, titanium dioxide, zinc oxide, iron oxide, cerium oxide, yttrium oxide, copper oxide, magnesium oxide, manganese oxide, indium-tin oxide, palladium, silver, gold and platinum.

Non-noble metals are also of commercial interest in nanocrystalline form. However, in this size regime, the surfaces of these particles are highly reactive and will oxidize when exposed to air. In the case of some metals, this oxidation causes violent combustion. Several methods to stabilize particles are under development and are expected to allow eventual commercialization of these metals. Additionally, fabrication of such materials as nanocrystalline carbides and nitrides will be attempted with modifications to the current physical vapor synthesis practices.

A metastable phase of a material generally results from physical vapor synthesis due to the high process temperatures and rapid solidification. Particle morphologies vary with material, although they are commonly equiaxed. Aluminum oxide particles produced appear perfectly spherical when imaged by SEM or TEM (see Figure 4).

PARTICLE SIZE CONTROL

Physical vapor synthesis provides sufficient control to allow concurrent adjustment of the specific surface area and the average particle size of production materials. Specific surface areas can be varied from approximately 30 to 90 m^2/g as desired. This corresponds to average particle sizes ranging from approximately 10 to 100 nanometers. Based on close correlation between average particle sizes measured from TEM images and calculated from BET specific surface areas, physical vapor synthesis particles are virtually nonporous.

More important than the average particle size in most applications is the particle size distribution, specifically the upper end of the distribution. Physical vapor synthesis materials have lognormal distributions, with one endpoint at a few nanometers and another between 300 and 500 nanometers (see Figure 5). Less than 1% of the particles are above 150 nanometers.

Figure 5

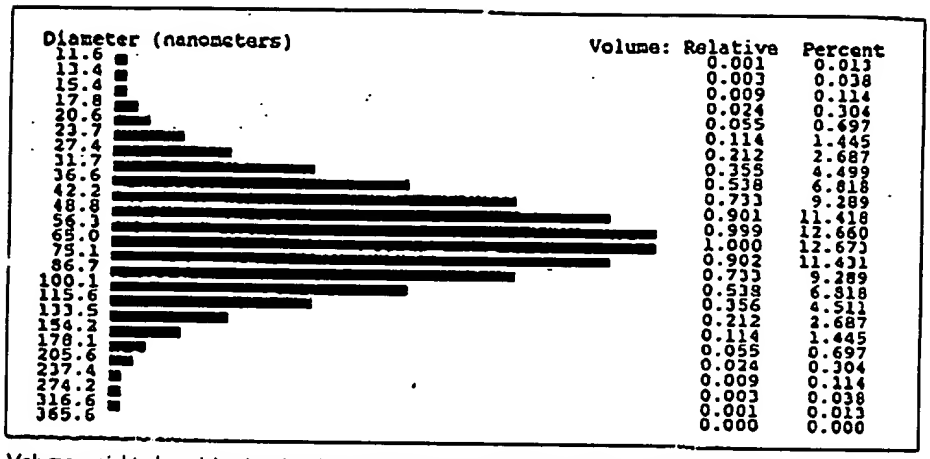

Volume-weighted particle size distribution of aluminum oxide produced by physical vapor synthesis.

When the particles are collected from physical vapor synthesis, they are weakly agglomerated up to tens of microns. The agglomerates can be broken down to the particle size distributions described above by such techniques as ultrasonication and media milling. Further refinement of these particle size distributions is also possible, eliminating particles above a specific size.

The overall purity of physical vapor synthesis nanocrystalline particles approximates the purity of the precursor material. Consequently, precursors commensurate with the overall purity requirements of the application are used. Specific impurities of concern for a given application can be engineered to desired levels.

APPLICATIONS

Applications for oxide particles produced by physical vapor synthesis have already been commercialized and include abrasives in polishing slurries for semiconductors, anti-fungal agents for health care and additives to increase the wear resistance of polymers. Additional applications for oxide and noble metal particles are also being developed. These include transparent conductive coatings, precious metal catalysts and additives to provide various functionalities to polymers. ❑

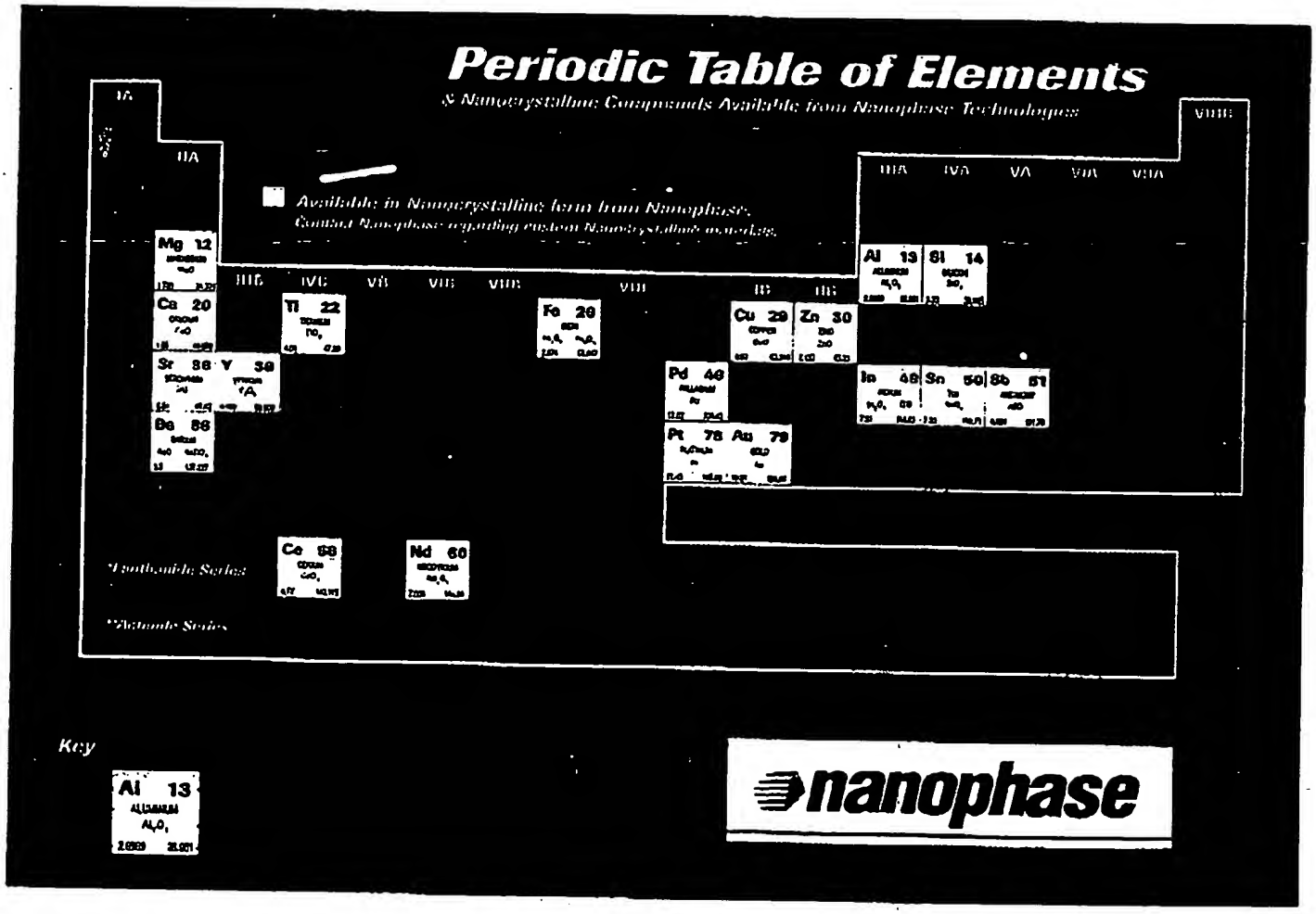

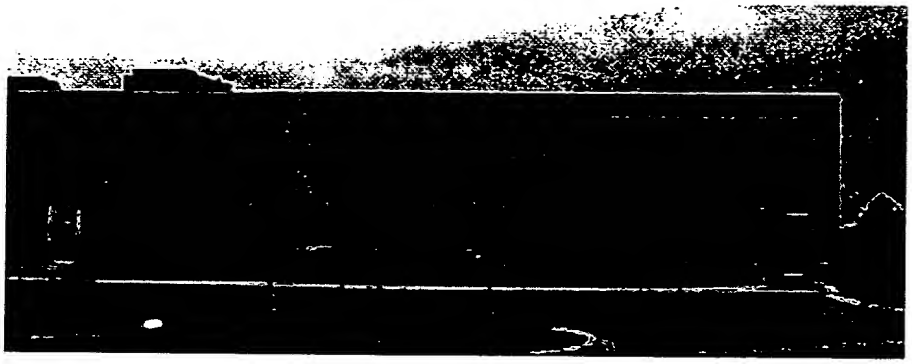

Nanophase Technologies Corporation is the world's leader in the development, production, and marketing of *nanocrystalline* materials for a wide range of industrial applications.

This web site is designed to provide information on our company, our technologies, our products, and applications for our *nanocrystalline* materials . We hope that you will visit this site often.

Corporate History

The origin of Nanophase can be traced back to research performed during the 1980s at Argonne National Laboratory, a U.S. Department of Energy facility. Interested in studying the properties of *nanocrystalline* materials, researchers at Argonne conceived a unique process to fabricate them. This process, commonly referred to today as *gas phase condensation*, could produce small quantities of materials with unique characteristics. Besides their sizes being measured in *nanometers*, the particles were of high purity, had no residual surface contaminants, were spherical, and were *non-porous*.

Convinced that these materials were commercially important and that *gas phase condensation* could be scaled to produce them in large quantities at reasonable cost, Argonne scientist Dr. Richard Siegel founded Nanophase in 1989. At that time, *gas phase condensation* could produce only a few grams of *nanocrystalline* material per day at a cost of approximately $1,000 per gram.

Several years of effort by scientists at Nanophase resulted in the development of a new process based generally on the principles of *gas phase condensation*, but with significantly improved fabrication rates and economies. This process, named Physical Vapor Synthesis (PVS) now allows Nanophase to produce tons of materials per year with costs as low as a few pennies per gram. PVS is patented and was recognized with an R&D 100 Award in 1995 as one of the year's most technologically significant new developments.

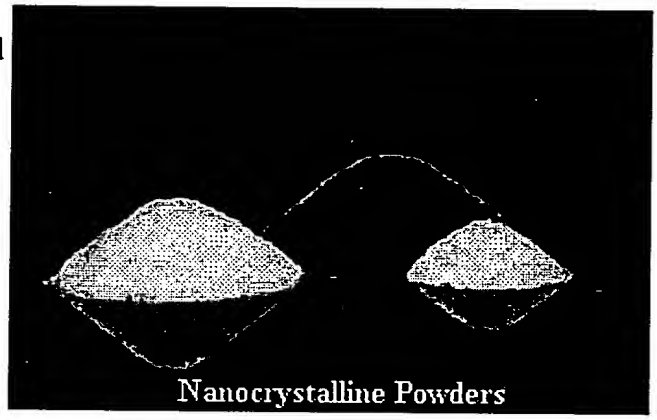

Nanocrystalline Powders

NanoTek® Aluminum Oxide

Product Code: 0100

Molecular Formula	Al_2O_3
Purity	99.5+%
Average Particle Size	27 - 56 nm (from SSA)
Specific Surface Area	30 - 60 m^2/g (BET)
Morphology	Spherical
Crystal Phase	Gamma
Distribution	2 - ~400 nm (by laser scattering, Horiba LA-910)
Refractive Index	1.7
Appearance	White to off white powder
Bulk Density	0.10 g/cc
True Density	3.6 g/cc

Pricing

Unit Size	Price
25g	$19.00
50g	$27.00
100g	$39.00
250g	$64.00
500g	$85.00
1kg	$135.00
2kg	$200.00
>2kg	Quote

Physical Vapor Synthesis (PVS)

Nanophase primarily employs its patented Physical Vapor Synthesis (PVS) process to produce *nanocrystalline* particles. PVS utilizes a plasma to heat a selected metal *precursor* in open atmosphere. As the temperature rises, the metal's atoms boil off into a stream of flowing gas, creating a *vapor*.

Collisions with atoms of a gas that is introduced to the process cool the metal atoms so that the *vapor condenses* into liquid molecular clusters. Cooling continues, freezing these molecular clusters into solid particles of *nanometric* size. The flowing gas transports the particles to a collection vessel. The presence of oxygen allows oxygen atoms to intermingle with metal atoms forming *nanocrystalline metal oxides* such as aluminum oxide and titanium dioxide.

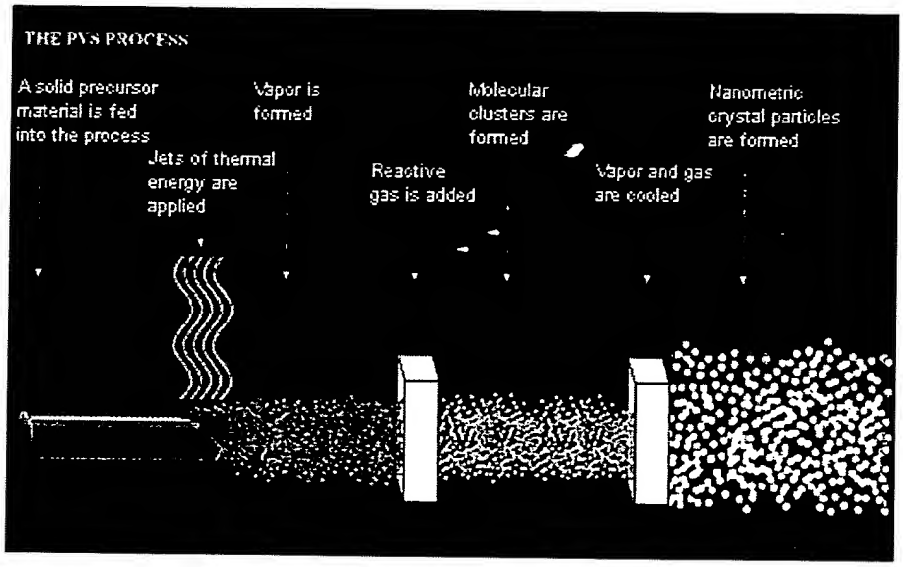

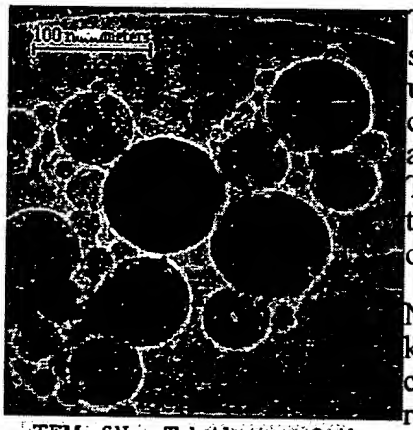

TEM of NanoTek Aluminum Oxide produced using PVS

The resultant powder consists of weakly *agglomerated* particles of spherical *morphology*. Purity of the powders is primarily dependent upon the purity of the *precursor* material. There are no residual chlorides or sulfides present on the surfaces of the particles as there are with materials produced by certain other combustion techniques. The clean nature of these surfaces enable treatments to be applied to tailor these materials for applications requiring *dispersion* in a variety of fluids.

Nanophase developed PVS from the general principles of a process known as *gas phase condensation*. *Gas phase condensation* is conducted under high vacuum conditions which limit it to producing research scale quantities of nanocrystalline materials. It typically employs a resistive heat source to generate a gas phase of the *precursor* material. Cooling of this gas phase to cause condensation and freezing to form nanocrystalline particles is accomplished using a liquid-nitrogen cooled collection surface. The materials produced by *gas phase condensation* are similar in *morphology*, purity, and size to those produced via PVS.

Gas phase condensation is practiced by many research scientists around the world as a means of fabricating materials for their experiments. Nanophase's patented PVS process is the only known method by which commercial quantities of these materials can be produced.

This Page is inserted by IFW Indexing and Scanning Operations and is not part of the Official Record

BEST AVAILABLE IMAGES

Defective images within this document are accurate representations of the original documents submitted by the applicant.

Defects in the images include but are not limited to the items checked:

- [x] BLACK BORDERS
- [ ] IMAGE CUT OFF AT TOP, BOTTOM OR SIDES
- [ ] FADED TEXT OR DRAWING
- [x] BLURED OR ILLEGIBLE TEXT OR DRAWING
- [ ] SKEWED/SLANTED IMAGES
- [ ] COLORED OR BLACK AND WHITE PHOTOGRAPHS
- [ ] GRAY SCALE DOCUMENTS
- [ ] LINES OR MARKS ON ORIGINAL DOCUMENT
- [ ] REPERENCE(S) OR EXHIBIT(S) SUBMITTED ARE POOR QUALITY
- [ ] OTHER: _____

IMAGES ARE BEST AVAILABLE COPY.
As rescanning documents *will not* correct images problems checked, please do not report the problems to the IFW Image Problem Mailbox